National Library of Canada
Acquisitions and Bibliographic Services Branch
395 Wellington Street
Ottawa, Ontario
K1A 0N4

Bibliothèque nationale du Canada
Direction des acquisitions et des services bibliographiques
395, rue Wellington
Ottawa (Ontario)
K1A 0N4

Your file Votre référence

Our file Notre référence

NOTICE

The quality of this microform is heavily dependent upon the quality of the original thesis submitted for microfilming. Every effort has been made to ensure the highest quality of reproduction possible.

If pages are missing, contact the university which granted the degree.

Some pages may have indistinct print especially if the original pages were typed with a poor typewriter ribbon or if the university sent us an inferior photocopy.

Reproduction in full or in part of this microform is governed by the Canadian Copyright Act, R.S.C. 1970, c. C-30, and subsequent amendments.

AVIS

La qualité de cette microforme dépend grandement de la qualité de la thèse soumise au microfilmage. Nous avons tout fait pour assurer une qualité supérieure de reproduction.

S'il manque des pages, veuillez communiquer avec l'université qui a conféré le grade.

La qualité d'impression de certaines pages peut laisser à désirer, surtout si les pages originales ont été dactylographiées à l'aide d'un ruban usé ou si l'université nous a fait parvenir une photocopie de qualité inférieure.

La reproduction, même partielle, de cette microforme est soumise à la Loi canadienne sur le droit d'auteur, SRC 1970, c. C-30, et ses amendements subséquents.

Canada

University of Alberta

Electro-hydrodynamic Instabilities in Nematic Liquid Crystals

by

Alexander Man Leung Nip

A thesis submitted to the Faculty of Graduate Studies and Research in partial fulfillment of the requirements for the degree of Doctor of Philosophy

in

Theoretical Physics

Department of Physics

Edmonton, Alberta

Fall 1995

National Library
of Canada

Acquisitions and
Bibliographic Services Branch

395 Wellington Street
Ottawa, Ontario
K1A 0N4

Bibliothèque nationale
du Canada

Direction des acquisitions et
des services bibliographiques

395, rue Wellington
Ottawa (Ontario)
K1A 0N4

Your file Votre référence

Our file Notre référence

THE AUTHOR HAS GRANTED AN IRREVOCABLE NON-EXCLUSIVE LICENCE ALLOWING THE NATIONAL LIBRARY OF CANADA TO REPRODUCE, LOAN, DISTRIBUTE OR SELL COPIES OF HIS/HER THESIS BY ANY MEANS AND IN ANY FORM OR FORMAT, MAKING THIS THESIS AVAILABLE TO INTERESTED PERSONS.

L'AUTEUR A ACCORDE UNE LICENCE IRREVOCABLE ET NON EXCLUSIVE PERMETTANT A LA BIBLIOTHEQUE NATIONALE DU CANADA DE REPRODUIRE, PRETER, DISTRIBUER OU VENDRE DES COPIES DE SA THESE DE QUELQUE MANIERE ET SOUS QUELQUE FORME QUE CE SOIT POUR METTRE DES EXEMPLAIRES DE CETTE THESE A LA DISPOSITION DES PERSONNE INTERESSEES.

THE AUTHOR RETAINS OWNERSHIP OF THE COPYRIGHT IN HIS/HER THESIS. NEITHER THE THESIS NOR SUBSTANTIAL EXTRACTS FROM IT MAY BE PRINTED OR OTHERWISE REPRODUCED WITHOUT HIS/HER PERMISSION.

L'AUTEUR CONSERVE LA PROPRIETE DU DROIT D'AUTEUR QUI PROTEGE SA THESE. NI LA THESE NI DES EXTRAITS SUBSTANTIELS DE CELLE-CI NE DOIVENT ETRE IMPRIMES OU AUTREMENT REPRODUITS SANS SON AUTORISATION.

ISBN 0-612-06266-X

Canada

University of Alberta

Library Release Form

Name of Author: Alexander Man Leung Nip

Title of Thesis: Electro-hydrodynamic Instabilities in Nematic Liquid Crystals

Degree: Doctor of Philosophy

Year this Degree Granted: 1995

Permission is hereby granted to the University of Alberta Library to reproduce single copies of this thesis and to lend or sell such copies for private, scholarly, or scientific research purposes only.

The author reserves all other publication and other rights in association with the copyright in the thesis, and except as hereinbefore provided, neither the thesis nor any substantial portion thereof may be printed or otherwise reproduced in any material form whatever without the author's prior written permission.

Alex Man Leung

10689-63 Ave.
Edmonton, Alberta
Canada T6H 1P7

Oct. 6, 95

University of Alberta

Faculty of Graduate Studies and Research

The undersigned certify that they have read, and recommend to the Faculty of Graduate Studies and Research for acceptance, a thesis entitled Electro-hydrodynamic Instabilties in Nematic Liquid Crystals submitted by Alexander Man Leung Nip in partial fulfillment of the requirements for the degree of doctor of philosophy in theoretical physics.

Dr. J.A. Tuszyński

Dr. F.C. Khanna

Dr. Z.W. Gortel

Dr. J. Jung

Dr. G.R. Freeman

Dr. M. Plischke

Dr. J.T. Gleeson

Abstract

We review some of the basic properties of the nematic liquid crystals and re-derive the fundamental quantities necessary for the development of a macroscopic continuum theory. Using this macroscopic theory as a basis, we carry out two separate investigations into the primary transitions of a nematic liquid crystal thin film subjected to an *a.c.* electric field. We first attempt to establish theoretically the critical behavior of the normal rolls observed slightly above the threshold voltage. A phenomenological free energy description is used and a set of bifurcation diagrams is constructed to illustrate the critical behavior. In our second investigation, we use the method of multi-scale analysis to illustrate the formation of oblique rolls at low frequencies when the director field is given only one rotational degree of freedom. The transformation from the normal to the oblique rolls is shown through the minimization of the neutral surface, thereby establishing the presence of a triple point. We furthermore examine the impact of the use of a restrictive director field on the small scale dynamics by deriving an amplitude equation.

Acknowledgements

My supervisor Prof. J.A. Tuszyński has certainly made a major contribution to this thesis. I am especially grateful to him for first introducing me to *nonlinear dynamical systems* in the earlier part of my graduate career and later to the *physics of liquid crystals*. His confidence in me has always been enormous; for that, I would like to extend to him my most sincere gratitude. I would also like to thank the other members of my examining committee—Prof. F.C. Khanna, Prof. Z.W. Gortel, Prof. J. Jung, Prof. G.R. Freeman, Prof. M. Plischke (Simon Fraser University) and Prof. J.T. Gleeson (University of Calgary)—for taking their valuable time to carefully assess this thesis and for their constructive criticisms and suggestions. I am also in debt to Prof. L. Kramer (Universität Bayreuth) for his insightful criticisms, which gave me the momentum necessary to continue what seemed to be an impossible task.

The people to whom I owed many thanks during the production of this thesis are too numerous to name here. Nevertheless, I would like to gratefully acknowledge the assistance I received from L. Chandler and P. Tripp. Their excellent secretarial skills made much of my graduate work almost enjoyable. Last, but not least, I want to thank my wonderful wife Kathy for taking total control of the house work and for putting up with many long hours of my hiding in the basement during the final stage of writing this thesis.

A.M.L. Nip

Contents

1 Introduction to Liquid Crystals **1**

1.1 Mesophases 2

2 Introduction to Nematodynamics **7**

2.1 Franck's Deformation Energy 8

2.2 Effects of External Fields 10

2.3 Molecular Field 15

2.4 Hydrostatics 18

2.5 Balance of Torques 24

2.6 Nematodynamics 27

2.6.1 Entropy Production 28

2.6.2 The Viscous Torque 31

2.6.3 Sources of Dissipation 34

2.6.4 Constitutive Equations 36

2.6.5 The Viscous Stress Tensor 38

2.7 Electro-hydrodynamic Instabilities 43

2.7.1 Helfrich Instability 43

2.7.2 Equations of Motion 47

3 Direct Bifurcation in Nematic Liquid Crystals **50**

3.1 The Director and The Electric Fields 51

3.2 The Fluid Velocity 58
3.3 The Rest State to Normal Rolls Transition Line 65
3.4 The Energy Method 72
3.4.1 A Phenomenological Free energy 73
3.4.2 Bifurcation Diagrams 83
3.5 Summary 92

4 Weakly Nonlinear Analysis **94**
4.1 The Multi-Scale Expansions 95
4.2 The Linear Balance 98
4.3 First Nonlinear Balance 111
4.4 The Amplitude Equation 117
4.5 Summary 124

5 Conclusions **126**

Bibliography **129**

A Anisotropic Tensors **133**

B Total Stress Tensor **135**

List of Tables

3.1 Physical parameters for the room temperature nematic liquid crystal MBBA [5, 6]. 68

4.1 Physical parameters for MBBA [6] and PAA [45] nematic liquid crystals. These values are used in the calculations of the stability diagrams in Figs. 4.5 and 4.6. The elastic constants k_{22} and k_{33} have been adjusted to yield optimal fits. 108

List of Figures

2.1 Three types of elementary deformation found in liquid crystals. . . . 10

2.2 A schematic diagram of a nematic cell. 44

2.3 Helfrich-Carr effect for a nematic liquid crystal with negative dielectric anisotropy and positive conductance anisotropy. 46

3.1 Typical plots of the solutions to the electro-hydrodynamic problem: (**a**) the director field, (**b**) the velocity field, (**c**) the induced current density at $t = 0$ and (**d**) the induced current density at $t = T/2$. . . . 64

3.2 The root-mean square voltage plotted as a function of the normalized domain spacing for various values of the reduced angular frequency. . 69

3.3 The normal-roll transition line. The solid line is the theoretical result derived from (3.72). The diamonds are the experimental measurements. 70

3.4 The normalized domain spacing plotted as a function of the threshold voltage. The solid line is calculated from the linear thoery; the dots represent the experimental measurements. 71

3.5 The fourth-order coefficient plotted as a function of the normalized domain spacing r at $\omega' = 0.5$ for different values of V_{rms}. 80

3.6 The second-order coefficient plotted as a function of the normalized domain spacing r at $\omega' = 0.5$ for different values of V_{rms}. 81

3.7 The transition line for the rest-state to normal-roll transition. The solid line is calculated by minimizing Eqn. (3.103) with respect to r; the dots represent the experimental measurements. 83

3.8 The transition line for the rest-state to normal-roll transition. The solid line is calculated at $\sigma_{\parallel}/\sigma_{\perp} = 1.15$; the dots represent the experimental measurements. 84
3.9 The trajectory made by the minimum of F in the positive quadrant of the parameter plane. 85
3.10 Bifurcation diagram for θ_o near criticality. 86
3.11 A log-log plot of the bifurcation diagram for θ_o. 87
3.12 Bifurcation diagram for the normalized domain width r. 89
3.13 Bifurcation diagram for r plotted over an extended range of ϵ. 89
3.14 A log-log plot of the bifurcation diagram for θ_o over an extend range of the reduced voltage ϵ. 90
3.15 Bifurcation curves for r for various values of the reduced angular frequency. 90
3.16 A log-log plot of the bifurcation curves for θ_o for different values of the reduced angular frequency. 91
3.17 The value of C_4 at the transition point plotted as a function of the reduced angular frequency. 91

4.1 Basic setup of a nematic liquid crystal cell. 96
4.2 Contour plots of the surface (4.36) at **a)** $\omega' > \omega_c'$; **b)** $\omega' \approx \omega_c'$ and **c)** $\omega' < \omega_c'$. 103
4.3 The threshold value of the state parameter r_y as a function of the modified angular frequency ω'. 104
4.4 Observed first transition thresholds of MBBA [13] (circle) and Merck Phase-V [15] ("+"). 105

4.5 Structure diagram for the low-order instabilities using MBBA material parameters. The solid and the dashed lines represent respectively the calculated threshold voltages for the normal- and the oblique-roll formations. The "+" and the dots, on the other hand, correspond to the experimentally measured threshold voltages for the normal- and the oblique-roll formations in Merck Phase-V, respectively. 106

4.6 Structure diagram for the low-order instabilities using PAA material parameters. The solid line is the theoretical transition line. The "+" and the diamonds correspond to the experimentally measured threshold voltages for the normal- and the oblique-roll formations in Merck Phase-V, respectively. 107

Chapter 1

Introduction to Liquid Crystals

It was first discovered and reported by an Austrian botanist named Friedrich Reinitzer that cholesterol and its derivatives possess two melting points [1]. The substance at one temperature T_1 turns into a cloudy liquid, then at a higher temperature T_2 it transforms into a clear liquid. It has the most unusual properties at temperatures intermediate between T_1 and T_2. It has the ability to scatter light in a way similar to solid; nevertheless, just as any liquid, it can be easily deformed and takes the shape of the container that contains it. The molecular structures of cholesterol and its derivatives were not known at the time; scientists were therefore unable to relate their peculiar properties to the fundamental interactions between molecules. But one thing was very certain. An unusual state of matter exists between these two melting temperatures. If a substance first melts at T_1, then what is melting at T_2? Could that be a new form of matter other than solid and liquid? These questions were one of the biggest mysteries in the scientific community at that time. This new form of matter was first referred to as the soft crystal, then the floating crystal. The name "liquid crystal" eventually came about and still remains in use today.

Of course, we now know that substances exhibiting liquid crystal phases share common molecular properties. They can be found in biological systems, or can be manufactured through chemical processes and synthesized in the laboratory. The

evolution from a pursuit of fundamental understanding of a basic form of matter into everyday applications is truly fascinating. In the last twenty years, liquid crystals have rapidly found their way into the information display industry. Liquid crystal displays (LCD's) have become the most dominant type of passive display devices available and can be found in use at every corner of our society. They are commonly used in digital watches, laptop computers, pocket televisions and other portable equipment.

1.1 Mesophases

We often distinguish the liquid from the solid phase by their densities and specific heats, but we can also characterize the individual phases in terms of the degree of orderliness. In the low temperature phase (the solid phase), the intermolecular forces are so strong that they overcome the molecules' thermal vibrations and restrictively confine the molecules to specific positions. The molecules are arranged in such a way that they form a regular repeating (lattice) pattern. This ordering is referred to as the positional order. In addition, there is also orientational order in solid. That is, all molecules in a solid are orientated in the same direction. There is a constant battle between the intermolecular forces and the thermal vibrations. The net result determines the amount of order a phase can possess. When the temperature becomes sufficiently high, the thermal excitation is eventually large enough to outweigh the intermolecular forces that hold the molecules rigidly in place. Thus, melting takes place. It becomes energetically more favorable for the molecules not to be confined to these specific positions but to wander freely throughout the volume. The mean intermolecular distance is therefore relatively greater than that of the solid phase. Most substances behave this way; they lose both the positional and the orientational orders all at once and transform spontaneously to isotropic liquids at the transition temperature. But there are some materials which go through an intermediate phase called mesophase before they transform to isotropic liquids. In principle, this can

be accomplished in two ways, depending on the sequence of which the orders are lost. If the orientational order is lost first but the positional order is retained, then this mesophase is called "plastic crystal." It maintains the lattice structure, but the molecules are randomly orientated. Alternatively, if the positional order is lost first but the orientational order is retained, the resultant mesophase is named "liquid crystal." A liquid crystal does not have a rigid lattice structure; its molecules can move about freely but they tend to orient in the same direction.

Ordinary substances, water for example, transform directly from solid to liquid as temperature rises. As is well known, this is a first order transition and is characterized by sudden changes in both density and specific heat. But for those substances whose molecules have elongated shapes with rigid centers and soft ends, there exists a mesophase between the solid and the liquid phases, namely, the liquid crystal phase. For instance, cholesteryl myristate, a substance which can be found in our cell membrances and has the molecular properties described above, possesses a liquid crystal phase between $71°C$ and $85°C$. As we have just mentioned, this phase of matter possesses partial properties from both the solid and the liquid phases. It retains some of the orientational order from the solid phase while, like liquid, it loses most of its positional order. On one hand, the lack of positional ordering allows the molecules to move about freely. The positional order, however, is not entirely lost; some liquid crystals do possess a small amount of positional order. The amount of positional order left in this mesophase gives rise to different kinds of liquid crystal phases. We shall explore these possibilities in the subsequent paragraphs. On the other hand, because of the presence of orientational order, it has the most unusual optical properties which are what most of our liquid crystal applications are based upon. These "finger-like" molecules tend to align themselves along the same direction. This preferred direction is represented by a vector field called the director. Note that the director can take either the "up" or the "down" direction. Mostly due to thermal fluctuations, the alignment of these molecules is not perfect. If we denote

the angle that the long molecular axis makes with the director by θ, there is a certain amount of spreading in the value of θ, depending on how much orientational order is present in the liquid crystal phase. To measure the orientational order, we average θ over the molecules in the sample. The average value $\bar{\theta}$ is zero if there is a perfect alignment or 100% orientational order, but increases as this order becomes weaker and weaker. The orientational order in fact disappears at $\bar{\theta} = 57^o$.

The parameter $\bar{\theta}$ serves an additional purpose. For those liquid crystal phases which have no positional order at all, the value of $\bar{\theta}$ indicates how far the liquid crystal is away from transforming to isotropic liquid. Since the spreading in the value of θ is subjected to thermal fluctuations, it's average $\bar{\theta}$ is a function of temperature. This implies that the transition of liquid crystal to isotropic liquid takes place at the temperature T_c such that $\bar{\theta}(T_c) = 57^o$. In order words, $\bar{\theta}$ serves as an order parameter as in Landau's theory of phase transition, except that it varies from 0^o to 57^o instead of from 1 to 0 as the system transforms from a symmetrical phase to a less symmetrical one. To make it a convenient measure of the order or the symmetry of the liquid crystal phase, it has been found that the quantity

$$\frac{1}{2}\left(3\cos^2\theta - 1\right) \tag{1.1}$$

should be average over the molecules in the sample instead [2]. We shall denote it's average value by p. As a result, perfect orientational order corresponds to $\cos\theta = 1$ and therefore $p = 1$. In the liquid phase, there is no orientational order. The molecules are equally likely to lie in any given direction. The average value of $\cos^2\theta$ in this case is $1/3$ and hence $p = 0$.

The above procedures work well in determining the orientational order present in a liquid crystal phase only if the director is fixed in space. A liquid crystal whose director is constant in space is named *nematic liquid crystal.* There are, however, liquid crystals whose directors rotate helically in space. Such liquid crystals are called *chiral nematic liquid crystals.* The above averaging process cannot be used in measuring the orientational order in this type of liquid crystals. Since the director

itself varies in space, not only does the order parameter change with temperature but it must also change in space. Therefore, averaging expression (1.1) over all molecules in the sample does not yield any physically meaningful measurement on the orientational order. However, if we define a spatial point $\vec{r}$ as a macroscopically small but microscopically big region of space centered at $\vec{r}$ and we average (1.1) over all molecules within this region, the result

$$p(\vec{r}, T) = \langle \frac{3\cos^2\theta - 1}{2} \rangle_{\vec{r}}, \tag{1.2}$$

where the subscript $\vec{r}$ on the right indicates that the average is local, is an accurate representation of the orientational order within the sample. Now, the order parameter $p(\vec{r}, T)$ varies both with temperature and in space. The above method is actually very similar to how we define the magnetization $\vec{M}(\vec{r})$ of a magnetic material. Magnetization $\vec{M}(\vec{r})$, by definition, is obtained by dividing the vector sum of the magnetic moments over all atoms in a small region of space centered at $\vec{r}$ by its own volume. Whether we are concerned with the order parameter in a chiral nematic liquid crystal or the magnetization in a ferromagnet, we take this volume of space to be sufficiently big so that it contains a statistically large number of molecules (or atoms).

We have mentioned previously that some liquid crystals do retain a small amount of positional order. Molecules in these liquid crystal phases arrange themselves in layers. They spend most of their time in the layers and very little time in between the layers. These liquid crystals are called *smectic liquid crystals.* There may or may not be any positional order within each layer. If there is no positional order within the layers at all, the molecules are free to move about in the layers or migrate from layer to layer. Because of the presence of orientational order, the molecules in each layer tend to align themselves along the director. The liquid crystal is called *smectic A* if the director is constant in space and is perpendicular to the planes. It is called *smectic C* if the spatially constant director makes an angle other than 90^o with the planes. Positional order can exist within the layers. In this case, the molecules tend to arrange themselves to appear at specific locations in the layer and form various

regular two-dimensional lattice patterns. If the director is perpendicular to the planes and the molecules appear in a hexagonal lattice pattern within each layer, the liquid crystal is called *smectic B*. It is named *smectic E* if the director is perpendicular to the planes but the molecules are organized in a rectangular lattice pattern in each plane.

What we have presented here is only a partial list of all the liquid crystals discovered so far and those that we have included are of the most fundamental types. Combining the properties of two of the above liquid crystals results in a new species. For example, chiral smectic liquid crystals can be derived from the chiral nematic and the smectic types. Molecules in these liquid crystals are arranged in layers, but the director rotates helically in space. In this thesis, we concern ourselves exclusively with the nematic liquid crystals. Through subsequent chapters, we explore the standard theories widely used to describe the nematic states at or out of equilibrium and focus on perhaps one of the most fascinating aspects of nematic liquid crystals — electrohydrodynamic instabilities.

Chapter 2

Introduction to Nematodynamics

Instabilities in nematic liquid crystals have attracted considerable interest in recent years [3, 4, 5, 6], mainly due to these systems' intrinsically large aspect ratios which make them ideal for the studying of pattern formation. It has been found that a thin (compared to the lateral dimensions) layer of nematic liquid crystal confined between two parallel plates can be excited either thermally [7, 8, 9, 10, 11, 12] or electrically [13, 14, 15, 16, 17] to produce a series of convective patterns. Most of what we know about these various patterns and the sequence of transformation is rather experimental [13, 14, 15, 16, 17, 18, 19]; theoretical treatments of these pattern formations have grown relatively slowly, largely due to the complexity of the underlying equations of motion and the inherent nonlinearities. Thus far, theoretical investigations have been limited to the low lying transition line: formation of normal rolls (straight convective rolls) and that of oblique rolls (zigzag rolls) from the rest state have been studied most extensively [3, 4, 5, 6]. Because the transition appears to be continuous, the convective state can be taken as a perturbation to the rest-state near criticality; therefore, the equations of motion can be linearized immediately, eliminating the need to deal with nonlinear couplings. The first theoretical investigation of the rest-state to normal-roll transition was initiated by Helfrich [3] and, today, the instability bears his name. His investigation concerned the formation of normal rolls from the rest

state in a nematic thin film placed in a uniform d.c. electric field and the question was essentially simplified to a one-dimensional problem. Dubois-Violette et al. [4] later expanded the calculation to the a.c. regime; Penz and Ford [5] extended it to a two-dimensional geometry. Recently, Bodenschatz et al. [6] took one step further, extending the calculation to a three-dimensional geometry and using it to describe the rest-state to oblique-roll transition at a frequency slightly below the triple point. Although these linear theories produce results which agree with the experimental observations very well at the transition points, they lack the ability to predict how patterns evolve. In this thesis, we address the issue of pattern evolution by examining the first transition from the rest state with a weakly nonlinear technique. We will carry out two theoretical investigations. The first one concerns the evolution of the stationary pattern beyond the transition threshold, while the second deals with small scale variations near the onset. But before we get to the heart of the matter, some preliminaries are useful. In this chapter, we introduce such important quantities as the deformation free energy, the dielectric free energy, the molecular field and the viscous stress tensor, because of the vital role they play in the development of the continuum theory. We then look at a possible explanation for the rest state going unstable and present the fundamental equation governing nematic liquid crystals. Let us now begin with a quick overview of the deformation energy.

2.1 Franck's Deformation Energy

In an ordinary crystal, stress causes atoms to become displaced; one part of the crystal could be displaced differently from the others. Deformation, in this case, is manifested by spatial variations in the displacement field. Nematic liquid crystals are systems of elongated molecules. In a suitable temperature range, these systems exhibit an unusual phase (the nematic phase) intermediate between the solid and the liquid phase. In this new phase, the molecules do not possess positional order, so

nematic liquid crystals can flow like fluids; however, the molecules maintain their orientational order, so these liquid crystals can demonstrate unusual optical properties. Since the molecules do not have a fixed center of mass, external stresses do not affect the way the centers of mass are distributed. Their alignment, however, is extremely sensitive to external stresses [20]; therefore, deformation in this case is characterized by the spatial variations in a vector field $\vec{n}$ called the director. The magnitude of the director is unity; its direction represents the locally preferred orientation of the molecular alignment in the same sense that $\vec{m}$ represents the local magnetization of a magnetic material. In addition, the variations of $\vec{n}$ are assumed small on the molecular scale. Since the nematic state $\vec{n}$ and $-\vec{n}$ correspond to the same physical state, the deformation energy F_d must be even with respect to $\vec{n}$. Furthermore, the undistorted state of a nematic liquid crystal corresponds to a uniform molecular aligment; therefore, F_d must be invariant under the transformation $x \longrightarrow -x$, $y \longrightarrow -y$ and $z \longrightarrow -z$. Using these symmetry arguments and neglecting the surface contributions, one can demonstrate that F_d is a linear combination of three independent terms, namely,

$$F = \frac{1}{2}k_{11}(\vec{\nabla} \cdot \vec{n})^2 + \frac{1}{2}k_{22}[\vec{n} \cdot (\vec{\nabla} \times \vec{n})]^2 + \frac{1}{2}k_{33}[\vec{n} \times (\vec{\nabla} \times \vec{n})]^2 \qquad (2.1)$$

This free energy is commonly referred to as the *Frank deformation energy* and the constants k_{11}, k_{22} and k_{33} the *Frank elastic constants* [21]. It is not difficult to see that, in general, the Frank elastic constants are non-zero and non-equivalent. This generality poses a great challenge to purely analytical approaches. In a few cases, the analyses can be considerably simplified by assuming these constants to be of the same value.

Each of the three independent terms in (2.1) corresponds to an elementary deformation in the nematic liquid crystals. These deformations are *splay*, *twist* and *bend* and are demonstrated in Fig. 2.1. They can be obtained by various surface arrangements. The first term on the right of (2.1) can be identified with the splay deformation since the presence of splay causes the director field to diverge. In the case

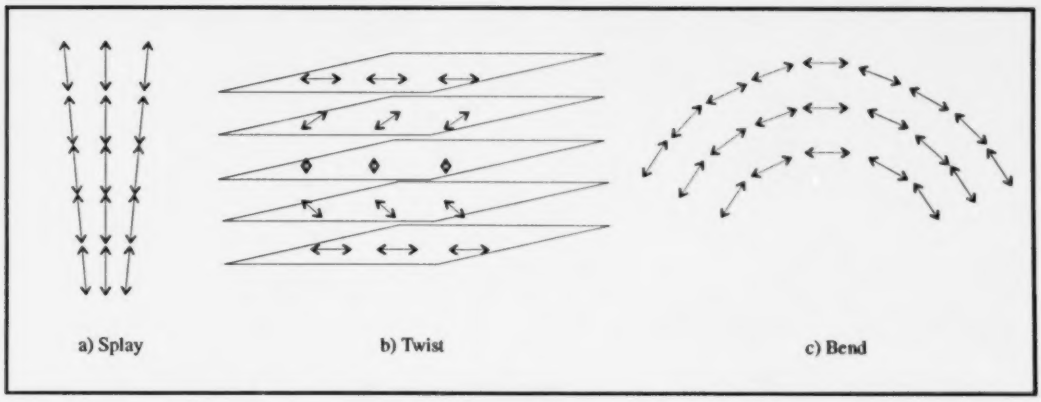

Figure 2.1: Three types of elementary deformation found in liquid crystals.

of the bend or the twist deformation, the director field is also rotational and therefore the vorticity $\vec{\omega} = \vec{\nabla} \times \vec{n}$ is non-zero. If twist is present alone, then the vorticity is orthogonal to the director field; the amount of twist is reflected by the cross product of the director and the vorticity. On the other hand, if bend is present alone, then the vorticity is parallel to the director; the amount of bend is characterized by the scalar product of the director and the vorticity. The second and the third terms in (2.1) correspond to the twist and the bend deformations, respectively. For this reason, the constants k_{11}, k_{22} and k_{33} (on the order of $10^{-12}N$ for a typical nematic liquid crystal) are also referred to as the splay, the twist and the bend elastic constants, respectively.

2.2 Effects of External Fields

Besides the boundary (wall) effect, alignment and deformation in nematic liquid crystals can be also induced by external electric and magnetic fields. Since the dielectric tensor is anisotropic, application of an electric field to a nematic liquid crystal induces a polarization along the long axis of the molecules. Typical nematic liquid crystal molecules are diamagnetic. For the nematic liquid crystal MBBA and PAA com-

monly used in experiments, their molecules have two aromatic rings which prefer to have the magnetic field in the plane of the rings. Depending on the magnetic and the electric anisotropies, these molecules can be made to align parallel or orthogonal to the fields. Therefore, in the presence of fields, not only is the director coupled to the intermolecular forces, it is also coupled to the external fields. It is the competition between these two kinds of couplings that determines the equilibrium state of the liquid crystal. The internal coupling is well characterized by the Frank deformation energy introduced in the last section. Similarly, the couplings with the external electric and magnetic fields are described by two additional free energies. It is our intention in this section to explore the explicit forms of these electromagnetic contributions. We shall now proceed to derive the electric and the magnetic free energies separately.

a) We first examine the magnetic contribution to the total free energy. We wish to derive an expression for the amount of work done on a magnetic sample placed tightly in a solenoid when the magnetic field is increased by an infinitesimal amount. The magnetization of the sample is assumed to be parallel to the external field. If the solenoid consists of N loops of wire and is connected to a battery, then, at any time, the applied (V) and the induced ($\mathcal{E}$) voltages are related to the current (i) by

$$V + \mathcal{E} = i\,R \tag{2.2}$$

where R is the resistance of the solenoid. To increase the magnetic field by an infinitesimal amount, the battery must do work against the back *emf*. Using the above expression, this amount of work can be written as

$$dW = V\,dq = -\mathcal{E}idt + i^2Rdt. \tag{2.3}$$

Quite clearly, the second term on the extreme right represents the irreversible ohmic loss while the first term is the amount of work responsible for raising the field and magnetizing the magnetic sample. The first term is what we are interested in. If we make use of Faraday's law of induction and the well known expression for the

magnetic induction H generated inside the solenoid, we can separate the first term on the extreme right of (2.3) into two parts in MKSA or SI units as

$$\frac{1}{\mu_o} vHdB = d\left(\frac{vH^2}{2}\right) + vHdM \tag{2.4}$$

where v is the volume of the sample and M is the magnetization. The first term on the right can be immediately identified with the energy required to establish the magnetic field. Then, the second term can be thought of as the amount of work required to magnetize the sample. Hence, the infinitesimal work done on the sample per unit volume is given by HdM. For a liquid crystal, regardless whether the molecules tend to align parallel or orthogonal to the field, this magnetic work increases the degree of alignment of the molecules and thereby lowers the free energy by the same amount i.e. reduces the maximum available energy for work at a later time. Consequently, the magnetic contribution to the change in the total free energy density is

$$df_M = -HdM. \tag{2.5}$$

This infinitesimal change in the magnetic free energy density can be appropriately applied to isotropic materials in which case the magnetization is along the direction of the external field. In a more general case, particularly for anisotropic materials, when the magnetization does not coincide with the external field, the above equation must be replaced by $df_M = -\vec{H} \cdot d\vec{M}$ or $df_M = -H_i dM_i$ where summation over repeated indices is implied. This expression can be further written in terms of the director field $\vec{n}$ and the magnetic intensity $\vec{H}$ if we make use of the magnetic susceptibility

$$\chi_{ij} = \chi_\perp \delta_{ij} + \triangle\chi n_i n_j \tag{2.6}$$

for a liquid crystal. Since nematic liquid crystals are anisotropic, their macroscopic response functions such as the magnetic susceptibility are 3×3 matrices. If the director is taken to be the principal axis, then χ can be written as a diagonal matrix

$$\chi = \begin{bmatrix} \chi_\perp & 0 & 0 \\ 0 & \chi_\perp & 0 \\ 0 & 0 & \chi_\parallel \end{bmatrix} \tag{2.7}$$

where $\chi_{\parallel}$ and $\chi_{\perp}$ are the magnetic susceptibilities measured along and orthogonal to the nematic axis respectively. After applying two consecutive rotations to the above expression, for a general director $\vec{n}$, the magnetic susceptibility takes on the form as shown in Eqn. (2.6). Since χ is a symmetric tensor, the infinitesimal change in the magnetic free energy density can also be written as

$$\begin{aligned} df_M &= -\vec{M} \cdot d\vec{H} \\ &= -\chi_{\perp} \vec{H} \cdot d\vec{H} - \triangle\chi(\vec{n} \cdot \vec{H})(\vec{n} \cdot d\vec{H}). \end{aligned} \tag{2.8}$$

Finally, the magnetic contribution to the total free energy density is obtained by integrating the above expression. This gives

$$f_M = -\frac{\chi_{\perp}\vec{H}^2}{2} - \frac{\triangle\chi}{2}(\vec{n} \cdot \vec{H})^2. \tag{2.9}$$

The first term on the right is independent of the director field and is a constant for a given $\vec{H}$. This term simply shifts the energy scale, so it can be discarded without loss of generality. The second term on the right however describes the coupling between the director and the magnetic field. If the magnetic anisotropy $\triangle\chi$ is positive, then the alignment with the magnetic field is energetically favorable. On the other hand, if the magnetic anisotropy is negative, then alignments orthogonal to the magnetic field are perferred.

b) We now turn our attention to the electric contribution to the total free energy density. We shall derive the electric free energy density in a way similar to that presented above. The magnitude of this energy must be equal to the amount of work required to polarize a dielectric material as an electric field is established in it. To calculate this amount of work, we consider a parallel-plate capacitor filled with a dielectric. The distance between the two plates is l. The capacitor has a capacitance C and is connected to an electrical power source. Similar to the magnetic case, we assume the polarization is parallel to the applied electric field. Having outlined the setup, we can immediately write down the infinitesimal work done dW that is required

to move an infinitesimal amount of charge dq from the negative plate to the positive one:

$$dW = V\,dq = Cl^2 E dE \tag{2.10}$$

where the relations $q = CV$ and $E = V/l$ have been used in writing the above equation. For a parallel-plate capacitor filled with a dielectric, the capacitance is given in gaussian units by $C = \varepsilon A/(4\pi l)$ where ε is the relative dielectric constant and A is the area of the parallel plates. Substituting this expression into equation (2.10), we can write the infinitesimal work done per unit volume in MKSA (SI) units as

$$DdE = (\epsilon_o E + P)dE = \epsilon_o d\left(\frac{E^2}{2}\right) + PdE \tag{2.11}$$

where P is the polarization. Of course, this amount of work is not only used to polarize the dielectric but is also used to establish the field. So it is not at all surprising that the first term on the right of (2.11) can be identified with the energy density of the field in free space; whereas, the second term reflects the amount of work that goes in to polarize the dielectric. Since, for nematic liquid crystals, an increment of the electric field induces further alignment of the molecules and thereby raises the polarization, the maximum available energy for doing work is reduced by the same amount that the power source puts in to produce the polarization. In other words, the infinitesimal change in the electric free energy density is given by $df_E = -PdE$. In the general case where the orientation of the polarization deviates from that of the applied electric field, the equation is written as

$$df_E = -\vec{P} \cdot d\vec{E} = -P_i dE_i. \tag{2.12}$$

We can proceed to express this infinitesimal change in the electric free energy density in terms of the director and the electric field by using the explicit form of the dielectric tensor

$$\varepsilon_{ij} = \varepsilon_\perp \delta_{ij} + \triangle\varepsilon n_i n_j \tag{2.13}$$

for a liquid crystal. Thus, we write (2.12) further as

$$\begin{aligned} df_E &= -\chi^e_{ij} E_j dE_i \\ &= -\frac{1}{4\pi}(\varepsilon_{ij} - \delta_{ij}) E_j dE_i \\ &= -\frac{1}{4\pi}(\varepsilon_\perp - 1)\vec{E}\cdot d\vec{E} - \frac{\triangle\varepsilon}{4\pi}(\vec{n}\cdot\vec{E})(\vec{n}\cdot d\vec{E}) \end{aligned} \tag{2.14}$$

where χ^e is the electric susceptibility tensor. Upon integration, we see that the electric contribution to the total free energy density is given in MKSA units by

$$f_E = -\frac{(\varepsilon_\perp - 1)}{2}\vec{E}^2 - \frac{\triangle\varepsilon}{2}(\vec{n}\cdot\vec{E})^2. \tag{2.15}$$

Similar to the magnetic free energy, the first term on the right in the above expression is independent of the director field and is also a constant at constant $\vec{E}$. Without loss of generality, we simply disregard this term. The second term, on the other hand, characterizes the coupling between the director and the electric field. This term favors the molecular alignment parallel to the applied field if the dielectric anisotropy $\triangle\varepsilon$ is positive; otherwise, alignments orthogonal to the external field are more favorable.

2.3 Molecular Field

On a very superficial level, liquid crystals respond to external stresses and stimuli in very much the same way ferromagnets respond to an external magnetic field. For example, for a liquid crystal with positive magnetic anisotropy, the molecules are made to conform with the applied magnetic field just as the magnetic spins in a ferromagnet are. Although these phenomena occur on different scales, this correspondence gives us certain advantages. As in the Weiss molecular-field approximation in the theory of ferromagnetism, instead of considering explicitly the interaction between each atomic pair, each atom is coupled to an internal field due to its surrounding neighbors in addition to the coupling with the external magnetic field. Analogously, in liquid crystals, we can avoid dealing with individual molecules by adopting a continuous

model and representing the internal forces by a continuous mean field. Then, the equilibrium configuration of the system is determined by the competition between this internal field and the external ones (such as electric and/or magnetic fields). Such a mean field approximation will continue to hold, so long as the physical phenomena of interest take place on a scale much greater than the inter-molecular distance. Below, we shall demonstrate how this internal field can be derived. The following derivation is in parallel with that presented by de Gennes [20].

In the absence of external fields, the bulk free energy of a nematic liquid crystal is given by the following functional:

$$F[n_\alpha, \partial_\alpha n_\beta] = \int f_d \, d^3r \tag{2.16}$$

where f_d is the Frank deformation energy density. The state of equilibrium then corresponds to the global minimum in the total free energy with respect to the variations of the director field. However, the variations cannot be arbitrary. Since the director field has a constant magnitude of unity, the variations have to be constructed in such a way that the norm of the director field remains constant i.e. $\vec{n}^2 = 1$. In other words, we wish to consider arbitrary rotations of the director field at each point in space. Furthermore, to obtain the conditions for equilibrium in the bulk, we must minimize the free energy in (2.16) with respect to $\vec{n}$ subjected to the constraint $\delta(\vec{n}^2) = 0$. This constraint equation can be further translated to $2\vec{n} \cdot \delta(\vec{n}) = 0$ and finally

$$\int \lambda(\vec{r})\vec{n} \cdot \delta(\vec{n}) \, d^3r = 0 \tag{2.17}$$

where $\lambda(\vec{r})$ is an arbitrary scalar function of $\vec{r}$. The total variation in F is given by

$$\begin{aligned} \delta F &= \int \left\{ \frac{\partial f_d}{\partial n_\beta} \delta n_\beta + \frac{\partial f_d}{\partial(\partial_\alpha n_\beta)} \frac{\partial(\delta n_\beta)}{\partial x_\alpha} \right\} d^3r \\ &= \int \left\{ \frac{\partial f_d}{\partial n_\beta} - \frac{\partial}{\partial x_\alpha} \frac{\partial f_d}{\partial(\partial_\alpha n_\beta)} \right\} \delta n_\beta \, d^3r. \end{aligned} \tag{2.18}$$

where integration by parts has been performed and the surface term has been ignored in writing the last equation. We now demand the total variation in F to vanish and

impose the above constraint on the variations in $\vec{n}$. This results in the following equation:

$$\int \left\{ \frac{\partial f_d}{\partial n_\beta} - \frac{\partial}{\partial x_\alpha} \frac{\partial f_d}{\partial(\partial_\alpha n_\beta)} + \lambda(\vec{r}) n_\beta \right\} \delta n_\beta \, d^3r = 0. \tag{2.19}$$

This is exactly equivalent to the method of Lagrange undetermined multipliers. Here, the arbitrary function $\lambda(\vec{r})$ plays the role of an undetermined multiplier. The coefficients of the variations δn_β in the above equation do not vanish identically since the variations themselves are not all independent. Although we can choose two of the δn_α independently, the third δn_α is connected to the first two through the constraint equation $2\vec{n} \cdot \delta(\vec{n}) = 0$. However, we can choose our $\lambda(\vec{r})$ at will. If we choose it in such a way that the coefficient of the third δn_α always vanishes, then equation (2.19) immediately implies

$$\frac{\partial}{\partial x_\alpha} \left\{ \frac{\partial f_d}{\partial(\partial_\alpha n_\beta)} \right\} - \frac{\partial f_d}{\partial n_\beta} = \lambda(\vec{r}) \, n_\beta. \tag{2.20}$$

If we define a molecular field $\vec{h}$ [20] as follows

$$h_\beta = \frac{\partial}{\partial x_\alpha} \left\{ \frac{\partial f_d}{\partial(\partial_\alpha n_\beta)} \right\} - \frac{\partial f_d}{\partial n_\beta}, \tag{2.21}$$

then, at equilibrium, the director must be at each point in space parallel to it: $\vec{h} = \lambda(\vec{r})\vec{n}$. Since the Frank deformation energy density consists of three independent terms, by substitution, the molecular field can also be separated into three independent contributions due to the splay, the twist and the bend elementary deformations. Hence, $\vec{h}$ can be further written as $\vec{h} = \vec{h}_{splay} + \vec{h}_{twist} + \vec{h}_{bend}$ with the three independent components given respectively as:

$$\begin{aligned} \vec{h}_{splay} &= k_{11} \nabla(\nabla \cdot \vec{n}), \\ \vec{h}_{twist} &= -k_{22}[A(\nabla \times \vec{n}) + \nabla \times (A\vec{n})], \\ \vec{h}_{bend} &= k_{33}[\vec{B} \times (\nabla \times \vec{n}) + \nabla \times (\vec{n} \times \vec{B})] \end{aligned} \tag{2.22}$$

where $A = \vec{n} \cdot (\nabla \times \vec{n})$ and $\vec{B} = \vec{n} \times (\nabla \times \vec{n})$.

In the presence of external fields, the molecular field in (2.21) picks up two additional contributions. Consider that the liquid crystal is placed in uniform electric and magnetic fields. Including gravity, the total free energy density is given by

$f = f_d + f_M + f_E + f_g$ where the last term on the right is the gravitational free energy density. The gravitational contribution to the total free energy density is perhaps the least significant. In fact, the nematic molecules respond strongly towards the internal molecular field and the electric field. Although alignments can be induced by a magnetic field, it has relatively low efficiency in comparison with an electric field [20]. To obtain the equilibrium condition, we must minimize the total free energy $\int f\, d^3r$ with respect to variations in the director consistent with the constraint equation (2.17), as opposed to minimizing only the total deformation energy. The same reasoning as we used in equations from (2.18) to (2.20) leads us to the same conclusion. That is, at equilibrium, the director field is everywhere parallel to the molecular field i.e. $\vec{h} = \lambda(\vec{r})\vec{n}$. However, in the presence of external fields, the molecular field takes on a different form:

$$h_\beta = \frac{\partial}{\partial x_\alpha}\left\{\frac{\partial f}{\partial(\partial_\alpha n_\beta)}\right\} - \frac{\partial f}{\partial n_\beta} \tag{2.23}$$

where the deformation energy density in (2.21) has been replaced by the above total free energy density. The gravitational free energy density $f_g = \rho\phi(\vec{r})$ (mass density $\times$ gravitational potential) is independent of the director; therefore, its contribution to the molecular field vanishes identically. If we use the expressions for the magnetic and the electric free energy densities as derived in Section 2.2 in the above expression, we arrive at

$$h_\beta = \frac{\partial}{\partial x_\alpha}\left\{\frac{\partial f_d}{\partial(\partial_\alpha n_\beta)}\right\} - \frac{\partial f_d}{\partial n_\beta} + \triangle\chi(\vec{n}\cdot\vec{H})H_\beta + \triangle\varepsilon(\vec{n}\cdot\vec{E})E_\beta. \tag{2.24}$$

It is therefore clear that the molecular field is an effective field which in general represents the net effects of the competition between the internal (molecular interactions) and various other external fields.

2.4 Hydrostatics

We have just looked at the equilibrium condition for systems whose director field is subjected to infinitesimal rotations. In this section, we shall examine the application

of a different kind of transformation to a nematic liquid crystal. In particular, we shall consider the displacements of the centers of mass of the molecules while retaining their orientations and we wish to compute the total change in the deformation free energy due to such a transformation. That this change in the deformation energy is non-zero is evident if we consider a nematic liquid crystal with only a bend deformation about the z-axis. If we rotate the centers of mass of all molecules by 90^o about the z-axis, the bend is transformed to a splay deformation. Hence, if the bend and the splay elastic constants are not the same, the deformation free energy $F_d = \int f_d \, d^3r$ will be different.

Consider the centers of mass of the molecules at each spatial point $\vec{r}$ to be displaced infinitesimally by $\vec{u}(\vec{r})$ while keeping the director frozen:

$$\vec{r} \rightarrow \vec{r}' = \vec{r} + \vec{u}(\vec{r}). \tag{2.25}$$

Although the orientation of the director is conserved in this transformation, its spatial derivatives undergo non-negligible changes. These changes denoted by $\delta(\partial_\beta n_\alpha)$ can be put into a more compact form as follows:

$$\begin{aligned} \delta(\partial_\beta n_\alpha) &= \frac{\partial n'_\alpha}{\partial r'_\beta} - \frac{\partial n_\alpha}{\partial r_\beta} \\ &= \frac{\partial n_\alpha}{\partial r_\gamma}\frac{\partial r_\gamma}{\partial r'_\beta} - \frac{\partial n_\alpha}{\partial r_\beta} \\ &= \frac{\partial n_\alpha}{\partial r_\gamma}\left(\frac{\partial r_\gamma}{\partial r'_\beta} - \delta_{\gamma\beta}\right). \end{aligned} \tag{2.26}$$

The transformation matrix $\partial r_\alpha / \partial r'_\beta$ can be written recursively as

$$\begin{aligned} \frac{\partial r_\alpha}{\partial r'_\beta} &= \frac{\partial}{\partial r'_\beta}[r'_\alpha - u_\alpha(\vec{r})] \\ &= \delta_{\alpha\beta} - \frac{\partial u_\alpha}{\partial r_\sigma}\frac{\partial r_\sigma}{\partial r'_\beta} \\ &= \delta_{\alpha\beta} - \frac{\partial u_\alpha}{\partial r_\sigma}(\delta_{\sigma\beta} - \ldots). \end{aligned} \tag{2.27}$$

Since the displacement $\vec{u}$ is infinitesimal, in the first order approximation, $\partial r_\alpha / \partial r'_\beta \approx \delta_{\alpha\beta} - \partial_\beta u_\alpha$. Inserting this expression into equation (2.26), the infinitesimal changes

in the derivatives of $\vec{n}$ can be simply written as

$$\delta(\partial_\alpha n_\beta) = -\frac{\partial n_\alpha}{\partial r_\gamma}\frac{\partial u_\gamma}{\partial r_\beta}. \tag{2.28}$$

Let us consider a volume element d^3r of a nematic liquid crystal. For an incompressible nematic, this volume element is preserved under the above transformation i.e. $d^3r = d^3r'$. Then, the infinitesimal change in the deformation energy of this volume element due to the above transformation is given by

$$d(\delta F_d) = \left\{\frac{\partial f_d}{\partial n_i}\delta n_i + \frac{\partial f_d}{\partial(\partial_i n_j)}\delta(\partial_i n_j)\right\} d^3r. \tag{2.29}$$

However, since the director is unaltered by the transformation, the first term on the right vanishes identically. We can use the expression (2.28) for the infinitesimal change in the director's derivatives in the second term. Then, the total change in the deformation energy is obtained by integration:

$$\delta F_d = \int \sigma^d_{ik}\frac{\partial u_k}{\partial r_i} d^3r \tag{2.30}$$

where

$$\sigma^d_{ik} = -\frac{\partial f_d}{\partial(\partial_i n_j)}\frac{\partial n_j}{\partial r_k}. \tag{2.31}$$

We can see what σ^d_{ik} corresponds to if we examine the generic expression for the elastic energy. The elastic energy for a deformable body is generally written as $F = \lambda_{ijkl}\ U_{ij}\ U_{kl}$ with the components of the strain tensor denoted by U_{ij} and those of the elastic modulus tensor by λ_{ijkl}. According to thermodynamics, at a constant temperature, the components of the stress tensor σ_{ij} can be obtained by differentiating the elastic energy with respect to the corresponding strain components [22] i.e. $\sigma_{ij} = \partial F/\partial U_{ij}$. Hence, in general, the components of the stress tensor are $\sigma_{ij} = \lambda_{ijkl}\ U_{kl}$ and the elastic energy simply becomes

$$F = \sigma_{ij}\ U_{ij} = \frac{1}{2}\sigma_{ij}\left(\frac{\partial u_i}{\partial r_j} + \frac{\partial u_j}{\partial r_i}\right). \tag{2.32}$$

We can now compare this energy expression with equation (2.30). We see immediately that the factor $\partial u_k/\partial r_i$ in (2.30) is associated with the components of the strain

tensor. Then, σ^d_{ij} must correspond to a deformation stress tensor. For this reason, σ^d_{ij} is commonly referred to as the *distortion stress tensor.*

To be as complete as possible, we should also take into account the magnetic, the electric and the gravitational contributions to the change in the total free energy under the transformation. As demonstrated in Section 2.2, the magnetic and the electric free energy densities are written respectively as $f_M = -\triangle\chi(\vec{n}\cdot\vec{H})^2/2$ and $f_E = -\triangle\varepsilon(\vec{n}\cdot\vec{E})^2/2$. Quite clearly, in view of the above transformation in which the director is unchanged, the electric and the magnetic fields do not contribute. On the other hand, the contribution from the gravitational field is non-vanishing. If the gravitational potential and the mass density are denoted by $\phi(\vec{r})$ and ρ respectively, then the corresponding free energy is $f_g = \rho\phi(\vec{r})$. Then the change in this free energy per unit volume due to the above transformation can be written as

$$\delta f_g = \rho\frac{\partial\phi}{\partial r_\alpha}\delta r_\alpha = \rho\frac{\partial\phi}{\partial r_\alpha}u_\alpha = \partial_\alpha f_g u_\alpha. \tag{2.33}$$

Putting together what we have obtained thus far, the total change in the free energy is given by

$$\begin{aligned}\delta F &= \delta F_d + \delta F_g \\ &= \int \sigma^d_{ik}\partial_i u_k d^3r + \int \partial_\alpha f_g u_\alpha d^3r.\end{aligned} \tag{2.34}$$

So far in our derivation, we have assumed that the liquid crystal is incompressible i.e. $\vec{\nabla}\cdot\vec{u} = 0$. However, this condition has not been imposed explicitly anywhere in our equations. This change in free energy is not yet applicable to incompressible nematics because the displacement $\vec{u}$ can still be chosen arbitrarily. In order to make sure that the minimum of F corresponds to an extremum with respect to variations u_α that leave the mass density unchanged, we add to the total change in the free energy an additional term, namely, $-\int p(\vec{r})\vec{\nabla}\cdot\vec{u}d^3r$. Since the divergence of $\vec{u}$ is zero anyway, this additional term will not have any effect on the total change in the free energy except that it limits the ways $\vec{u}$ is chosen. We shall call the scalar function $p(\vec{r})$ pressure, which plays the role of a Lagrange multiplier and can be

determined from a set of hydrodynamic equations to be derived later in the chapter. With this incompressibility condition in place, the change in free energy finally takes the following form:

$$\delta F = \int \sigma^e_{ik} \partial_i u_k d^3r + \int \partial_\alpha f_g \; u_\alpha d^3r \tag{2.35}$$

where

$$\sigma^e_{ik} = \sigma^d_{ik} - p(\vec{r})\delta_{ik} \tag{2.36}$$

is called the Ericksen stress tensor.

In addition to displacing the centers of mass of the molecules, we shall extend our transformation to include infinitesimal variations in the director field. Furthermore, we shall calculate the total change in the free energy for such a general transformation. In previous cases, we were mainly interested in energies due to the bulk of the sample and, therefore, all surface terms were ingored. These surface terms appeared in the deformation energy and also in the molecular field derived earlier. Here, we are interested in the total change in the free energy; thus, we must be careful not to drop the surface terms. The surface terms once omitted should also be reinstated. Particularly, in what follows, the deformation free energy density f_d will no longer refer to only the Frank deformation energy density; it will also contain the additional surface terms. Now, in the presence of the magnetic, the electric as well as the gravitational fields, the total free energy density is written as $f = f_d + f_M + f_E + f_g$ and the change in the total free energy due to infinitesimal variations in the director is given by

$$\begin{aligned} \delta F &= \int \left\{ \frac{\partial f}{\partial n_\beta} \delta n_\beta + \frac{\partial f}{\partial(\partial_\alpha n_\beta)} \frac{\partial(\delta n_\beta)}{\partial x_\alpha} \right\} d^3r \\ &= \int \left\{ \frac{\partial f_d}{\partial(\partial_\alpha n_\beta)} \partial_\alpha(\delta n_\beta) + \left[\frac{\partial f_d}{\partial n_\beta} - \Delta\chi(\vec{n}\cdot\vec{H})H_\beta \right. \right. \\ &\quad \left. \left. - \Delta\varepsilon(\vec{n}\cdot\vec{E})E_\beta \right] \delta n_\beta \right\} d^3r. \end{aligned} \tag{2.37}$$

The first term on the right can be converted to a surface integrai plus a volume

integral through an integration by parts:

$$\int \frac{\partial f_d}{\partial(\partial_\alpha n_\beta)} \partial_\alpha(\delta n_\beta)\, d^3r = \int \frac{\partial f_d}{\partial(\partial_\alpha n_\beta)} \delta n_\beta\, dS_\alpha - \int \partial_\alpha \left[\frac{\partial f_d}{\partial(\partial_\alpha n_\beta)}\right] \delta n_\beta\, d^3r. \qquad (2.38)$$

Here, to write down the surface integral, we have assumed that the sample is a slab (layer) of nematic liquid crystal. The differential $d\vec{S}$ is a vectorial surface element on the boundary of the sample with an outward-drawn normal. The surface integral above is to be evaluated on the closed boundary of the liquid crystal and therefore represents a surface contribution to the change in the free energy. Clearly, this surface term is equivalent to the amount of work required to change the director on the boundary by an infinitesimal amount. As mentioned previously, this surface term is not to be dropped. Combining equations (2.35) and (2.37), we have, for the total change in free energy as the molecules are displaced and the director varies infinitesimally,

$$\begin{aligned} \delta F &= \int \frac{\partial f_d}{\partial(\partial_\alpha n_\beta)} \delta n_\beta\, dS_\alpha + \int (\sigma^e_{ik}\partial_i u_k + \partial_\alpha f_g\, u_\alpha)\, d^3r \\ &\quad + \int \left\{ \frac{\partial f_d}{\partial n_\beta} - \partial_\alpha \left[\frac{\partial f_d}{\partial(\partial_\alpha n_\beta)}\right] - \triangle\chi(\vec{n}\cdot\vec{H})H_\beta - \triangle\varepsilon(\vec{n}\cdot\vec{E})E_\beta \right\} \delta n_\beta\, d^3r \\ &= \int (\sigma^e_{ik}\partial_i u_k + \partial_\alpha f_g\, u_\alpha - h_\beta \delta n_\beta)\, d^3r + \int \frac{\partial f_d}{\partial(\partial_\alpha n_\beta)} \delta n_\beta\, dS_\alpha \qquad (2.39) \end{aligned}$$

where we have used the definition of the bulk molecular field (2.24). We see that the first volume term represents the amount of work associated with a typical elastic deformation; the second volume term corresponds to the amount of work needed to deform the director in the presence of the gravitational field and, finally, the last volume term expresses the work required to rotate the director against the intermolecular forces, the electric and the magnetic fields. We gain another surface term by integrating the first term on the right in the last equation by parts:

$$\delta F = \int -(u_\alpha J_\alpha + h_\beta \delta n_\beta)\, d^3r + \int \left[\sigma^e_{\beta\alpha} u_\alpha + \frac{\partial f_d}{\partial(\partial_\beta n_\alpha)} \delta n_\alpha\right] dS_\beta \qquad (2.40)$$

where

$$J_\alpha = \partial_\beta \sigma^e_{\beta\alpha} - \partial_\alpha f_g. \qquad (2.41)$$

We can think of this change in the total free energy as the work that is required to cause the infinitesimal variations. Then, in the volume integral on the right, the first term can be regarded as the amount of work per unit volume needed to displace the molecules in the bulk; whereas, the second term corresponds to the amount of work that is necessary to change the director against the molecular field. Similarly, for the surface integral which is to be evalulated on a fixed boundary, the first term can be interpreted as the work put in to move the molecules infinitesimally on the boundary surface and the second term can be looked upon as the work that is needed to change the director on the surface of the sample. Now, returning to the first term in the volume integral, we see that this term must represent an energy (or work). Since u_α is a displacement, J_α must be the force per unit volume in the bulk of the sample. It is then logical to conclude that, at hydrostatic equilibrium in which the fluid particles are not in motion, the bulk force must vanish i.e. $\vec{J} = 0$.

Before closing this section, we must emphasize that the expression for the change in the total free energy (2.40) is valid for incompressible nematics whose director is allowed to vary arbitrarily. This is because the condition for the conservation of the magnitude of the director $\vec{n}^2 = 1$ has not been imposed anywhere in this part of the derivation. However, we must bear in mind that, at equilibrium, the director is everywhere parallel to the bulk molecular field (2.24) only for variations that leave the magnitude of the director at unity. This equilibrium condition can be used wherever possible to reinforce that the magnitude of the director remains invariant.

2.5 Balance of Torques

The deformation energy of a liquid crystal is doubtlessly invariant with respect to a uniform rotation of the sample. After all, simply rotating the observer's point of view could not have altered the equilibrium state of the system in any way. Furthermore, this invariance property leads to a rotational identity which displays the balance

between the body torques and the surface torques at equilibrium. Below, we shall derive this rotational identity and identify various body and surface torques.

A uniform rotation of the liquid crystal sample by an angle ω corresponds exactly to rotations of the centers of mass of the molecules and the director by the same amount. If $\vec{\omega}$ is the angular displacement vector whose direction is along the axis of rotation, then the variations $\vec{u}$ and $\delta\vec{n}$ are respectively written as

$$\vec{u} = \vec{\omega} \times \vec{r} \Longrightarrow u_\alpha = \varepsilon_{\alpha\mu\beta}\omega_\mu r_\beta, \tag{2.42}$$

$$\delta\vec{n} = \vec{\omega} \times \vec{n} \Longrightarrow \delta n_\alpha = \varepsilon_{\gamma\mu\rho}\omega_\mu n_\rho \tag{2.43}$$

where $\varepsilon_{\gamma\mu\rho}$ is the *Levi-Civita* symbol. The changes in the deformation energy have already been worked out previously in Section 2.4. There, we found that the change due to displacements of the centers of mass of the molecules was given by (See Eqn. (2.30))

$$\int \sigma^d_{\beta\alpha}\partial_\beta u_\alpha \, d^3r, \tag{2.44}$$

while the change due to variations of the director, according to Eqn. (2.18) was

$$\int \left\{ \frac{\partial f_d}{\partial(\partial_\alpha n_\beta)}\partial_\alpha(\delta n_\beta) + \frac{\partial f_d}{\partial n_\beta}\delta n_\beta \right\} d^3r. \tag{2.45}$$

Then, the total change in the deformation energy must vanish identically when the centers of mass of the molecules and the director are rotated by the same amount. Substituting the expressions (2.42) and (2.43) into (2.44) and (2.45) respectively, we are led to the following:

$$\begin{aligned} 0 = \delta F_d &= \int \left\{ \sigma^d_{\beta\alpha}\partial_\beta u_\alpha + \frac{\partial f_d}{\partial(\partial_\alpha n_\beta)}\partial_\alpha(\delta n_\beta) + \frac{\partial f_d}{\partial n_\beta}\delta n_\beta \right\} d^3r \\ &= \omega_\mu \int \left\{ \sigma^d_{\beta\alpha}\varepsilon_{\alpha\mu\beta} + \frac{\partial f_d}{\partial(\partial_\alpha n_\beta)}\varepsilon_{\beta\mu\rho}\partial_\alpha n_\rho + \frac{\partial f_d}{\partial n_\beta}\varepsilon_{\beta\mu\rho}n_\rho \right\} d^3r. \end{aligned} \tag{2.46}$$

Clearly, the integral in the last equation must correspond to the net torque on the system. Since the components of the angular displacement vector can be chosen arbitrarily, this net torque must vanish identically. So,

$$\int \left\{ \sigma^d_{\beta\alpha}\varepsilon_{\alpha\mu\beta} + \frac{\partial f_d}{\partial(\partial_\alpha n_\beta)}\varepsilon_{\beta\mu\rho}\partial_\alpha n_\rho + \frac{\partial f_d}{\partial n_\beta}\varepsilon_{\beta\mu\rho}n_\rho \right\} d^3r = 0. \tag{2.47}$$

Although still in its early form, this is the rotational identity we sought. If the nematic sample is placed in uniform magnetic and electric fields, the electromagnetic contributions to the above identity can be brought in through the molecular field as defined in (2.24) as follows

$$\frac{\partial f_d}{\partial n_\beta} = -h_\beta + \frac{\partial}{\partial x_\alpha}\left\{\frac{\partial f_d}{\partial(\partial_\alpha n_\beta)}\right\} + \triangle\chi(\vec{n}\cdot\vec{H})H_\beta + \triangle\varepsilon(\vec{n}\cdot\vec{E})E_\beta. \tag{2.48}$$

This turns the identity (2.47) into

$$\int\Big\{\sigma^d_{\beta\alpha}\varepsilon_{\alpha\mu\beta} - (\vec{n}\times\vec{h})_\mu + \partial_\alpha\left[\frac{\partial f_d}{\partial(\partial_\alpha n_\beta)}\varepsilon_{\beta\mu\rho}n_\rho\right] + \triangle\chi(\vec{n}\cdot\vec{H})(\vec{n}\times\vec{H})_\mu + \triangle\varepsilon(\vec{n}\cdot\vec{E})(\vec{n}\times\vec{E})_\mu\Big\}\,d^3r = 0. \tag{2.49}$$

Recall that $\chi_{ij} = \chi_\perp\delta_{ij} + \triangle\chi n_i n_j$; therefore, the magnetization $\vec{M} = \chi_\perp\vec{H} + \triangle\chi(\vec{n}\cdot\vec{H})\vec{n}$ and the torque that the magnetic field exerts on the bulk of the sample is $\vec{M}\times\vec{H} = \triangle\chi(\vec{n}\cdot\vec{H})(\vec{n}\times\vec{H})$. Similarly, the bulk torque due to the electric field is given by $\vec{P}\times\vec{E} = \vec{D}\times\vec{E} = \triangle\varepsilon(\vec{n}\cdot\vec{E})(\vec{n}\times\vec{E})$. Since the left hand side of equation (2.49) is the sum of torques that act on the system, the term $-(\vec{n}\times\vec{h})$ can be regarded as the torque per unit volume that the molecular field exerts on the director. However, it vanishes identically at equilibrium because the director would be everywhere parallel to the molecular field. Thus, at equilibrium, the rotational identity becomes

$$\int\left[\sigma^d_{\beta\alpha}\varepsilon_{\alpha\mu\beta} + (\vec{M}\times\vec{H})_\mu + (\vec{P}\times\vec{E})_\mu\right]\,d^3r + \int\frac{\partial f_d}{\partial(\partial_\alpha n_\beta)}\varepsilon_{\beta\mu\rho}n_\rho\,dS_\alpha = 0 \tag{2.50}$$

where we have applied Gauss's law to convert the volume integral of the total differential to a surface integral.

Two of the body (bulk) torques have already become apparent in the rotational identity. What remains to be done is to transform the term involving the distortion stress tensor and the surface integral into a more physically interpretable form. To do this, we make use of the condition for hydrostatic equilibrium; namely, the bulk force density $\vec{J}$ must vanish. If this is so, the bulk torque also vanishes

$$0 = \int\vec{r}\times\vec{J}\,d^3r = \int\varepsilon_{\mu\rho\alpha}r_\rho J_\alpha\,d^3r = \int\left(\varepsilon_{\mu\rho\alpha}r_\rho\partial_\beta\sigma^e_{\beta\alpha} - \varepsilon_{\mu\rho\alpha}r_\rho\partial_\alpha f_g\right)\,d^3r \tag{2.51}$$

where we have used the definition (2.41) for the bulk force density $\vec{J}$ in writing the last equation. The last term on the right can be immediately identified with the torque due to the gravitational force, since $-\varepsilon_{\mu\rho\alpha} r_\rho \partial_\alpha f_g = -(\vec{r} \times \vec{\nabla} f_g)_\mu = (\vec{r} \times \vec{F}_g)_\mu = G_\mu$, where $\vec{F}_g$ is the gravitational force density. Then, if we integrate the first term on the right of (2.51) by parts and re-arrange, we get

$$\int \varepsilon_{\mu\beta\alpha} \sigma^e_{\beta\alpha} \, d^3r = \int \varepsilon_{\mu\rho\alpha} r_\rho \sigma^e_{\beta\alpha} \, dS_\beta + \int G_\mu \, d^3r. \tag{2.52}$$

After we insert the definition (2.36) for Ericksen stress tensor into the left hand side of the above equation, we see that the pressure term vanishes identically and we are left with

$$\int \varepsilon_{\mu\beta\alpha} \sigma^d_{\beta\alpha} \, d^3r = \int \varepsilon_{\mu\rho\alpha} r_\rho \sigma^e_{\beta\alpha} \, dS_\beta + \int G_\mu \, d^3r. \tag{2.53}$$

Combining this equation with the rotational identity (2.50), we finally arrive at

$$\int \varepsilon_{\mu\rho\alpha} \left[r_\rho \sigma^e_{\beta\alpha} + \frac{\partial f_d}{\partial(\partial_\beta n_\alpha)} n_\rho \right] dS_\beta + \int \left[(\vec{M} \times \vec{H})_\mu + (\vec{P} \times \vec{E})_\mu + G_\mu \right] d^3r = 0. \tag{2.54}$$

Or, if we denote the sum $\sigma^e_{\beta\alpha} dS_\beta$ by $(d\vec{S}{:}\sigma^e)_\alpha$ and similarly for the other term above, the above identity can be simply written as:

$$\int \vec{r} \times (d\vec{S}{:}\sigma^e) + \int \vec{n} \times (d\vec{S}{:}\Omega) + \int \left[(\vec{M} \times \vec{H})_\mu + (\vec{P} \times \vec{E})_\mu + G_\mu \right] d^3r = 0. \tag{2.55}$$

where $\Omega_{\alpha\beta} = \partial f_d / \partial(\partial_\alpha n_\beta)$. Hence, from this rotational identity, we see that, at hydrostatic equilibrium, the body torques due to the external fields are balanced by the surface torques. Evidently, there are two surface torques: a torque derivable from the second rank tensor Ω is exerted on the director at the boundary surface and another torque due to Ericksen stress tensor is exerted on the centers of mass of the molecules.

2.6 Nematodynamics

Thus far, we have been considering the hydrostatic equilibrium of the nematic liquid crystals. Now, we turn our attention to the nonequilibrium situation. Once the fluid

particles are in motion, the director is no longer coupled internally only to the molecular field, but also to the velocity field of the moving fluid particles. In a more complex situation in which a magnetic or an electric field exists, the director also interacts with this external field. Then, it is not a trivial matter to minimize the corresponding free energy to obtain the equilibrium configuration, when dissipations and so many types of couplings co-exist. It is well known that fluid dynamical systems obey an equation, analogous to the Newton's second law, known as the Navier-Stokes equation [23]. But because of the couplings between the director and the electromagnetic fields, this hydrodynamic equation alone does not suffice. Maxwell's equations must also be added to the system of equations to describe the electromagnetic interactions. The resultant set of equations adequately expresses the interplay among the director field, the internal field (the molecular field) and the external ones (the magnetic and the electric fields). The study of these electro-hydrodynamic phenomena in nematic liquid crystals is commonly known as *nematodynamics*. In this section, we will examine some of the fundamentals in nematodynamics and derive a very important tensor — the total stress tensor — which is a main ingredient in the hydrodynamic equation. Again, our presentation in this section follows closely the approach given by de Gennes [20].

2.6.1 Entropy Production

Non-uniform flows give rise to internal friction which in turn leads to irreversible dissipative losses. As pointed out by de Gennes [20], there are two types of dissipative losses in nematic liquid crystals: losses due to the conventional viscosity effects and losses caused by the rotation of the director with respect to the background fluid. These kinds of losses are represented by a quantity called the entropy production, which amounts to the heat dissipated at the expense of the system's internal energy. Let's consider a system which consists of a nematic liquid crystal maintained at a constant temperature. From the first law of thermodynamics, an increase in the

internal energy is expressed by

$$dE = dQ' - p\,dV. \tag{2.56}$$

Since the volume of the system is unchanged, the increase in the internal energy is exactly the amount of heat absorbed i.e. $dE = dQ'$. In other words, the amount of heat released by the system dQ is equivalent to the decrease in energy: $dQ = -dE \Longrightarrow$ $T\,dS = -dE$ where dS represents the decrease in entropy (assuming the process to be reversible). Then, for isothermal processes, the amount of heat produced per unit time is given by

$$\frac{dQ}{dt} = T\frac{dS}{dt} = T\dot{S} = -\frac{dE}{dt}. \tag{2.57}$$

This is the entropy production we mentioned earlier. We shall assume that all gravitational effects are small enough to be ignored and that a uniform magnetic field is present. Then, the total energy of the system is given by $\int(\rho\vec{v}^2/2 + f_o + f_d + f_M)\,dV$, where the first term represents the kinetic energy of the system, ρ is the mass density and f_o is the internal energy not available for doing work at a constant temperature. Then, the entropy production is simply the negative of the sum of the rates of change of the respective energies.

Since the entropy production represents the dissipative losses of the system, in principle, it can be expressed in terms of the viscous stress tensor. This can be achieved by making use of the hydrodynamic equation:

$$\frac{\partial}{\partial t}(\rho v_i) = -\frac{\partial \Pi_{ik}}{\partial x_k} \tag{2.58}$$

where Π is the momentum flux density tensor which, for a viscous fluid, is defined as $\Pi_{ik} = -\sigma_{ik} + \rho v_i v_k$. The total stress tensor σ is further written in terms of the viscous stress tensor σ' as $\sigma_{ik} = -p\delta_{ik} + \sigma'_{ik}$. With these definitions, it is not difficult to see that, for an incompressible fluid ($\vec{\nabla}\cdot\vec{v} = 0$ and $\rho = \text{const.}$), the hydrodynamic equation can be equivalently written as

$$\frac{d}{dt}(\rho v_i) = \partial_k \sigma_{ki} \tag{2.59}$$

where the derivative on the left is the material derivative $d/dt = \partial/\partial t + (\vec{v} \cdot \vec{\nabla})$ which measures the time rate of change in a frame of reference that travels with the fluid. Having said that, the rate of change of the kinetic energy for an incompressible nematic can be written as follows:

$$\frac{d}{dt}\int \frac{1}{2}\rho\vec{v}^2 \, d^3r = \int v_\alpha \frac{\partial}{\partial t}(\rho v_\alpha) \, d^3r = \int v_\alpha \partial_k \sigma_{k\alpha} \, d^3r - \frac{\rho}{2}\int v_k \partial_k (v_\alpha v_\alpha) \, d^3r \qquad (2.60)$$

where we have made use of equation (2.59). If we integrate the second term by parts, we have

$$\frac{d}{dt}\int \frac{1}{2}\rho\vec{v}^2 \, d^3r = \int v_\alpha \partial_k \sigma_{k\alpha} \, d^3r - \frac{\rho}{2}\int v_k \vec{v}^2 \, dS_k + \frac{\rho}{2}\int (\vec{\nabla} \cdot \vec{v})\vec{v}^2 \, d^3r. \qquad (2.61)$$

The last term on the right vanishes identically because of the incompressibility condition. If we limit ourselves to the entropy productions associated with the bulk of the sample only, then all surface contributions, such as the second term on the right of the above equation, can be dropped. Consequently, after integrating the first term on the right by parts, the entropy production associated with the motion of the fluid in the bulk is given by

$$\frac{d}{dt}\int \frac{1}{2}\rho\vec{v}^2 \, d^3r = -\int \sigma_{k\alpha}\partial_k v_\alpha \, d^3r. \qquad (2.62)$$

The entropy productions associated with the deformation and the magnetic free energies can be dealt with at the same time. We have already shown in Section 2.4 that, for a liquid crystal placed in a magnetic and the gravitational fields, the total change in free energy due to infinitesimal displacements of the centers of mass of the molecules and variations in the director field is given by Eqn. (2.39):

$$\delta F = \int (\sigma^e_{\beta\alpha}\partial_\beta u_\alpha + u_\alpha \partial_\alpha f_g - h_\gamma \delta n_\gamma) \, d^3r + \text{surface term} \qquad (2.63)$$

where $F = F_d + F_M + F_g$. If we ignore the gravitational effect and drop the surface term, we find that the total change in free energy per unit time is simply given by

$$\frac{\delta F}{\delta t} = \int \left[\sigma^e_{\beta\alpha}\partial_\beta\left(\frac{u_\alpha}{\delta t}\right) - h_\gamma \frac{\delta n_\gamma}{\delta t}\right] d^3r. \qquad (2.64)$$

Then, the displacement per unit time $u_\alpha/\delta t$ can be regarded as the velocity of the fluid $\vec{v}$. In the frame of reference that travels along with the fluid, the variations in the director per unit time $\delta n_\gamma/\delta t$ can be interpreted as the material derivative of the director: $\dot{\vec{n}} = d\vec{n}/dt = \partial\vec{n}/\partial t + (\vec{v}\cdot\vec{\nabla})\vec{n}$. Therefore, the dissipative losses associated with the deformation and the magnetic free energies are written jointly as

$$\frac{d}{dt}(F_d + F_M) = \int (\sigma^e_{\beta\alpha}\partial_\beta v_\alpha - h_\gamma \dot{n}_\gamma)\, d^3r. \tag{2.65}$$

Finally, we note that the internal energy density f_o depends only on the mass density ρ at a constant temperature. Since, for an incompressible nematic, the mass density is a constant, the internal energy does not contribute to the total entropy production. Combining equations (2.62) and (2.65), we can express the total entropy production as

$$T\dot{S} = \int \left[(\sigma_{k\alpha} - \sigma^e_{k\alpha})\,\partial_k v_\alpha + \vec{h}\cdot\dot{\vec{n}}\right]\, d^3r. \tag{2.66}$$

Obviously, the terms on the right correspond to dissipative processes. From this point of view, since $\partial_k v_\alpha$ is related to the components of the strain tensor, the quantity

$$\sigma'_{k\alpha} = \sigma_{k\alpha} - \sigma^e_{k\alpha} \tag{2.67}$$

must be the viscous stress tensor.

2.6.2 The Viscous Torque

Since the Ericksen stress tensor is not necessarily symmetric, the viscous stress tensor, in general, is not symmetric either. We shall demonstrate in this section that the antisymmetric part of the viscous stress tensor corresponds to the viscous torque that the director exerts on the fluid flow. In the following discussions, we will be dealing with cases where the body of the fluid is in a non-uniform motion. In other words, viscous forces are present and the systems are not at hydrostatic equilibrium. A further complication may come from the dissipative losses due to the motion of the fluid and of the director at the boundary surface. To simplify our analysis, we

avoid dealing with the latter of these surface losses by assuming a strong anchoring boundary condition so that the director is held fixed at the boundary by the surface effect (by rubbing or treating the limiting walls with appropriate chemicals). To proceed, we examine the net torque $\vec{T}$ exerted on a nematic liquid crystal in the presence of a uniform magnetic field only (gravitational effects are ignored):

$$\begin{aligned} \vec{T} &= \frac{d\vec{L}}{dt} = \frac{d}{dt}\int (\vec{r}\times\rho\vec{v})\, d^3r \\ &= \int (\varepsilon_{ijk} r_j \partial_\alpha \sigma_{\alpha k} - \varepsilon_{ijk}\rho r_j v_\alpha \partial_\alpha v_k)\, d^3r \end{aligned} \tag{2.68}$$

where we have made use of the hydrodynamic equation (2.59). The second term on the right can be integrated by parts to yield a surface term and a volume term:

$$\int \rho\varepsilon_{ijk} r_j v_\alpha v_k\, dS_\alpha - \int \rho\varepsilon_{ijk}\partial_\alpha(r_j v_\alpha) v_k\, d^3r. \tag{2.69}$$

It is not too difficult to show that the integrand of the volume integral can be written as a sum of two terms: one is proportional to $\vec{v}\times\vec{v}$ and the other is proportional to $\vec{\nabla}\cdot\vec{v}$. In view of the incompressibility condition, the contribution of this volume term is clearly zero. The surface integral vanishes for the same reason. Since the integral is to be evaluated at the boundary of the sample, the factor v_α in the integrand is the velocity component on the boundary surface. If the fluid is to be confined within a fixed volume V, then the normal component of $\vec{v}$ must vanish at the surface and, consequently, $\vec{v}$ must be orthogonal to the surface element $d\vec{S}$ everywhere on the boundary surface. If the no-slip (realistic) boundary condition is applied, $\vec{v}$ vanishes on the boundary surfaces. Thus, the surface integral vanishes identically and the net torque is nothing but

$$\vec{T} = \int \varepsilon_{ijk} r_j \partial_\alpha \sigma_{\alpha k}\, d^3r. \tag{2.70}$$

Carrying out this integration by parts, we obtain again a surface term and a volume term:

$$\begin{aligned} \vec{T} &= \int \varepsilon_{ijk} r_j \sigma_{\alpha k}\, dS_\alpha - \int \varepsilon_{ijk}\sigma_{jk}\, d^3r \\ &= \int \left[\vec{r}\times(d\vec{S}\!:\!\sigma)\right]_i - \int \varepsilon_{ijk}(\sigma'_{jk} + \sigma^e_{jk})\, d^3r. \end{aligned} \tag{2.71}$$

If we now define the antisymmetric part of the viscous stress tensor as $\vec{\Gamma}$ such that $\Gamma_i = \varepsilon_{ijk}\sigma'_{kj}$, the net torque can be written as

$$\vec{T} = \int \left[\vec{r} \times (d\vec{S}{:}\sigma)\right]_i + \int \Gamma_i \, d^3r - \int \varepsilon_{ijk}\sigma^e_{jk} \, d^3r. \tag{2.72}$$

We now utilize a rotational identity from Section 2.5. Since this identity was derived by using a symmetry argument on the deformation free energy, it continues to remain valid even when the fluid is no longer at rest. Then, according to Eqn. (2.49), the rotational identity for a non-equilibrium system placed in a uniform magnetic field is given by

$$\int \left[\varepsilon_{\mu\beta\alpha}\sigma^d_{\beta\alpha} - (\vec{n} \times \vec{h})_\mu + (\vec{M} \times \vec{H})_\mu\right] \, d^3r = -\int \left[\vec{n} \times (d\vec{S}{:}\Omega)\right]_\mu \tag{2.73}$$

where we have used Gauss's law to convert the volume integral associated with the tensor Ω to a surface integral. Once again, we note that the sum $\varepsilon_{\mu\beta\alpha}\sigma^d_{\beta\alpha}$ is equivalent to $\varepsilon_{\mu\beta\alpha}\sigma^e_{\beta\alpha}$ since the pressure term $p\varepsilon_{\mu\beta\alpha}\delta_{\beta\alpha}$ vanishes identically. Combining Eqn. (2.73) with Eqn. (2.72), we can rewrite the net torque $\vec{T}$ as

$$\begin{aligned} \vec{T} \;=\; & \int \left[\vec{r} \times (d\vec{S}{:}\sigma)\right]_i + \int \Gamma_i \, d^3r - \int (\vec{n} \times \vec{h})_i \, d^3r \\ & + \int (\vec{M} \times \vec{H})_i \, d^3r + \int \left[\vec{n} \times (d\vec{S}{:}\Omega)\right]_i . \end{aligned} \tag{2.74}$$

There is another way to construct the net torque. Already seen in Section 2.5 is the balance of the surface and the volume torques at hydrostatic equilibrium. Equation (2.55) not only describes this state of affair very clearly, it also indicates what the net torque is made up of — terms at the left hand side of the equation. Thus, following Equation (2.55), we can simply write the net torque at hydrostatic equilibrium as

$$\vec{T} = \int \left[\vec{r} \times (d\vec{S}{:}\sigma^e)\right]_i + \int \left[\vec{n} \times (d\vec{S}{:}\Omega)\right]_i + \int \left[(\vec{M} \times \vec{H})_i + (\vec{P} \times \vec{E})_i + G_i\right] \, d^3r. \tag{2.75}$$

With a minor modification, this expression can be used to describe the net torque even for systems out of equilibrium. The body torques are well accounted for in the above equation even for non-equilibrium cases. However, once the fluid is in non-uniform

motion, viscous forces result and so the Ericksen stress tensor which gives rise to the torque that acts on the molecules at the boundary surface must be replaced by the total stress tensor in order to account for the viscous torque at the boundary. Finally, since the director is strongly anchored at the boundary surface, the expression for the torque that acts on the director at the boundary is left unchanged. Therefore, the net torque for non-equilibrium systems placed in a uniform magnetic field is given by

$$\vec{T} = \int \left[\vec{r} \times (d\vec{S}{:}\sigma)\right]_i + \int \left[\vec{n} \times (d\vec{S}{:}\Omega)\right]_i + \int (\vec{M} \times \vec{H})_i \, d^3r. \tag{2.76}$$

Comparing this equation with (2.74), we see that the antisymmetric part of the viscous stress tensor is equivalent to the viscous torque (per unit volume) that the director exerts on the molecular field (the flow):

$$\vec{\Gamma} = \vec{n} \times \vec{h}. \tag{2.77}$$

Therefore, in view of the equilibrium condition derived earlier, this torque is nonzero only for systems out of equilibrium.

2.6.3 Sources of Dissipation

We are almost in a position to write down the final form of the entropy production and identify the sources of dissipation. To make our final expression easier to interpret, we express the entropy production in terms of the symmetric and the antisymmetric parts of the tensor $\partial_\alpha v_\beta$ given respectively by $A_{\alpha\beta} = (\partial_\alpha v_\beta + \partial_\beta v_\alpha)/2$ and $\omega_{\alpha\beta} = (\partial_\alpha v_\beta - \partial_\beta v_\alpha)/2$. Furthermore, we wish to incorporate the viscous torque derived above into the final expression. Therefore, we also separate the viscous stress tensor σ' into a symmetric part S' and an antisymmetric part $\Gamma_{\alpha\beta} = (\sigma'_{\alpha\beta} - \sigma'_{\beta\alpha})/2$. We now recall from Section 2.6.1 that the entropy production associated with the bulk of the nematic is given in (2.66) as

$$T\dot{S} = \int \left(\sigma'_{\alpha\beta}\partial_\alpha v_\beta + \vec{h} \cdot \dot{\vec{n}}\right) \, d^3r. \tag{2.78}$$

The surface terms can be totally omitted, so long as we assume that the director is strongly anchored and the rigid (no-slip) boundary condition ($\vec{v} = 0$) applies so that there is no dissipation at the surface. Both of these assumptions are quite realistic. Strong anchoring can be guaranteed by proper treatments of the boundary surfaces so that the director is held fixed by the surface effect mentioned earlier. Since the liquid crystal is confined by rigid limiting walls, at the boundary, the normal component of the velocity must vanish. For a viscous fluid, the layer immediately adjacent to the surface of a solid body is brought to rest by means of molecular attraction and "sticks" to the surface; therefore, the tangential component of the velocity must vanish at the boundaries as well. Having justified our assumptions, we now proceed to convert the entropy production to a more physically suggestive form. The first term of the integrand in equation (2.78) can be rewritten as follows:

$$\begin{aligned} {S'}_{\alpha\beta}\partial_\alpha v_\beta &= ({S'}_{\alpha\beta} + \Gamma_{\alpha\beta})(A_{\alpha\beta} + \omega_{\alpha\beta}) \\ &= {S'}_{\alpha\beta}A_{\alpha\beta} + {S'}_{\alpha\beta}\omega_{\alpha\beta} + \Gamma_{\alpha\beta}A_{\alpha\beta} + \Gamma_{\alpha\beta}\omega_{\alpha\beta} \\ &= {S'}_{\alpha\beta}A_{\alpha\beta} + \Gamma_{\alpha\beta}\omega_{\alpha\beta}. \end{aligned} \tag{2.79}$$

Note that terms such as ${S'}_{\alpha\beta}\omega_{\alpha\beta}$ vanish identically due to the antisymmetry of ω. Since the diagonal elements of the antisymmetric tensors are identically zero, the second sum on the right in the above equation is simply reduced to

$$\begin{aligned} \Gamma_{\alpha\beta}\omega_{\alpha\beta} &= 2(\Gamma_{yz}\omega_{yz} + \Gamma_{zz}\omega_{zz} + \Gamma_{xy}\omega_{xy}) \\ &= -\varepsilon_{ijk}{\sigma'}_{kj}\left(\frac{1}{2}\varepsilon_{ilm}\partial_l v_m\right) \\ &= -\vec{\Gamma}\cdot\vec{\omega} \end{aligned} \tag{2.80}$$

where, as demonstrated in Section 2.6.2, $\vec{\Gamma} = \vec{n} \times \vec{h}$ is the viscous torque that the director exerts on the flow and $\vec{\omega} = (\vec{\nabla} \times \vec{v})/2$ is the local angular velocity of the fluid. Using equations (2.79) and (2.80), the entropy production (2.78) can be written as

$$T\dot{S} = \int \left[S' \| A - \vec{\Gamma}\cdot\vec{\omega} + \vec{h}\cdot\dot{\vec{n}}\right] d^3r$$

$$= \int \left[S' \| A - (\vec{n} \times \vec{h}) \cdot \vec{\omega} + \vec{h} \cdot \dot{\vec{n}} \right] \, d^3r$$
$$= \int \left\{ S' \| A + \vec{h} \cdot \left[\dot{\vec{n}} - (\vec{\omega} \times \vec{n}) \right] \right\} \, d^3r \tag{2.81}$$

where $(S' \| A)$ denotes the direct sum $S'_{\alpha\beta} A_{\alpha\beta}$. At this point, we define a vector

$$\vec{N} = \dot{\vec{n}} - (\vec{\omega} \times \vec{n}). \tag{2.82}$$

As we pointed out previously, $\dot{\vec{n}}$ is the total time rate of change of the director in the moving frame of reference that flows with the fluid. On the other hand, since $\vec{\omega}$ is the local angular velocity of the fluid, $\vec{\omega} \times \vec{n}$ is the rate of change of the director due to the local rotation of the fluid. Then, we see that the vector $\vec{N}$ represents the rate of change of the director with respect to the background flow. The entropy production therefore takes the final form:

$$T\dot{S} = \int \left(S' \| A + \vec{h} \cdot \vec{N} \right) \, d^3r. \tag{2.83}$$

The first term on the right involves a symmetric tensor constructed from the velocity gradient, while the second term involves the time rate of change of the director. Therefore, there are two types of dissipation in nematic liquid crystals. One type is associated with the shear motion of the fluid and the other type is due to the rotation of the director.

2.6.4 Constitutive Equations

Having found the sources of dissipation, we follow what is usually done in irreversible thermodynamics and rewrite the entropy production as a sum of products of the generalized thermodynamic fluxes Y_i and the conjugate forces X_i:

$$T\dot{S} = \sum_i X_i Y_i.$$

This procedure can be justified generally. An example of such a procedure is given in the monograph by Kreuzer [24] and so we will not repeat it here. There is a certain

amount of arbitrariness in choosing the generalized forces and fluxes, but the choice is usually guided by the concept of cause and effect as well as by physical interpretations. In view of the entropy production (2.83), we can think of the rotation of the director being caused by the fluid flow represented by the molecular field and the viscous forces being caused by the non-uniform motion of the fluid. Therefore, we can choose to regard the components of the molecular field h_α and those of the symmetric part of the viscous stress tensor ${S'}_{\alpha\beta}$ as generalized forces. Then, the components of $\vec{N}$ and A become the generalized fluxes conjugate to the molecular field and the viscous forces, respectively.

We now postulate a set of constitutive equations which describe the response of the nematic systems to these thermodynamic forces. To do this, we make use of *Truesdell's principle of equipresence*. As quoted in the book by Jaunzemis [25],

> As the last of the general rules, we record Truesdell's principle of equipresence, which states that if an independent variable is present in one constitutive equation, then it should be present in all, unless its presence contradicts other principles or known properties (e.g. material symmetry), or is excluded by some type of linearization.

Then, for sufficiently small deviations from equilibrium, the fluxes are small; therefore, we can assume that the generalized forces are linear functions of the conjugate fluxes. Due to Truesdell's principle of equipresence, we expand the generalized forces as linear combinations of all conjugate fluxes:

$$ {S'}_{\alpha\beta} = L_{\alpha\beta\gamma\delta} A_{\gamma\delta} + M_{\alpha\beta\gamma} N_\gamma, \tag{2.84} $$

$$ h_\gamma = {M'}_{\gamma\alpha\beta} A_{\alpha\beta} + P_{\gamma\delta} N_\delta. \tag{2.85} $$

Or equivalently, if we denote the generalized forces by $Y^i_{\alpha\beta\ldots}$ and the conjugate fluxes by $X^i_{\gamma\delta\ldots}$, then the constitutive equations are simply

$$ Y^i_{\alpha\beta\ldots} = L^{ij}_{(\alpha\beta\ldots)(\gamma\delta\ldots)} X^j_{\gamma\delta\ldots}. $$

According to Onsager's reciprocal relation [26], $L^{ij}_{(\alpha\beta\ldots)(\gamma\delta\ldots)} = L^{ji}_{(\alpha\beta\ldots)(\gamma\delta\ldots)}$. Clearly, in Eqns. (2.84) and (2.85), the coefficient $M_{\alpha\beta\gamma}$ corresponds to $L^{12}_{(\alpha\beta\ldots)(\gamma\delta\ldots)}$ whereas the coefficient $M'_{\alpha\beta\gamma}$ corresponds to $L^{21}_{(\alpha\beta\ldots)(\gamma\delta\ldots)}$. Hence, from Onsager's reciprocal relation,

$$M_{\alpha\beta\gamma} = M'_{\alpha\beta\gamma}. \tag{2.86}$$

In addition, the tensors L, M and P must be compatible with the symmetry requirements of the nematic liquid crystals. They are in fact determined by the properties of the medium in equilibrium, i.e. they must be functions of the components of the director $\vec{n}$. Analogous to the theory of elasticity, due to the existing symmetry, many of their components vanish identically. Since nematic liquid crystals have a local cylindrical symmetry about the director, the above constitutive equations should be invariant with respect to rotations about the nematic axis. Then, in a rotated frame of reference, equations (2.84) and (2.85) are transformed as follows:

$$\bar{S}'_{\alpha\beta} = L_{\alpha\beta\gamma\delta}\bar{A}_{\gamma\delta} + M_{\alpha\beta\gamma}\bar{N}_{\gamma}, \tag{2.87}$$

$$\bar{h}_{\gamma} = M'_{\gamma\alpha\beta}\bar{A}_{\alpha\beta} + P_{\gamma\delta}\bar{N}_{\delta} \tag{2.88}$$

where the barred quantities represent the transformed components. Because the rotation took place about the axis of symmetry, the tensorial coefficients L, M and P are unaffected by the transformation. Tensors with this transformation property are named transverse isotropic tensors [25].

2.6.5 The Viscous Stress Tensor

In this section, we shall determine first the explicit forms of the tensors L, M and P, and then a clear expression for the viscous stress tensor. As we have already pointed out above, the tensors L, M and P are invariant with respect to rotations about the nematic axis; therefore, they are transverse isotropic tensors. Let us first focus on the third-rank tensor M. Following the development outlined in Appendix A, there

exist three independent vectors $\vec{u}$, $\vec{v}$ and $\vec{w}$ such that the scalar polynomial

$$Q = M_{\alpha\beta\gamma} u_\alpha v_\beta w_\gamma \tag{2.89}$$

is form-invariant under rotations about the nematic axis. According to a representation theorm of Cauchy [25], a scalar function of vectors $\vec{v}_1$, $\vec{v}_2$, $\cdots$, $\vec{v}_m$ is isotropic if it depends on the scalar products $\vec{v}_i \cdot \vec{v}_j$ only where i and j may take on any of the values 1, 2, $\cdots$, m. Therefore, we see that the basis of Q must at least consist of the scalar products $\vec{u} \cdot \vec{v}$, $\vec{v} \cdot \vec{w}$ and $\vec{u} \cdot \vec{w}$. In addition, since Q is transverse isotropic (invariant with respect to rotations about the director), it also depends on the rotational invariances $\vec{n} \cdot \vec{u}$, $\vec{n} \cdot \vec{v}$ and $\vec{n} \cdot \vec{w}$. Then, according to Eqn. (A.2), the most general form of Q is a linear combination of the products $(\vec{n} \cdot \vec{u})(\vec{v} \cdot \vec{w})$, $(\vec{n} \cdot \vec{v})(\vec{u} \cdot \vec{w})$, $(\vec{n} \cdot \vec{w})(\vec{u} \cdot \vec{v})$ and $(\vec{n} \cdot \vec{u})(\vec{n} \cdot \vec{v})(\vec{n} \cdot \vec{w})$. In other words,

$$\begin{aligned} Q &= a_1 n_\alpha u_\alpha v_\beta w_\beta + a_2 n_\beta v_\beta u_\alpha w_\alpha + a_3 n_\gamma w_\gamma u_\alpha v_\alpha + a_4 n_\alpha u_\alpha n_\beta v_\beta n_\gamma w_\gamma \\ &= \left(a_1 n_\alpha \delta_{\beta\gamma} + a_2 n_\beta \delta_{\alpha\gamma} + a_3 \delta_{\alpha\beta} n_\gamma + a_4 n_\alpha n_\beta n_\gamma\right) u_\alpha v_\beta w_\gamma \end{aligned} \tag{2.90}$$

where the a_i's are constant coefficients. From Eqn. (A.3), we see that

$$M_{\alpha\beta\gamma} = a_1 n_\alpha \delta_{\beta\gamma} + a_2 n_\beta \delta_{\alpha\gamma} + a_3 \delta_{\alpha\beta} n_\gamma + a_4 n_\alpha n_\beta n_\gamma. \tag{2.91}$$

This third-rank tensor is to appear in the expression (2.84) for the symmetric part of the viscous stress tensor $S'_{\alpha\beta}$; therefore, it must be symmetric with respect to the exchange of its first two indices i.e. $M_{\alpha\beta\gamma} = M_{\beta\alpha\gamma}$. This symmetry requirement leads us to the following expression for M:

$$M_{\alpha\beta\gamma} = a_1(n_\alpha \delta_{\beta\gamma} + n_\beta \delta_{\alpha\gamma}) + (a_3 \delta_{\alpha\beta} + a_4 n_\alpha n_\beta) n_\gamma. \tag{2.92}$$

Similarly, for the second-rank transverse isotropic tensor P, the scalar form-invariant polynomial $W = P_{\gamma\delta} u_\gamma v_\delta$ depends on the invariances $\vec{u} \cdot \vec{v}$, $\vec{n} \cdot \vec{u}$ and $\vec{n} \cdot \vec{v}$. Hence, we may express W as a linear combination of the products $\vec{u} \cdot \vec{v}$ and $(\vec{n} \cdot \vec{u})(\vec{n} \cdot \vec{v})$. Again, using equation (A.3), we can easily show that

$$P_{\gamma\delta} = c_1 \delta_{\gamma\delta} + c_2 n_\gamma n_\delta \tag{2.93}$$

where the c_i's are constants. The method for determining the tensor L is essentially the same although slightly more tedious due to a larger number of basis elements (invariances). We shall not repeat the steps here but simply present the result:

$$\begin{aligned} L_{\alpha\beta\gamma\delta} &= d_1\delta_{\alpha\beta}\delta_{\gamma\delta} + d_2\delta_{\alpha\gamma}\delta_{\beta\delta} + d_3\delta_{\alpha\delta}\delta_{\gamma\beta} + d_4\delta_{\alpha\beta}n_\gamma n_\delta + d_9\delta_{\gamma\delta}n_\alpha n_\beta \\ &\quad + d_5\delta_{\alpha\gamma}n_\beta n_\delta + d_7\delta_{\beta\gamma}n_\alpha n_\delta + d_6\delta_{\alpha\delta}n_\beta n_\gamma + d_8\delta_{\beta\delta}n_\alpha n_\gamma \\ &\quad + d_{10}n_\alpha n_\beta n_\gamma n_\delta \end{aligned} \tag{2.94}$$

where the d_i's are constants. This fourth-rank tensor is necessarily symmetric with respect to interchanging the indices α and β, since it is to be used to construct the symmetric part of the viscous stress tensor S' according to equation (2.84). In addition, we note that the sum $L_{\alpha\beta\gamma\delta}A_{\gamma\delta}$ in equation (2.84) represents a linear combination of all distinct components of A. Since A is symmetric, terms such as $L_{\alpha\beta lm}A_{lm}$ and $L_{\alpha\beta ml}A_{ml}$ are not independent of each other. Therefore, we can choose to define L such that it is also symmetric with respect to the interchange of its last two indices. Altogether, we require $L_{\alpha\beta\gamma\delta} = L_{\beta\alpha\gamma\delta} = L_{\alpha\beta\delta\gamma}$. Exercising these symmetry requirements leads us to the following expression for L:

$$\begin{aligned} L_{\alpha\beta\gamma\delta} &= d_1\delta_{\alpha\beta}\delta_{\gamma\delta} + d_2(\delta_{\alpha\gamma}\delta_{\beta\delta} + \delta_{\alpha\delta}\delta_{\beta\gamma}) + d_4\delta_{\alpha\beta}n_\gamma n_\delta + d_9\delta_{\gamma\delta}n_\alpha n_\beta \\ &\quad + d_5(\delta_{\alpha\gamma}n_\beta n_\delta + \delta_{\beta\gamma}n_\alpha n_\delta + \delta_{\alpha\delta}n_\beta n_\gamma + \delta_{\beta\delta}n_\alpha n_\gamma) \\ &\quad + d_{10}n_\alpha n_\beta n_\gamma n_\delta. \end{aligned} \tag{2.95}$$

An expression for the symmetric part of the viscous stress tensor is now within reach. Inserting equations (2.92) and (2.95) into the constitutive equation (2.84), we get

$$\begin{aligned} S'_{\alpha\beta} &= d_1\delta_{\alpha\beta}A_{\mu\mu} + d_9n_\alpha n_\beta A_{\mu\mu} + d_4\delta_{\alpha\beta}n_\gamma n_\mu A_{\gamma\mu} + \alpha_1 n_\alpha n_\beta n_\mu n_\rho A_{\mu\rho} + \alpha_4 A_{\alpha\beta} \\ &\quad + \frac{1}{2}(\alpha_5 + \alpha_6)(n_\alpha A_{\mu\beta} + n_\beta A_{\mu\alpha})n_\mu + \frac{1}{2}\gamma_2(n_\alpha N_\beta + n_\beta N_\alpha) \\ &\quad + (a_3\delta_{\alpha\beta} + a_4 n_\alpha n_\beta)(\vec{n}\cdot\vec{N}) \end{aligned} \tag{2.96}$$

where we have made use of the symmetric property of the tensor A to simplify the expression and renamed some of the constants for later conveniences. Recall that

$\vec{N}$ is the time rate of change of the director with respect to the background flow. Since the magnitude of the director is held fixed at unity, $\vec{N}$ must be orthogonal to $\vec{n}$ itself and, consequently, the very last term on the right of the above equation must vanish identically. Furthermore, if we reinforce the incompressibility condition $\vec{\nabla} \cdot \vec{v} = 0$, then sums such as $A_{\mu\mu}$ in the above equation must also vanish. Lastly, if we consider the entropy production due to the viscosity effect: $\int S'_{\alpha\beta} A_{\alpha\beta}\, d^3r$, we see that the third term on the right makes no contribution at all to the dissipation because $A_4 \delta_{\alpha\beta} n_\gamma n_\mu A_{\gamma\mu} A_{\alpha\beta} = A_4 n_\gamma n_\mu A_{\gamma\mu} A_{\alpha\alpha} = 0$. Therefore, it can be dropped without loss of generality. To sum up, we thus write S' as

$$\begin{aligned} S'_{\alpha\beta} &= \alpha_1 n_\alpha n_\beta n_\mu n_\rho A_{\mu\rho} + \alpha_4 A_{\alpha\beta} + \frac{1}{2}(\alpha_5 + \alpha_6)(n_\alpha A_{\mu\beta} + n_\beta A_{\mu\alpha}) n_\mu \\ &\quad + \frac{1}{2}\gamma_2 (n_\alpha N_\beta + n_\beta N_\alpha). \end{aligned} \tag{2.97}$$

An expression for the molecular field $\vec{h}$ is obtained by substitution. Inserting equations (2.92) and (2.93) into the second constitutive equation (2.85), we find

$$\begin{aligned} h_\gamma &= \frac{1}{2}\gamma_2 (n_\alpha A_{\alpha\gamma} + n_\beta A_{\gamma\beta}) + a_3 n_\gamma A_{\alpha\alpha} + a_4 (n_\alpha n_\beta A_{\alpha\beta}) n_\gamma \\ &\quad + \gamma_1 N_\gamma + c_2 n_\gamma (\vec{n} \cdot \vec{N}). \end{aligned} \tag{2.98}$$

Again, because $\vec{N}$ is orthogonal to the director, the very last term on the right vanishes identically. If we consider the entropy production due to the rotation of the director: $\int \vec{h} \cdot \vec{N}\, d^3r$, we see immediately that the third term on the right does not contribute since $a_4 (n_\alpha n_\beta A_{\alpha\beta})(\vec{n} \cdot \vec{N}) = 0$ due to the orthogonality of $\vec{n}$ and $\vec{N}$. Therefore, we can omit this term without loss of generality. Finally, the second term on the right is removed by the incompressibility condition. Since the tensor A is symmetric with respect to the interchange of its two indices, the molecular field is simply reduced to

$$h_\gamma = \gamma_2 n_\alpha A_{\alpha\gamma} + \gamma_1 N_\gamma. \tag{2.99}$$

Having derived the symmetric part of the viscous stress tensor, we must combine it with the antisymmetric part to form the total viscous stress tensor. Recall that

we have previously defined this antisymmetric part in two different ways. When deriving the viscous torque in Section 2.6.2, the antisymmetric part was defined as $\Gamma_i = \varepsilon_{ijk}\sigma'_{kj}$ and, in obtaining the final form of the entropy production in Section 2.6.3, it was defined as $\Gamma_{\alpha\beta} = (\sigma'_{\alpha\beta} - \sigma'_{\beta\alpha})/2$. The first definition was introduced to reflect the physical significance of the antisymmetric part of the viscous stress tensor, while the latter was introduced for computational conveniences. These definitions do not lead to any ambiguity and, indeed, they are related to each other in a consistent way: $\Gamma_{\alpha\beta} = -\varepsilon_{\alpha\beta i}\Gamma_i/2$. Also, since $\vec{\Gamma}$ is the viscous torque $\vec{n} \times \vec{h} = \varepsilon_{ijk}n_j h_k$, $\Gamma_{\alpha\beta}$ can be rewritten as $\Gamma_{\alpha\beta} = -(n_\alpha h_\beta - n_\beta h_\alpha)/2$. Then, using equation (2.97) and (2.99), we can write the total viscous stress tensor as

$$\begin{aligned}
\sigma'_{\alpha\beta} &= S'_{\alpha\beta} + \Gamma_{\alpha\beta} \\
&= \alpha_1 n_\alpha n_\beta n_\mu n_\rho A_{\mu\rho} + \alpha_4 A_{\alpha\beta} + \frac{1}{2}(\alpha_5 + \alpha_6 - \gamma_2) n_\alpha n_\mu A_{\mu\beta} \\
&\quad + \frac{1}{2}(\alpha_5 + \alpha_6 + \gamma_2) n_\beta n_\mu A_{\mu\alpha} + \frac{1}{2}(\gamma_2 - \gamma_1) n_\alpha N_\beta \\
&\quad + \frac{1}{2}(\gamma_2 + \gamma_1) n_\beta N_\alpha .
\end{aligned} \tag{2.100}$$

We now define

$$\alpha_2 = \frac{1}{2}(\gamma_2 - \gamma_1) \tag{2.101}$$

and

$$\alpha_3 = \frac{1}{2}(\gamma_2 + \gamma_1) \tag{2.102}$$

or, inversely, $\gamma_1 = \alpha_3 - \alpha_2$ and $\gamma_2 = \alpha_3 + \alpha_2$. Furthermore, it has been shown by Leslie [27] that $\gamma_2 = \alpha_6 - \alpha_5$. This leads to the relation

$$\alpha_3 + \alpha_2 = \gamma_2 = \alpha_6 - \alpha_5 \tag{2.103}$$

known as the Parodi relation [28]. As a result, the total viscous stress tensor is finally written as

$$\begin{aligned}
\sigma'_{\alpha\beta} &= \alpha_1 n_\alpha n_\beta n_\mu n_\rho A_{\mu\rho} + \alpha_4 A_{\alpha\beta} + \alpha_5 n_\alpha n_\mu A_{\mu\beta} + \alpha_6 n_\beta n_\mu A_{\mu\alpha} \\
&\quad + \alpha_2 n_\alpha N_\beta + \alpha_3 n_\beta N_\alpha
\end{aligned} \tag{2.104}$$

where the viscosity coefficients $\alpha's$ are commonly referred to as the Leslie coefficients. Not all of these coefficients are independent; four of them are connected by the Parodi relation (2.103). Hence, for an incompressible nematic liquid crystal, there are altogether five independent viscosity coefficients.

In hydrodynamical calculations, the equation of motion is written in terms of the total stress tensor σ. For completeness, it is therefore important to recapitulate what the total stress tensor is composed of. Restating equation (2.67),

$$\sigma_{\alpha\beta} = \sigma'_{\alpha\beta} + \sigma^e_{\alpha\beta} = \sigma'_{\alpha\beta} + \sigma^d_{\alpha\beta} - p\delta_{\alpha\beta}. \tag{2.105}$$

We see that the total stress tensor consists of an irreversible part due to viscous forces and a reversible part due to the elasticity of the liquid crystal.

2.7 Electro-hydrodynamic Instabilities

Under proper experimental conditions, a thin layer (typically 50 μm thick with the lateral dimensions of 2 $\times$ 3 cm) of a nematic liquid crystal can be excited by an *a.c.* electric field, at appropriate frequency values, to produce a sequence of convective patterns similar to those observed in the Rayleigh-Bénard convection of the isotropic fluids [29]. This transition sequence includes the familiar **normal rolls**, the **oblique rolls**, the **skewed varicose** and the **bimodal** patterns [16]. In this section, we examine these experimental conditions and present a proposed scenario which explains why the initial configuration becomes unstable. Finally, we present the governing equations of motion, which form the basis for our subsequent analysis.

2.7.1 Helfrich Instability

We consider a thin layer of nematic liquid crystal with a positive conductive anisotropy ($\triangle\sigma = \sigma_\parallel - \sigma_\perp > 0$) but a negative dielectric anisotropy ($\triangle\epsilon = \epsilon_\parallel - \epsilon_\perp < 0$). The latter anisotropy implies that the molecules prefer to align orthogonal to the external

electric field. The liquid crystal is to be sandwiched between two parallel glass plates. The upper and the lower limiting plates are specially treated so that the molecules align parallel to the plates uniformly in the undistorted configuration. We shall label this direction x and the vertical direction z. The plates are also coated with a thin layer of transparent but conductive material to provide visual inspection as well as a uniform electric field in the vertical direction. To avoid dealing with charge injection [20] (due to complex chemical reactions at the electrodes) at the electrodes, a low frequency electric field $\vec{E} = E_o \cos(\omega t)\ \vec{k}$ is used so that the switching electric field does not allow enough time for the chemical reactions to take place. A schematic diagram of the nematic cell is shown in Fig. 2.2.

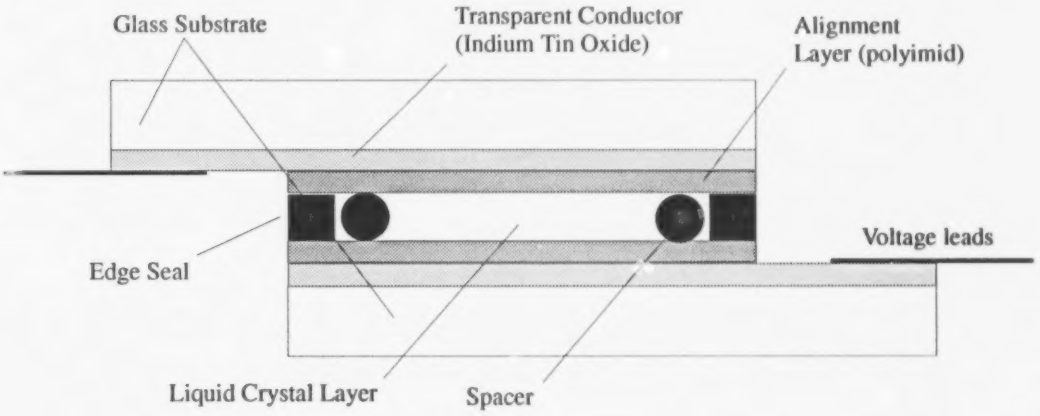

Figure 2.2: A schematic diagram of a nematic cell.

Since nematic liquid crystals are capable of transmitting torques, it appears that a logical starting point for our investigation would be to examine the different types of torques that are exerted on the director when the system slightly deviates from the undistorted configuration. Suppose that an infinitesimal periodic perturbation along the x-direction is present in the director field. First, there is a restoring torque on the director due to the increase in the deformation free energy. Secondly, there is a dielectric torque due to the external electric field. Although this electric field

is oscillatory, it effectively exerts a torque on the molecules so as to align them orthogonal to the field. So, this torque too is a restoring torque.

Now, the periodic perturbation in the director means that the director is slightly "bent" locally away from the x-axis i.e. $\vec{n} = (n_x, 0, n_z)$. Due to the anisotropy of the conductivity tensor ($J_i = \sigma_{ij} E_j$), the external electric field along z drives a current with a non-zero x-component. Because the deviation of the director away from the x-axis is periodic in x, this current has different orientations in different regions of the sample. Since the sample is electrically neutral to begin with, this current implies a local charge separation and charge accumulation (periodic in x) occurs producing a secondary electric field. While the vertical component of this secondary field is stabilizing, its horizontal component tries to align the director along the z-axis, resulting in a driving torque exerted on the director. At the same time, the accumulated charges are pulled by the external electric field and this gives rise to a convective flow which exerts a viscous torque on the director driving it away from the x-axis. Hence, this is also a driving torque. This situation is depicted in Fig. 2.3.

In summary, the director experiences three kinds of torques: the elastic, the dielectric and the viscous torques denoted respectively by τ_d, τ_E and τ_v. Using the linear approximation and the orders of magnitude of the physical parameters for a typical nematic liquid crystal, one can show that these torques are on the order of $\epsilon^{1/2}$ where ϵ is the reduced voltage $(V^2 - V_c^2)/V_c^2$ and V_c is a transition voltage. The system's configuration is then dictated by the competition among these torques. If the restoring torques dominate, then the parallel alignment is energetically favorable. On the other hand, if the restoring torques are balanced by the driving torques due to an increase in the applied electric field, then the parallel alignment becomes unstable and the system will bifurcate into a new configuration with a finite periodicity in the x-direction. The above scenario was originally due to Helfrich and Carr [3, 30] . The instability is therefore commonly referred to as the *Helfrich-Carr instability.*

As described above, there are two easily accessible control parameters (V and

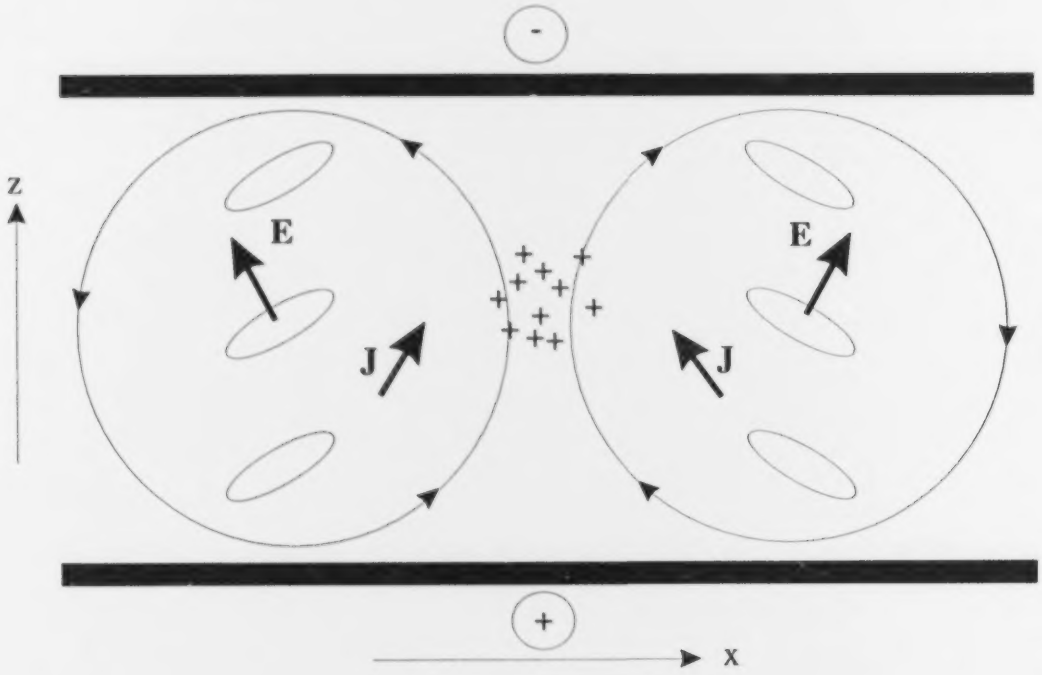

Figure 2.3: Helfrich-Carr effect for a nematic liquid crystal with negative dielectric anisotropy and positive conductance anisotropy.

ω) in a typical electro-convection experiment involving nematic liquid crystals. The stability diagram for various convective patterns is therefore constructed in the V-ω parameter plane. A cut-off (or critical) angular frequency ω_c divides the stability diagram into two regimes. For all angular frequencies $\omega < \omega_c$, the periodic pattern corresponds to a static distortion in the director and oscillating charges. This regime is called the conduction regime. Once the angular frequency exceeds the cut-off point ($\omega > \omega_c$), the charges can no longer follow the excitation; the charges become static whereas the alignment pattern becomes oscillatory. This regime is called the dielectric regime.

2.7.2 Equations of Motion

Helfrich and Carr's interpretation of the electro-hydrodynamic instabilities has gained wide acceptance over the years. It has been used in linear theories to calculate the critical voltages for transitions from the rest state to the normal rolls as well as from the rest state to the oblique rolls at low frequencies; the results obtained so far agree with the experimental observations reasonably well. In view of these successes, Helfrich's scenario will form the backbone of our analysis. We list below the governing equations of motion for a typical electro-convective experiment.

Let us consider the identical setup as described in the previous subsection. In addition, we shall assume that the nematic is incompressible i.e.

$$\vec{\nabla} \cdot \vec{v} = 0. \tag{2.106}$$

As we have pointed out earlier, not only is the director coupled to the velocity field, because each molecule carries an electric dipole, it also interacts with the external electric field. Furthermore, the impurity ions immersed in the liquid crystal will also respond to the field and be ultimately responsible for sustaining the fluid flow. Therefore, the hydrodynamic equation alone does not suffice to determine the stable configuration of the system; it must be supplemented by Maxwell's equations. In the

absence of a magnetic field, the required Maxwell equations in MKSA (SI) units are:

$$\vec{\nabla} \cdot \vec{D} = q, \tag{2.107}$$

$$\vec{J} + \frac{\partial \vec{D}}{\partial t} = 0, \tag{2.108}$$

$$\vec{\nabla} \times \vec{E} = 0. \tag{2.109}$$

If we take the divergence on both sides of Ampére's law and combine it with Gauss's law, we obtain the equation for the conservation of charge:

$$\vec{\nabla} \cdot \vec{J} + \frac{\partial q}{\partial t} = 0. \tag{2.110}$$

Because the impurity ions are dragged by the external field, there is now an additional body force in the hydrodynamic equation:

$$\rho \frac{dv_\beta}{dt} = \partial_\alpha \sigma_{\alpha\beta} + qE_\beta \tag{2.111}$$

where the derivative dv_β/dt on the left is the material derivative $\partial/\partial t + (\vec{v} \cdot \vec{\nabla})$ and σ is the stress tensor derived previously. Finally, based on Helfrich-Carr scenario, the sum of torques should be zero for a stable stationary state such as the convective straight rolls in which the director and the velocity are time independent. Hence, we have the following torque-balance equation:

$$\tau_d + \tau_E + \tau_v = 0. \tag{2.112}$$

Equations (2.106), (2.107), (2.109), (2.110), (2.111) and (2.112) constitute a set of fundamental equations. Together with the rigid boundary conditions:

$$\vec{v}(z = \pm d/2) = 0 \tag{2.113}$$

$$E_{(x,y)}(z = \pm d/2) = 0 \tag{2.114}$$

$$\delta\vec{n}(z = \pm d/2) = 0, \tag{2.115}$$

where we have placed the origin of our coordinate system in the center of the nematic cell and d is the thickness of the layer, they completely specify the nematic

system. These equations are in principle solvable; however, the presence of nonlinearities makes them impossible to be handled exactly. Thus, approximation must be employed. These equations have been linearized and the solutions have been obtained in the past [3, 4, 5, 6]. In the chapters that follow, we will provide two different ways to incorporate nonlinearities into the model.

Chapter 3

Direct Bifurcation in Nematic Liquid Crystals

Under the experimental conditions we prescribed in the last chapter, at sufficiently high field frequencies, the nematic layer is transformed into a set of normal rolls at the first transition voltage. Normal rolls are convective rolls. Due to the coupling between the molecules and various other fields as described in the Helfrich-Carr scenario, the director of the normal rolls is sinusoidally modulated only in the direction of the previously preferable axis (the x-axis) and remains parallel to the vertical (xOz) plane. Since nematic liquid crystals are birefringent, when placed between a pair of crossed polarizers, the liquid crystal appears as a set of straight parallel rolls orthogonal to the x-axis. In an experiment performed by Rasenat et al. [17], the normal rolls exhibited a power-law behavior as the applied voltage continued to increase beyond the onset. These authors showed that the modulational amplitude of the director θ_o increased as a square root of the reduced voltage $\epsilon = (V^2 - V_c^2)/V_c^2$ where V and V_c are the applied rms voltage and the rms threshold voltage of the transition, respectively. This phenomenon is reminiscent of a direct bifurcation, in which case, the amplitude θ_o could be taken as an order parameter. So far, this critical behavior has eluded all theoretical attempts. Although the application of the multi-scale technique in this

regime will certainly lead to interesting results as we will demonstrate in the next chapter, the leading order in the ϵ-expansion of the solutions:

$$u(x,y,z,t) = \epsilon^{1/2}\left(u_o + \epsilon^{1/2}u_1 + \epsilon u_2 + \ldots\right) \tag{3.1}$$

is a priori chosen so as to achieve detailed balance (balance the linear growth rate by a nonlinearity satisfying the symmetry requirements of the system) in the final equation of state. The correct critical behavior is therefore not a direct consequence of the proposed model. In this chapter, we examine this critical behavior by proposing a phenomenological free energy for the nematic system. We regard the amplitude θ_o as an infinitesimal order parameter and expand the unknown field variables in powers of θ_o. After solving for the linear solutions and their first nonlinear corrections, we proceed to construct the free energy and finally obtain a set of bifurcation diagrams for a continuous transition by means of minimization.

3.1 The Director and The Electric Fields

The geometry we adopt here is exactly the same as described in the previous chapter. Since, according to experimental observations, the convective pattern has no apparent variation in the y-direction and the director and the velocity remain parallel to the xOz plane, we can legitimately consider the bifurcation as a two-dimensional problem and regard all remaining field components independent of y. Then, the director can be parameterized by the tilt angle θ measured with respect to the x-axis i.e. $\vec{n} = (n_x, 0, n_z) = (\cos\theta, 0, \sin\theta)$. If we are not far beyond the threshold, the perturbations to the uniform state remain infinitesimally small, we can expand n_x and n_y in powers of θ. But we will have to be cautious to keep terms up to the second-order. Similarly, the velocity field has only two non-vanishing components: $\vec{v} = (v_x, 0, v_z)$. For the electric field, because there is an internal field due to the charge separation, we write the total electric field as $\vec{E} = (E_x, 0, E_z = E'_z + E_a)$ where $E_a = E_o\cos(\omega t)$ is the applied electric field.

To use the conservation of charge equation (2.110), we must first determine the charge density q and the current density $\vec{J}$. We do this by making use of the constitutive equations $D_i = \varepsilon_{ij}E_j$ and $J_i = \sigma_{ij}E_j$ for anisotropic materials and Gauss's law. Note that we have omitted the convective term $q\vec{v}$ in the current density $\vec{J}$ for simplicity. This term however has been considered in [6]. Knowing from the previous chapter that the dielectric tensor is $\varepsilon = \varepsilon_\perp \delta_{ij} + \Delta\varepsilon n_i n_j$, we can write the displacement field as follows:

$$\begin{aligned} D_x &= (\varepsilon_\perp + \Delta\varepsilon n_x^2)E_x + \Delta\varepsilon n_x n_z E_z, \\ D_y &= 0, \\ D_z &= \Delta\varepsilon n_x n_z E_x + (\varepsilon_\perp + \Delta\varepsilon n_z^2)E_z. \end{aligned} \tag{3.2}$$

Because the conductivity tensor takes on the same form as the dielectric tensor, the current density $\vec{J}$ is expressed similarly as

$$\begin{aligned} J_x &= (\sigma_\perp + \Delta\sigma n_x^2)E_x + \Delta\sigma n_x n_z E_z, \\ J_y &= 0, \\ J_z &= \Delta\sigma n_x n_z E_x + (\sigma_\perp + \Delta\sigma n_z^2)E_z. \end{aligned} \tag{3.3}$$

It is now necessary to expand each component of the director in powers of the tilt angle θ. Since we intend to incorporate the first nonlinear corrections into our calculation, we are careful to keep terms up to the second-order. This transforms the above displacement field to

$$\begin{aligned} D_x &= \varepsilon_\parallel E_x + \Delta\varepsilon\theta E_z, \\ D_y &= 0, \\ D_z &= \Delta\varepsilon\theta E_x + (\varepsilon_\perp + \Delta\varepsilon\theta^2)E_z. \end{aligned} \tag{3.4}$$

The same procedure transforms the components of $\vec{J}$ to the similar expressions. This is quite straightforward and so we will not display these expressions here. Using

Gauss's law, the charge density q can be written as

$$\begin{aligned} q &= \varepsilon_{\parallel}\frac{\partial E_x}{\partial x} + \Delta\varepsilon\theta\frac{\partial E'_z}{\partial x} + \Delta\varepsilon\frac{\partial\theta}{\partial x}(E_a + E'_z) + \Delta\varepsilon\theta\frac{\partial E_x}{\partial z} \\ &\quad + \Delta\varepsilon\frac{\partial\theta}{\partial z}E_x + \varepsilon_{\perp}\frac{\partial E'_z}{\partial z} + 2\Delta\varepsilon\theta\frac{\partial\theta}{\partial z}E_a. \end{aligned} \tag{3.5}$$

Substituting the above expression for q and the expansions for the components of $\vec{J}$ in equation (2.110), we find

$$\begin{aligned} &\sigma_{\parallel}\frac{\partial E_x}{\partial x} + \Delta\sigma\theta\frac{\partial E'_z}{\partial x} + \Delta\sigma\frac{\partial\theta}{\partial x}(E_a + E'_z) + \Delta\sigma\theta\frac{\partial E_x}{\partial z} + \Delta\sigma\frac{\partial\theta}{\partial z}E_x \\ &+ \sigma_{\perp}\frac{\partial E'_z}{\partial z} + 2\Delta\sigma\theta\frac{\partial\theta}{\partial z}E_a + \varepsilon_{\parallel}\frac{\partial^2 E_x}{\partial x\partial t} + \Delta\varepsilon\theta\frac{\partial^2 E'_z}{\partial x\partial t} + \Delta\varepsilon\frac{\partial\theta}{\partial x}(\frac{\partial E_a}{\partial t} + \frac{\partial E'_z}{\partial t}) \\ &+ \Delta\varepsilon\theta\frac{\partial^2 E_x}{\partial z\partial t} + \Delta\varepsilon\frac{\partial\theta}{\partial z}\frac{\partial E_x}{\partial t} + \varepsilon_{\perp}\frac{\partial^2 E'_z}{\partial z\partial t} + 2\Delta\varepsilon\theta\frac{\partial\theta}{\partial z}\frac{\partial E_a}{\partial t} = 0. \end{aligned} \tag{3.6}$$

We can see intuitively that the hydrodynamic equations and the torque-balance equation will also contain second-order nonlinear terms. The presence of these nonlinearities makes it very difficult to solve this set of equations exactly, if not impossible. Therefore, we shall not proceed exactly but resort to a technique involving perturbative expansions.

Since we are only interested in the immediate neighborhood of the critical point, the scale on which the bifurcation takes place is infinitesimally small. This scale is presumbly on the order of θ_o (the modulational amplitude of the director in the linear limit). Hence, we can employ a technique similar to the method of multiple-scale expansion commonly used in hydrodynamic calculations. We expand each observable quantity in powers of θ_o. Then, by substitution, each fundamental equation can be broken down into sub-equations, each associated with a different order of θ_o. Subsequently, by solving these sets of simultaneous equations in a consecutive way, we will be able to obtain the linear solutions and their nonlinear corrections. Therefore, we formally expand the tilt angle, the velocity, the electric field and the pressure as

$$\begin{aligned} \theta &= u_1\theta_o + u_2\theta_o^2 + \cdots, \\ E_x &= E_{x1}\theta_o + E_{x2}\theta_o^2 + \cdots, \end{aligned}$$

$$\begin{aligned} E'_z &= E_{z1}\theta_o + E_{z2}\theta_o^2 + \cdots, \\ v_x &= v_{x1}\theta_o + v_{x2}\theta_o^2 + \cdots, \\ v_z &= v_{z1}\theta_o + v_{z2}\theta_o^2 + \cdots, \\ p &= p_o + p_1\theta_o + p_2\theta_o^2 + \cdots \end{aligned} \tag{3.7}$$

where the coefficients of various orders of θ_o are all functions of x and z and probably t. Below the bifurcation point, the pressure $p = p_o$. Hence, p_o is the hydrostatic pressure. For a thin layer of liquid crystal, we can regard p_o as constant without any loss of generality. Also, according to Faraday's law and the incompressibility condition, that

$$\frac{\partial E_{xi}}{\partial z} = \frac{\partial E_{zi}}{\partial x} \tag{3.8}$$

and

$$\frac{\partial v_{xi}}{\partial x} = -\frac{\partial v_{zi}}{\partial z} \tag{3.9}$$

for $i = 1, 2, \cdots$. If we now substitute the expansions for θ, E_x and E'_z as in (3.7) into equation (3.6) and collect like order terms, then the first- and the second-order terms must vanish independently. This leads us to the first- and the second-order equations written respectively as

$$\begin{aligned} &\triangle\sigma\, E_o \cos(\omega t)\frac{\partial u_1}{\partial x} - \triangle\varepsilon\, E_o\omega \sin(\omega t)\frac{\partial u_1}{\partial x} + \sigma_\perp \frac{\partial E_{z1}}{\partial z} + \varepsilon_\perp \frac{\partial^2 E_{z1}}{\partial z \partial t} \\ &+ \sigma_\parallel \frac{\partial E_{x1}}{\partial x} + \varepsilon_\parallel \frac{\partial^2 E_{x1}}{\partial x \partial t} = 0 \end{aligned} \tag{3.10}$$

where ω (rad/sec) is the angular frequency of the electric field, and

$$\begin{aligned} &\triangle\sigma\, E_{x1}\frac{\partial u_1}{\partial z} + 2\triangle\sigma\, E_o \cos(\omega t)\, u_1 \frac{\partial u_1}{\partial z} - 2\triangle\varepsilon\, E_o\omega \sin(\omega t)\, u_1 \frac{\partial u_1}{\partial z} \\ &+ \triangle\sigma\, E_{z1}\frac{\partial u_1}{\partial x} + \triangle\sigma\, E_o \cos(\omega t)\frac{\partial u_2}{\partial x} - \triangle\varepsilon\, E_o\omega \sin(\omega t)\frac{\partial u_2}{\partial x} \\ &+ \triangle\varepsilon \frac{\partial u_1}{\partial z}\frac{\partial E_{x1}}{\partial t} + \triangle\varepsilon \frac{\partial u_1}{\partial x}\frac{\partial E_{z1}}{\partial t} + \triangle\sigma\, u_1 \frac{\partial E_{x1}}{\partial z} + \sigma_\perp \frac{\partial E_{z2}}{\partial z} \\ &+ \triangle\varepsilon\, u_1 \frac{\partial^2 E_{x1}}{\partial z \partial t} + \varepsilon_\perp \frac{\partial^2 E_{z2}}{\partial z \partial t} + \sigma_\parallel \frac{\partial E_{x2}}{\partial x} + \triangle\sigma\, u_1 \frac{\partial E_{z1}}{\partial x} + \varepsilon_\parallel \frac{\partial^2 E_{x2}}{\partial x \partial t} \\ &+ \triangle\varepsilon\, u_1 \frac{\partial^2 E_{z1}}{\partial x \partial t} = 0. \end{aligned} \tag{3.11}$$

Although we have not obtained the remaining first- and second-order equations, it seems appropriate that we pause to examine the boundary conditions for this nematic system before we proceed any further with the above two equations. The upper and the lower plates of the nematic cell are coated with a thin layer of transparent and conductive material to provide a uniform external field. So, we can regard these plates as perfect conductors and hence the tangential component of the electric field at the boundary must vanish identically. If we assume that the thickness of the cell is d and we place the origin of our coordinate system in the center of the cell, then

$$E_x(z = \pm d/2) = 0. \tag{3.12}$$

Since these plates have been specially treated (coated with a polyimid rubbed in one direction for example) to produce the desirable surface effect, for strong anchoring, the z-component of the director must be zero at the boundary:

$$\theta(z = \pm d/2) = 0. \tag{3.13}$$

For the velocity field, the "no slip" condition and the rigid limiting walls imply that the fluid velocity must be zero at the boundary:

$$\vec{v}(z = \pm d/2) = 0. \tag{3.14}$$

According to our previous discussions, if the director is strongly anchored and the fluid is motionless at the boundaries, then there is no dissipation at the surfaces. Thus, this set of rigid boundary conditions makes certain that the surface contributions do not enter into our calculations. Therefore, we shall disregard all surface terms in the rest of our analysis. Returning to the first- and the second-order equations we have just derived, we see that the first-order equation consists of only the first-order coefficients introduced in equations (3.7) whereas the second-order equation consists of coefficients up to the second-order. This is actually very typical of the ϵ-expansions: the n-th order equations generally contain coefficients up to the n-order. Therefore, these equations must be solved in a consecutive manner. It is now well known that

analytic solutions to the set of first-order equations do not exist if the above fully rigid boundary conditions are to be insisted upon. However, if one of the conditions is relaxed, allowing the tangential velocity at the boundary to be small but non-zero, then the linear solutions can indeed be written down in analytical form. For these semi-rigid boundary conditions, the linear solutions have been found to be expressed in terms of the lowest-order harmonics [5, 6, 2]:

$$u_1 = \sin(px)\cos(qz), \tag{3.15}$$

$$E_{x1} = \bar{E}_{x1}(t)\sin(px)\cos(qz), \tag{3.16}$$

$$E_{z1} = r\bar{E}_{x1}(t)\cos(px)\sin(qz), \tag{3.17}$$

$$v_{x1} = \bar{v}_{x1}\sin(px)\sin(qz), \tag{3.18}$$

$$v_{z1} = \frac{1}{r}\bar{v}_{x1}\cos(px)\cos(qz) \tag{3.19}$$

where $r = q/p$, $p = 2\pi/\lambda$ and $q = \pi/d$. To be consistent with the periodicity of the normal rolls, $\lambda/2$ is the width of the rolls so that r represents the normalized domain spacing and is approximately 1 for the observed stationary straight rolls. It is easy to check that these linear solutions satisfy Faraday's law (3.8) and the incompressibility condition (3.9) automatically.

Equation (3.10) can be used immediately to determine the time dependent amplitude $\bar{E}_{x1}(t)$. Substituting equation (3.15) to (3.17) into (3.10), we get

$$\bar{E}_{x1}(t) = -\frac{E_o}{g}[a\omega\sin(\omega t) + b\cos(\omega t)] \tag{3.20}$$

where

$$a = \triangle\sigma\tau - \triangle\varepsilon, \tag{3.21}$$

$$b = \triangle\varepsilon\tau\omega^2 + \triangle\sigma, \tag{3.22}$$

$$g = (\sigma_\parallel + \sigma_\perp r^2)(\tau^2\omega^2 + 1), \tag{3.23}$$

$$\tau = (\varepsilon_\parallel + \varepsilon_\perp r^2)/(\sigma_\parallel + \sigma_\perp r^2). \tag{3.24}$$

Having determined the first-order coefficients for the tilt angle and the components of the electric field, we can subsequently substitute them in the second-order equation

(3.11) to obtain an equation only for the second-order coefficients. Although the algebra is more tedious, it can be shown that, after substitution, the second-order equation takes on the following form:

$$\begin{aligned}
&\frac{qE_o}{2g}[A_1\omega\sin(\omega t)A_2\cos(\omega t)][\sin(2qz)-2\cos(2px)\sin(2qz)] \\
&+E_o[\Delta\sigma\cos(\omega t)-\Delta\varepsilon\omega\sin(\omega t)][\frac{\partial u_2}{\partial x}-\frac{q}{2}\cos(2px)\sin(2qz)] \\
&+\sigma_\perp\frac{\partial E_{z2}}{\partial z}+\varepsilon_\perp\frac{\partial^2 E_{z2}}{\partial z\partial t}+\sigma_\parallel\frac{\partial E_{x2}}{\partial x}+\varepsilon_\parallel\frac{\partial^2 E_{x2}}{\partial x\partial t}=0
\end{aligned} \tag{3.25}$$

with

$$A_1 = \Delta\sigma a+\Delta\varepsilon(g-b), \tag{3.26}$$

$$A_2 = \Delta\sigma(b-g)+\Delta\varepsilon a\omega^2. \tag{3.27}$$

The spatially dependent parts of the coefficients must be made up of the second-harmonics in x and z. Knowing that, in the conduction regime, the director is static in time, we can assume that

$$u_2=\frac{q}{4p}\sin(2px)\sin(2qz). \tag{3.28}$$

This kills the second term on the left of Equation (3.25) and we are left with an equation that connects only the field components E_{x2} and E_{z2}. However, this equation can be written in terms of E_{x2} alone, if we differentiate it with respect to x and then use Faraday's law (3.8). This results in the equation

$$\begin{aligned}
&\frac{2qpE_o}{g}[A_1\omega\sin(\omega t)+A_2\cos(\omega t)]\sin(2px)\sin(2qz) \\
&\quad+\sigma_\perp\frac{\partial^2 E_{x2}}{\partial z^2}+\varepsilon_\perp\frac{\partial^3 E_{x2}}{\partial^2 z\partial t}+\sigma_\parallel\frac{\partial^2 E_{x2}}{\partial x^2}+\varepsilon_\parallel\frac{\partial^3 E_{x2}}{\partial^2 x\partial t} = 0.
\end{aligned} \tag{3.29}$$

The spatial part of E_{x2} is now obvious, so we write

$$E_{x2}=\bar{E}_{x2}(t)\sin(2px)\sin(2qz) \tag{3.30}$$

and, by substitution, the time dependent amplitude is found to be

$$\bar{E}_{x2}(t)=A\sin(\omega t)+B\cos(\omega t) \tag{3.31}$$

where

$$A = \frac{qpE_o\omega}{2g}\left[\frac{A_1(\sigma_\perp q^2+\sigma_\parallel p^2)+A_2(\varepsilon_\perp q^2+\varepsilon_\parallel p^2)}{(\sigma_\perp q^2+\sigma_\parallel p^2)^2+\omega^2(\varepsilon_\perp q^2+\varepsilon_\parallel p^2)^2}\right], \tag{3.32}$$

$$B = \frac{qpE_o}{2g}\left[\frac{A_2(\sigma_\perp q^2+\sigma_\parallel p^2)-A_1\omega^2(\varepsilon_\perp q^2+\varepsilon_\parallel p^2)}{(\sigma_\perp q^2+\sigma_\parallel p^2)^2+\omega^2(\varepsilon_\perp q^2+\varepsilon_\parallel p^2)^2}\right]. \tag{3.33}$$

The field component E_{z2} can be recovered by using Faraday's law (3.8) once again. Accordingly, by means of integration, this second-order z-component can be written as

$$E_{z2} = -\frac{q}{p}\bar{E}_{x2}(t)\cos(2px)\cos(2qz)+h(z,t) \tag{3.34}$$

where the function $h(z,t)$ has appeared as a result of the integration. The function $h(z,t)$ can be determined by using the second-order equation (3.25). Therefore, if we substitute the solutions (3.28), (3.30) and (3.34) in (3.25) and simplify, we obtain an equation for $h(z,t)$:

$$\frac{E_oq}{2g}\left[A_1\omega\sin(\omega t)+A_2\cos(\omega t)\right]\sin(2qz)+\varepsilon_\perp\frac{\partial^2 h}{\partial z\partial t}+\sigma_\perp\frac{\partial h}{\partial z}=0. \tag{3.35}$$

The spatial part of h can only be $\cos(2qz)$. If we write

$$h(z,t)=\bar{E}_{z2}(t)\cos(2qz), \tag{3.36}$$

we find, by substitution, that

$$\bar{E}_{z2}(t)=\frac{E_o}{4g}\frac{(A_2\varepsilon_\perp+A_1\sigma_\perp)\omega\sin(\omega t)+(A_2\sigma_\perp-A_1\omega^2\varepsilon_\perp)\cos(\omega t)}{\sigma_\perp^2+\omega^2\varepsilon_\perp^2}. \tag{3.37}$$

Hence, we have obtained, through the equation of charge conservation, the second-order corrections to the director field and the electric field. Note that u_2 and E_{x2} vanish identically at the upper and the lower plates; hence, the boundary conditions are satisfied automatically at this stage.

3.2 The Fluid Velocity

Since the director and the electric field are already known, the two hydrodynamic equations can be combined to eliminate the pressure term and to yield a relation connecting the two velocity components v_x and v_z. With the incompressibility condition

($\vec{\nabla} \cdot \vec{v} = 0$), one of the components can be entirely eliminated from the equation. Then, the remaining component can be determined almost immediately by inspection. But first, we must apply the perturbative expansions in (3.7) to break down the hydrodynamic equations into two sub-systems of the first- and the second-order.

The essential ingredient in this equation is the total stress tensor given by $\sigma = \sigma' + \sigma^e$. The viscous stress tensor σ' has been defined previously in (2.104) and the Ericksen stress tensor σ^e in (2.36). Although the algebra becomes very tedious, the total stress tensor can be obtained quite straightforwardly. Since the derivation is not particularly instructive for our purposes, we will simply omit it here. Nevertheless, for the interested reader, the non-vanishing components of the total stress tensor are listed in Appendix B. Before we go on, we make another simplifying assumption. We assume that the velocity field is sufficiently small so that convective terms such as $(\vec{v} \cdot \vec{\nabla})F_i$, where F_i can be any field component, can be safely ignored. These terms are present in the viscous stress tensor σ' because the vector field $\vec{N}$ appearing in the definition of σ' (2.104) is the rate of rotation of the director with respect to the background flow and therefore the total time derivative $\dot{\vec{n}}$ in Eqn. (2.82) corresponds to the material derivative $\partial\vec{n}/\partial t + (\vec{v}\cdot\vec{\nabla})\vec{n}$. In the conduction regime, where $\vec{n}$ and $\vec{v}$ are stationary, the explicit time derivatives of these vector fields vanish. Then, according to equations (2.111) and (B.1) to (B.5), if we expand the director in powers of the tilt angle θ, the x- and the z-components of the hydrodynamic equations (accurate to the second-order infinitesimal) are respectively

$$
\begin{aligned}
&(\alpha_1 + \alpha_4 + \alpha_5 + \alpha_6)\frac{\partial^2 v_x}{\partial x^2} + \frac{1}{2}(2\alpha_1 + \alpha_5 + \alpha_6 - \alpha_2 - \alpha_3)\left(\theta\frac{\partial^2 v_x}{\partial x \partial z} + \frac{\partial\theta}{\partial x}\frac{\partial v_x}{\partial z}\right) \\
&+ \frac{1}{2}(2\alpha_1 + \alpha_5 + \alpha_6 + \alpha_2 + \alpha_3)\left(\theta\frac{\partial^2 v_z}{\partial x^2} + \frac{\partial\theta}{\partial x}\frac{\partial v_z}{\partial x}\right) - 2k_{33}\frac{\partial\theta}{\partial x}\frac{\partial^2\theta}{\partial x^2} - \frac{\partial p}{\partial x} \\
&+ \frac{1}{2}(\alpha_3 + \alpha_4 + \alpha_6)\frac{\partial^2 v_x}{\partial z^2} + \frac{1}{2}(\alpha_4 + \alpha_6 - \alpha_3)\frac{\partial^2 v_z}{\partial z \partial x} + \alpha_6\left(\theta\frac{\partial^2 v_z}{\partial z^2} + \frac{\partial\theta}{\partial z}\frac{\partial v_z}{\partial z}\right) \\
&+ (\alpha_1 + \alpha_5)\left(\frac{\partial^2 v_x}{\partial z \partial x} + \frac{\partial\theta}{\partial z}\frac{\partial v_x}{\partial x}\right) + qE_x - k_{11}\left(\frac{\partial\theta}{\partial z}\frac{\partial^2\theta}{\partial z \partial x} + \frac{\partial^2\theta}{\partial z^2}\frac{\partial\theta}{\partial x}\right)
\end{aligned}
$$

$$+\alpha_3\left(v_x\frac{\partial^2\theta}{\partial z\partial x}+\frac{\partial v_x}{\partial z}\frac{\partial\theta}{\partial x}+v_z\frac{\partial^2\theta}{\partial z^2}+\frac{\partial v_z}{\partial z}\frac{\partial\theta}{\partial z}\right)=0 \tag{3.38}$$

and

$$\begin{aligned}
&\frac{1}{2}(\alpha_2+\alpha_4+\alpha_5)\frac{\partial^2 v_x}{\partial z\partial x}+\frac{1}{2}(\alpha_4+\alpha_5-\alpha_2)\frac{\partial^2 v_z}{\partial x^2}+(\alpha_1+\alpha_6)\left(\theta\frac{\partial^2 v_x}{\partial x^2}+\frac{\partial\theta}{\partial x}\frac{\partial v_x}{\partial x}\right)\\
&+\alpha_2\left(v_z\frac{\partial^2\theta}{\partial z\partial x}+\frac{\partial v_x}{\partial x}\frac{\partial\theta}{\partial x}+v_x\frac{\partial^2\theta}{\partial x^2}+\frac{\partial v_z}{\partial x}\frac{\partial\theta}{\partial z}\right)+\alpha_5\left(\theta\frac{\partial^2 v_z}{\partial x\partial z}+\frac{\partial\theta}{\partial x}\frac{\partial v_z}{\partial z}\right)\\
&-k_{33}\left(\frac{\partial\theta}{\partial x}\frac{\partial^2\theta}{\partial z\partial x}+\frac{\partial^2\theta}{\partial x^2}\frac{\partial\theta}{\partial z}\right)+\frac{1}{2}(\alpha_5+\alpha_6+\alpha_2+\alpha_3)\left(\theta\frac{\partial^2 v_x}{\partial z^2}+\frac{\partial\theta}{\partial z}\frac{\partial v_x}{\partial z}\right)\\
&+\frac{1}{2}(\alpha_5+\alpha_6-\alpha_2-\alpha_3)\left(\theta\frac{\partial^2 v_z}{\partial z\partial x}+\frac{\partial\theta}{\partial z}\frac{\partial v_z}{\partial x}\right)+\alpha_4\frac{\partial^2 v_z}{\partial z^2}-2k_{11}\frac{\partial\theta}{\partial z}\frac{\partial^2\theta}{\partial z^2}\\
&-\frac{\partial p}{\partial z}+qE_z=0.
\end{aligned} \tag{3.39}$$

The y-component equation vanishes identically since the y-component of the electric field is zero, the pressure is independent of y and all other related components of the total stress tensor vanish identically. If we now substitute the expansions (3.7) in the x-component equation and collect like order terms, we obtain the first- and the second-order equations respectively as

$$\begin{aligned}
&\frac{1}{2}\left(\alpha_3+\alpha_4+\alpha_6\right)\frac{\partial^2 v_{x1}}{\partial^2 z}-\frac{1}{2}\left(\alpha_3-\alpha_4-\alpha_6\right)\frac{\partial^2 v_{z1}}{\partial x\partial z}-\frac{\partial p_1}{\partial x}\\
&+\left(\alpha_1+\alpha_4+\alpha_5+\alpha_6\right)\frac{\partial^2 v_{x1}}{\partial^2 x}=0
\end{aligned} \tag{3.40}$$

and

$$\begin{aligned}
&\alpha_6\frac{\partial u_1}{\partial z}\frac{\partial v_{z1}}{\partial z}+\frac{1}{2}\left(\alpha_3+\alpha_4+\alpha_6\right)\frac{\partial^2 v_{x2}}{\partial^2 z}+\alpha_6\,u_1\frac{\partial^2 v_{z1}}{\partial^2 z}-\frac{\partial p_2}{\partial x}\\
&+\frac{1}{2}\left(2\,\alpha_1-\alpha_2-\alpha_3+\alpha_5+\alpha_6\right)\frac{\partial v_{x1}}{\partial z}\frac{\partial u_1}{\partial x}-k_{11}\frac{\partial^2 u_1}{\partial^2 z}\frac{\partial u_1}{\partial x}\\
&+\left(\alpha_1+\alpha_5\right)\frac{\partial u_1}{\partial z}\frac{\partial v_{z1}}{\partial x}+\frac{1}{2}\left(2\,\alpha_1+\alpha_2+\alpha_3+\alpha_5+\alpha_6\right)\frac{\partial u_1}{\partial x}\frac{\partial v_{z1}}{\partial x}\\
&-k_{11}\frac{\partial u_1}{\partial z}\frac{\partial^2 u_1}{\partial x\partial z}+\frac{1}{2}\left(4\,\alpha_1-\alpha_2-\alpha_3+3\,\alpha_5+\alpha_6\right)u_1\frac{\partial^2 v_{x1}}{\partial x\partial z}\\
&-\frac{1}{2}\left(\alpha_3-\alpha_4-\alpha_6\right)\frac{\partial^2 v_{z2}}{\partial x\partial z}+\left(\alpha_1+\alpha_4+\alpha_5+\alpha_6\right)\frac{\partial^2 v_{x2}}{\partial^2 x}\\
&+\frac{1}{2}\left(2\,\alpha_1+\alpha_2+\alpha_3+\alpha_5+\alpha_6\right)u_1\frac{\partial^2 v_{z1}}{\partial^2 x}-2\,k_{33}\frac{\partial u_1}{\partial x}\frac{\partial^2 u_1}{\partial^2 x}
\end{aligned}$$

$$+E_{x1}\left[\Delta\varepsilon\, E_a \frac{\partial u_1}{\partial x} + \varepsilon_\perp \frac{\partial E_{z1}}{\partial z} + (\Delta\varepsilon + \varepsilon_\perp)\frac{\partial E_{x1}}{\partial x}\right] = 0. \tag{3.41}$$

Similarly, the z-component equation can also be broken down into the first-order equation

$$\begin{aligned}
&-\frac{\partial p_1}{\partial z} + \alpha_4 \frac{\partial^2 v_{z1}}{\partial^2 z} + \frac{1}{2}(\alpha_2 + \alpha_4 + \alpha_5)\frac{\partial^2 v_{x1}}{\partial x \partial z} - \frac{1}{2}(+\alpha_2 - \alpha_4 - \alpha_5)\frac{\partial^2 v_{z1}}{\partial^2 x} \\
&+ E_a\left[\Delta\varepsilon\, E_a \frac{\partial u_1}{\partial x} + \varepsilon_\perp \frac{\partial E_{z1}}{\partial z} + (\Delta\varepsilon + \varepsilon_\perp)\frac{\partial E_{x1}}{\partial x}\right] = 0
\end{aligned} \tag{3.42}$$

and the second-order equation

$$\begin{aligned}
&-\frac{\partial p_2}{\partial z} + \frac{1}{2}(\alpha_2 + \alpha_3 + \alpha_5 + \alpha_6)\frac{\partial u_1}{\partial z}\frac{\partial v_{x1}}{\partial z} - 2\,k_{11}\frac{\partial u_1}{\partial z}\frac{\partial^2 u_1}{\partial^2 z} \\
&+ \frac{1}{2}(\alpha_2 + \alpha_3 + \alpha_5 + \alpha_6)\, u_1 \frac{\partial^2 v_{x1}}{\partial^2 z} + \alpha_4 \frac{\partial^2 v_{z2}}{\partial^2 z} + \alpha_5 \frac{\partial v_{z1}}{\partial z}\frac{\partial u_1}{\partial x} \\
&+ (\alpha_1 + \alpha_6)\frac{\partial u_1}{\partial x}\frac{\partial v_{x1}}{\partial x} - \frac{1}{2}(\alpha_2 + \alpha_3 - \alpha_5 - \alpha_6)\frac{\partial u_1}{\partial z}\frac{\partial v_{z1}}{\partial x} \\
&- k_{33}\frac{\partial u_1}{\partial x}\frac{\partial^2 u_1}{\partial x \partial z} + \frac{1}{2}(\alpha_2 + \alpha_4 + \alpha_5)\frac{\partial^2 v_{x2}}{\partial x \partial z} - k_{33}\frac{\partial u_1}{\partial z}\frac{\partial^2 u_1}{\partial^2 x} \\
&- \frac{1}{2}(\alpha_2 + \alpha_3 - 3\,\alpha_5 - \alpha_6)\, u_1 \frac{\partial^2 v_{z1}}{\partial x \partial z} + (\alpha_1 + \alpha_6)\, u_1 \frac{\partial^2 v_{x1}}{\partial^2 x} \\
&+ E_{z1}\left[\Delta\varepsilon\, E_a \frac{\partial u_1}{\partial x} + \varepsilon_\perp \frac{\partial E_{z1}}{\partial z} + (\Delta\varepsilon + \varepsilon_\perp)\frac{\partial E_{x1}}{\partial x}\right] \\
&+ E_a\left\{\Delta\varepsilon\, E_{x1}\frac{\partial u_1}{\partial z} + 2\,\Delta\varepsilon\, E_a\, u_1 \frac{\partial u_1}{\partial z} + \Delta\varepsilon\left[E_{z1}\frac{\partial u_1}{\partial x} + E_a \frac{\partial u_2}{\partial x}\right]\right. \\
&\left. + \Delta\varepsilon\, u_1 \frac{\partial E_{x1}}{\partial z} + \varepsilon_\perp \frac{\partial E_{z2}}{\partial z} + (\Delta\varepsilon + \varepsilon_\perp)\frac{\partial E_{x2}}{\partial x} + \Delta\varepsilon\, u_1 \frac{\partial E_{z1}}{\partial x}\right\} \\
&- \frac{1}{2}(\alpha_2 - \alpha_4 - \alpha_5)\frac{\partial^2 v_{z2}}{\partial^2 x} = 0.
\end{aligned} \tag{3.43}$$

Just as before, the two first-order equations involve only the first-order coefficients of the velocity field and the pressure while the second-order equations involve coefficients up to the second-order. Therefore, we must again solve these equations consecutively. Since pressure is not a major concern in our calculation, we simply eliminate it by combining the two first-order equations. It we differentiate this combined equation with respect to z and apply the incompressibility condition and Faraday's law, we

find

$$\eta_3\frac{\partial^4 v_{x1}}{\partial z^4}+(\eta_1-\eta_2-\eta_5)\frac{\partial^4 v_{x1}}{\partial x^2\partial z^2}+\eta_4\frac{\partial^4 v_{x1}}{\partial x^4}$$
$$=\ \triangle\varepsilon E_a^2\frac{\partial^3 u_1}{\partial x^2\partial z}+E_a\left(\varepsilon_\perp\frac{\partial^3 E_{x1}}{\partial z^3}+\varepsilon_\parallel\frac{\partial^3 E_{x1}}{\partial x^2\partial z}\right) \tag{3.44}$$

where

$$\eta_1 = \alpha_1+\alpha_4+\alpha_5+\alpha_6, \tag{3.45}$$
$$\eta_2 = \frac{1}{2}(\alpha_4+\alpha_6-\alpha_3), \tag{3.46}$$
$$\eta_3 = \frac{1}{2}(\alpha_3+\alpha_4+\alpha_6), \tag{3.47}$$
$$\eta_4 = \frac{1}{2}(\alpha_4+\alpha_5-\alpha_2), \tag{3.48}$$
$$\eta_5 = \frac{1}{2}(\alpha_5-\alpha_4+\alpha_2). \tag{3.49}$$

Inserting the linear solutions (3.15), (3.16) and (3.18) into the above equation, we get for the amplitude of v_{x1}

$$\bar{v}_{x1}=\frac{E_o^2 r^2 d(\triangle\varepsilon-\tau\triangle\sigma)}{2\pi(\tau^2\omega^2+1)\xi} \tag{3.50}$$

where

$$\xi=\eta_3 r^4+(\eta_1-\eta_2-\eta_5)r^2+\eta_4. \tag{3.51}$$

Hence, the first-order coefficients have been completely determined. Not surprisingly, we can readily see that these expressions are exactly the solutions obtained in the linear thoery. This is encouraging because it indicates that our present technique is at least consistent with the analyses done in the past.

Next, we solve for the second-order coefficients v_{x2} and v_{z2}. If we substitute the first-order coefficients in the second-order x-component equation and differentiate it with respect to z, we obtain, after applying the condition of incompressibility,

$$\eta_3\frac{\partial^3 v_{x2}}{\partial z^3}-\frac{\partial^2 p_2}{\partial x\partial z}+(\eta_1-\eta_2)\frac{\partial^3 v_{x2}}{\partial x^2\partial z}+A_x\sin(2px)\sin(2qz)=0 \tag{3.52}$$

with

$$A_x = \frac{pq}{2}\left[(2\eta_5+4\eta_2+6\eta_3-4\eta_1)Aq-k_{11}q^2-\frac{aE_o^2\triangle\sigma}{2g}\right.$$

$$+2(\eta_1-\eta_2-\eta_4)\frac{Ap}{r}-p^2(k_{11}r^2+2k_{33})\Big]. \tag{3.53}$$

If the same is done to the second-order z-component equation except that we carry out the differentiation with respect to x instead, we get

$$\eta_4\frac{\partial^3 v_{z2}}{\partial x^3}-\frac{\partial^2 p_2}{\partial x\partial z}+\eta_5\frac{\partial^3 v_{x2}}{\partial x^2\partial z}+A_z\sin(2px)\sin(2qz)=0 \tag{3.54}$$

with

$$\begin{aligned} A_z &= -\frac{pqE_o^2}{4g^2}\left\{[5ab-(4bg+3a^2\omega^2)\tau](\sigma_\parallel+\sigma_\perp r^2)+4g^2\Delta\varepsilon\right\} \\ &\quad -p^3[q(k_{33}+k_{11}r^2)+(\eta_1-\eta_2-3\eta_4-2\eta_5)A]-pq^2A(\eta_3+\eta_5). \end{aligned} \tag{3.55}$$

Since the same pressure term appears in both of the above equations, it can be removed by subtracting the two equations. If we then differentiate the resultant equation with respect to z, we can use the incompressibility condition once more to transform it to an equation involving only the second-order coefficient v_{x2}:

$$\eta_4\frac{\partial^4 v_{x2}}{\partial x^4}+\eta_3\frac{\partial^4 v_{x2}}{\partial z^4}+(\eta_1-\eta_2-\eta_5)\frac{\partial^4 v_{x2}}{\partial x^2\partial z^2}+2q(A_x-A_z)\sin(2px)\cos(2qz)=0. \tag{3.56}$$

Since the derivatives in the above equation are of even order, the spatial part of v_{x2} must be made up of the second-order harmonics $\sin(2px)\cos(2qz)$. Hence, if we put

$$v_{x2}=B\sin(2px)\cos(2qz), \tag{3.57}$$

we find, by substitution, that

$$B=\frac{-q(A_x-A_z)}{8[p^4\eta_4+q^4\eta_3+p^2q^2(\eta_1-\eta_2-\eta_5)]}. \tag{3.58}$$

Then, the second-order coefficient v_{z2} can be found through the incompressibility condition. It is not difficult to see that v_{z2} must have the following form:

$$v_{z2}=-\frac{p}{q}B\cos(2px)\sin(2qz)+h'(x). \tag{3.59}$$

An equation for $h'(x)$ can be found if we simply combine Eqns. (3.52) and (3.54) to get rid of the pressure term and substitute (3.59) into the resultant equation. This leads us to the equation

$$\eta_4\frac{\partial^3 h'}{\partial x^3}=0. \tag{3.60}$$

Since η_4 is in general non-vanishing, we assume $h'(x)$ to be zero and omit it in the rest of the calculation.

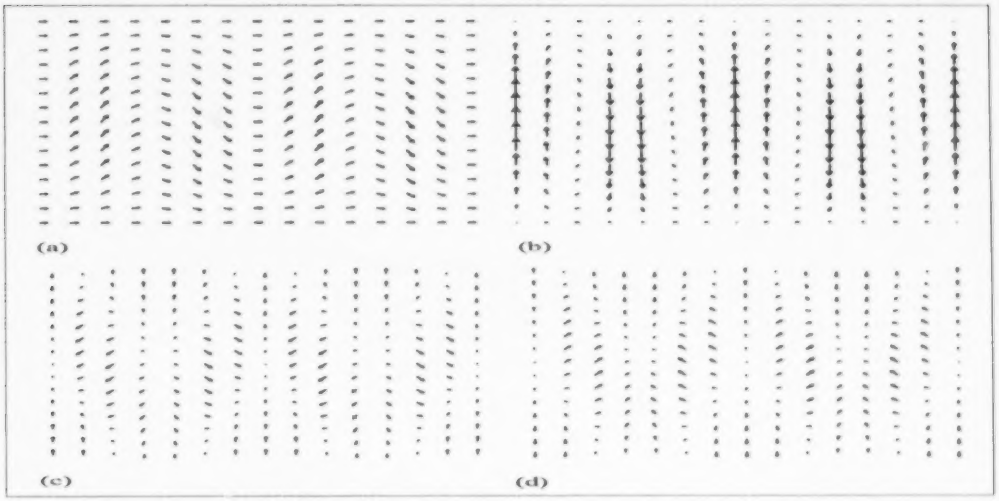

Figure 3.1: Typical plots of the solutions to the electro-hydrodynamic problem: (**a**) the director field, (**b**) the velocity field, (**c**) the induced current density at $t = 0$ and (**d**) the induced current density at $t = T/2$.

Therefore, we have finally obtained the second-order corrections to the linear solutions. For illustration purpose, typical plots of the director, the velocity and the current density are displayed in Fig. 3.1. Note that the nonlinear effects are much too subtle to be detectable on these plots. However, these nonlinear terms will play an invaluable role later in the chapter, when we use these solutions to construct a phenomenological free energy for the nematic system. Although this is only the first step beyond the linear approximation, the equations and the algebra involved are already very complex. Going beyond this order of approximation becomes exceedingly cumbersome. For this reason, we shall restrict ourselves to expansions up to the second-order in θ_o only. Doing so will, no doubt, affect the accuracy of our

final results. One foreseen disadvantage is that the high order coefficients in the final expansion of the free energy would be inexact and this could compromise the validity of the expansion over an extended range in the parameter (the r-θ_o) plane.

3.3 The Rest State to Normal Rolls Transition Line

The transition from the rest state to the normal rolls takes place at a well defined threshold voltage and this voltage increases with the electric field angular frequency. The points at which the bifurcation takes place in the voltage-angular frequency plane form the transition line. In this subsection, we demonstrate how the frequency dependence of the threshold voltage can be calculated from the torque-balance equation, as a consequence of Helfrich-Carr scenario. Since we are only concerned with the transition voltage, the perturbation and, in particular, the amplitude θ_o can be taken to be arbitrarily small. Under these circumstances, the non-linear terms and the second-order corrections to the solutions are unimportant to the calculation and therefore can be dropped. As a result, what we are about to demonstrate is equivalent to the linear version of the theory established rigorously by many authors. The steps and the discussions we present here can also be found in [4, 5, 6].

Since this is a two-dimensional problem, the x- and the z-components of the torques vanish identically. Then, in our frame of reference, the y-component of the torque is defined as

$$\Gamma = \frac{\delta f}{\delta \theta} \tag{3.61}$$

where f is a free energy density and the derivative on the right is the functional derivative:

$$\frac{\delta}{\delta \theta} = \frac{\partial}{\partial \theta} - \sum_i \frac{d}{dx_i}\left[\frac{\partial}{\partial(\partial_i \theta)}\right]. \tag{3.62}$$

Let us first consider the torque exerted by the total electric field on the director.

From Section 2.2, we know that the dielectric free energy density is given by

$$f_E = -\frac{\Delta\varepsilon}{2}(\vec{n}\cdot\vec{E})^2 = -\frac{\Delta\varepsilon}{2}(E_x\cos\theta + E_z\sin\theta)^2. \tag{3.63}$$

Then, in the linear approximation, once the linear solutions have been inserted, the dielectric torque is given by

$$\Gamma_E = -\Delta\varepsilon E_a^2\left[1 - \frac{(\Delta\sigma\tau - \Delta\varepsilon)\omega\sin(\omega t) + (\Delta\varepsilon\tau\omega^2 + \Delta\sigma)\cos(\omega t)}{(\sigma_\parallel + \sigma_\perp r^2)(\tau^2\omega^2+1)\cos(\omega t)}\right]u_1\theta_o \tag{3.64}$$

and its time average is simply

$$\Gamma_E = -\frac{\Delta\varepsilon E_o^2}{2}\left[\frac{\tau^2\omega^2(\sigma_\parallel + \sigma_\perp r^2) + \sigma_\perp(r^2+1) - \Delta\varepsilon\tau\omega^2}{(\sigma_\parallel + \sigma_\perp r^2)(\tau^2\omega^2+1)}\right]u_1\theta_o. \tag{3.65}$$

To derive the deformation torque, we use Frank's deformation energy (2.1). Since the distortion of the director in the normal rolls consists of the splay and the bend only, the twist term drops out completely. Thus, the deformation energy density is written as

$$f_d = \frac{k_{11}}{2}(\cos\theta\frac{\partial\theta}{\partial z} - \sin\theta\frac{\partial\theta}{\partial x})^2 + \frac{k_{33}}{2}(\sin\theta\frac{\partial\theta}{\partial z} + \cos\theta\frac{\partial\theta}{\partial x})^2. \tag{3.66}$$

Then, according to the definition (3.61), the elastic torque is written, in the linear approximation, as

$$\Gamma_d = (k_{33}p^2 + k_{11}q^2)u_1\theta_o. \tag{3.67}$$

Finally, for the viscous torque, we recall from Section 2.6.2 that the antisymmetric part of the viscous stress tensor is the torque that the director exerts on the flow: $(\vec{n}\times\vec{h})_i = \varepsilon_{ijk}\sigma'_{kj}$. In the linear approximation, the tensor components σ'_{zx} and σ'_{xz} are respectively given by

$$\sigma'_{zx} = \frac{1}{2}(\alpha_3 + \alpha_4 + \alpha_6)\frac{\partial v_x}{\partial z} + \frac{1}{2}(\alpha_4 + \alpha_6 - \alpha_3)\frac{\partial v_z}{\partial x} \tag{3.68}$$

and

$$\sigma'_{xz} = \frac{1}{2}(\alpha_4 + \alpha_5 + \alpha_2)\frac{\partial v_x}{\partial z} + \frac{1}{2}(\alpha_4 + \alpha_5 - \alpha_2)\frac{\partial v_z}{\partial x}. \tag{3.69}$$

Then, clearly, the viscous torque that the flow exerts on the director can be written as

$$\begin{aligned}\Gamma_v &= -(\sigma'_{xz} - \sigma'_{zx}) \\ &= -\eta_6 \frac{\partial v_x}{\partial z} - (\eta_4 - \eta_2)\frac{\partial v_z}{\partial x} \\ &= -\frac{(\Delta\varepsilon - \Delta\sigma\tau)E_o^2(\alpha_2 - \alpha_3 r^2)}{2(\tau^2\omega^2+1)\xi} u_1\theta_o \end{aligned} \tag{3.70}$$

where the Parodi relation (2.103) has been used in the numerator in the last equation to eliminate the viscosity coefficients α_5 and α_6 and $\xi = \xi(r)$ is given in (3.51). Now, the sum of the above three torques should be zero for stationary patterns. However, the torques derived above are all proportional to the first order coefficient u_1 and the amplitude θ_o. For nontrivial solutions, these factors drop out of the torque-balance equation, leaving behind an equation which describes the dependence of the magnitude of the external field E_o on the field angular frequency ω and the normalized domain spacing r:

$$\begin{aligned} -\frac{\Delta\varepsilon E_o^2 d^2}{2}\left[\frac{\tau^2\omega^2(\sigma_\parallel + \sigma_\perp r^2) + \sigma_\perp(r^2+1) - \Delta\varepsilon\tau\omega^2}{(\sigma_\parallel + \sigma_\perp r^2)(\tau^2\omega^2+1)}\right] = \\ \frac{(\Delta\sigma\tau - \Delta\varepsilon)E_o^2 d^2(\alpha_3 r^2 - \alpha_2)}{2(\tau^2\omega^2+1)\xi(r)} - k_{33}\left(\frac{2\pi d}{\lambda}\right)^2 - k_{11}\pi^2. \end{aligned} \tag{3.71}$$

But once we recognize that the root-mean-square voltage V_{rms} is given by $E_o d/\sqrt{2}$, the above equation can be converted to a more useful form:

$$\begin{aligned} V_{rms}^2 &= \frac{\pi^2(k_{11}r^2 + k_{33})(\tau^2\omega^2+1)}{r^2(r^2+1)}\left\{\frac{(\alpha_3 r^2 - \alpha_2)(\sigma_\parallel\varepsilon_\perp - \varepsilon_\parallel\sigma_\perp)}{(\sigma_\parallel + \sigma_\perp r^2)\xi(r)}\right. \\ &\quad \left. +\Delta\varepsilon\left[\frac{\sigma_\perp}{\sigma_\parallel + \sigma_\perp r^2} + \frac{\tau^2\omega^2\varepsilon_\perp}{\varepsilon_\parallel + \varepsilon_\perp r^2}\right]\right\}^{-1}. \end{aligned} \tag{3.72}$$

We see that V_{rms}^2 is even with respect to r. This means that for a given angular frequency, there are two degenerate states denoted by $r_\pm$ as the applied voltage is increased beyond the threshold and that this threshold voltage must correspond to the minimum of the two-dimensional curve $V_{rms}^2(r)$. Before we proceed to compute the threshold voltages, there is an additional experimental condition we must be

k_{11}	6.10×10^{-12} N
k_{33}	7.25×10^{-12} N
α_1	6.5×10^{-3} Kg/m/s
α_2	-77.5×10^{-3} Kg/m/s
α_3	-1.2×10^{-3} Kg/m/s
α_4	83×10^{-3} Kg/m/s
α_5	46×10^{-3} Kg/m/s
α_6	-35×10^{-3} Kg/m/s
$\varepsilon_{\parallel}$	$4.72 \times \varepsilon_o$
$\varepsilon_{\perp}$	$5.25 \times \varepsilon_o$
$\sigma_{\parallel}/\sigma_{\perp}$	≈ 1.5

Table 3.1: Physical parameters for the room temperature nematic liquid crystal MBBA [5, 6].

aware of. Although the above expression is made up of physical parameters, all but two parameters are known experimentally. Due to technical difficulties, so far, the conductivities $\sigma_{\parallel}$ and $\sigma_{\perp}$ have not been measured independently. Only the ratio of $\sigma_{\parallel}$ to $\sigma_{\perp}$ has been established approximately for the most popular room temperature nematic liquid crystals [30, 31]. MBBA, a room temperature nematic liquid crystal on which the rest of our analysis is based, is among them and the ratio $\sigma_{\parallel}/\sigma_{\perp}$ has been found to be roughly 1.5 [31]. The rest of the physical parameters for MBBA is listed in Table 3.1 for reference.

Without a precise value for either $\sigma_{\parallel}$ or $\sigma_{\perp}$, it appears that we are unable to proceed with our comparison with experimental observations. However, we can avoid dealing with the precise values of $\sigma_{\parallel}$ and $\sigma_{\perp}$ temporarily if we introduce the (dimensionless) reduced field angular frequency $\omega' = \omega\varepsilon_{\parallel}/\sigma_{\parallel}$. Then, expression (3.72) can be rewritten so that the conductivities $\sigma_{\parallel}$ and $\sigma_{\perp}$ always appear in the ratio $\sigma_{\parallel}/\sigma_{\perp}$. Now, we have sufficient information to plot (3.72) and obtain the threshold voltage for each

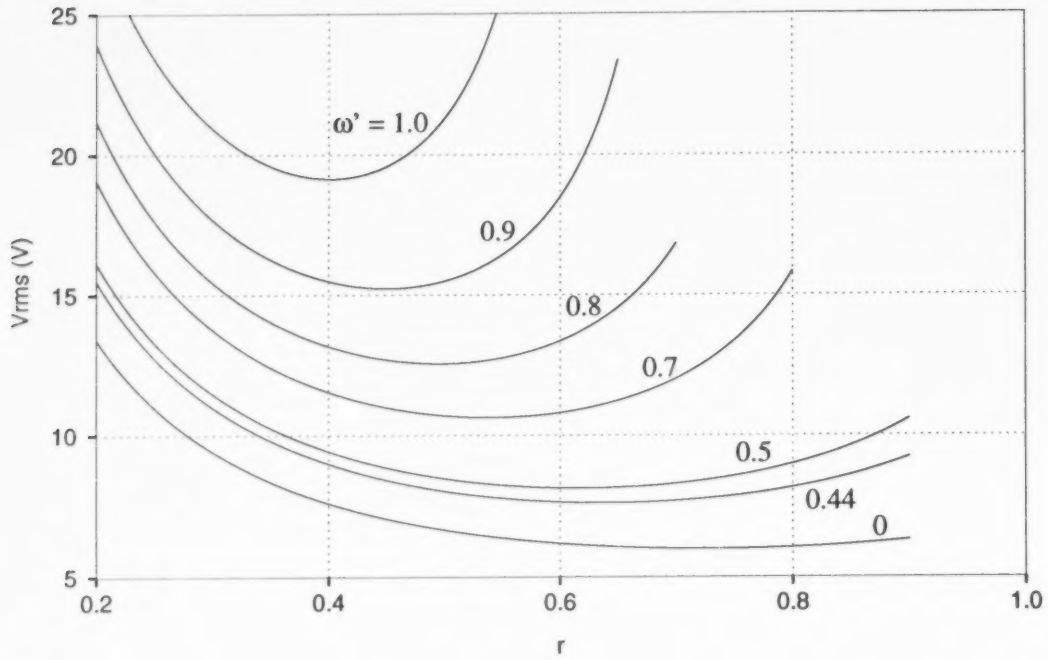

Figure 3.2: The root-mean square voltage plotted as a function of the normalized domain spacing for various values of the reduced angular frequency.

given ω' by minimizing the root-mean-square voltage with respect to r. Later, either $\sigma_{\parallel}$ or $\sigma_{\perp}$ will be chosen so that it yields the best possible fit to the experimental data. Therefore, we do have an adjustable parameter in our model. However, we should not regard this as a deficiency of the theory since this is merely due to the lack of experimental information (currently at our disposal).

The root-mean-square voltage is plotted as a function of the normalized domain spacing r for various values of ω' in Figure 3.2. The figure shows that the threshold voltage increases with the field angular frequency and that there appears to be a cut-off angular frequency at which the threshold voltage becomes infinitely large. Beyond this cut off point, formation of normal rolls become impossible. Figure 3.3 displays

the transition line, as a result of minimizing the root-mean-square voltage numerically

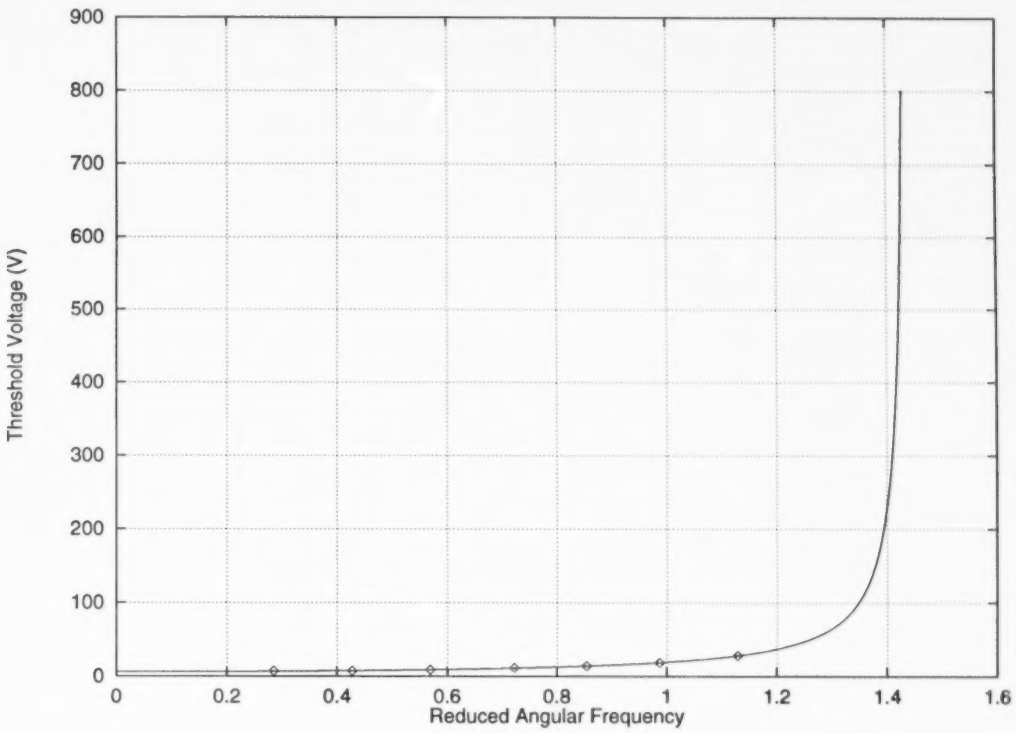

Figure 3.3: The normal-roll transition line. The solid line is the theoretical result derived from (3.72). The diamonds are the experimental measurements.

with respect to r, and the experimental measurements for MBBA performed by the Orsay group [13]. First, we note that the reduced cut-off angular frequency at roughly $\omega' = 1.43$ has become more apparent on this plot. Secondly, we have chosen the conductivity $\sigma_{\|}$ to be $1.87 \times 10^{-8}\Omega^{-1}m^{-1}$ so that the experimental measurement on the extreme right of the graph lies exactly on our transition line. We see that the agreement with the experimental observations is not bad at all. The transition line is slightly lower at low frequencies, but this is probably due to the semi-rigid boundary conditions that we have assumed. Thus, we see that, although the boundary conditions are less realistic, they do not lead to an unacceptable discrepancy after all.

Finally, we plot the normalized domain spacing as a function of the threshold voltage in Figure 3.4, thereby eliminating the reduced angular frequency ω' and the need to

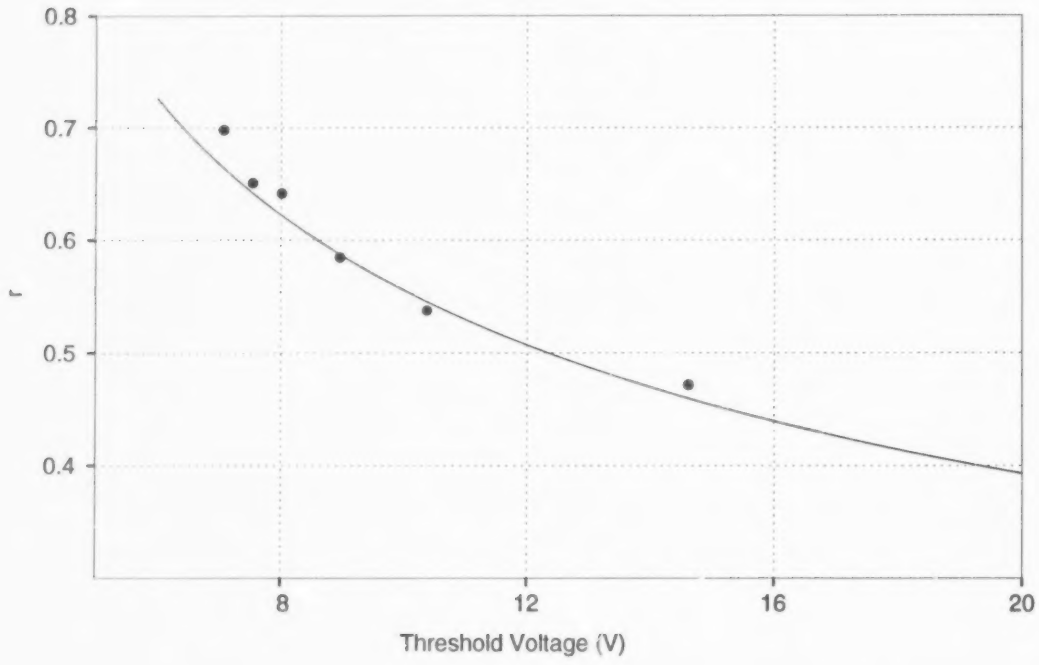

Figure 3.4: The normalized domain spacing plotted as a function of the threshold voltage. The solid line is calculated from the linear thoery; the dots represent the experimental measurements.

adjust the conductivity $\sigma_{\parallel}$. Thus, the result is independent of any parametrization. The experimental data due to Meyerhofer and Sussman [14] are superimposed in the figure to demonstrate the good agreement between the linear theory and the observations.

3.4 The Energy Method

In the above section, we have seen that the linear version of the continuum theory does produce threshold voltages that agree with experimental observations very well. Nevertheless, the theory was unable to provide information as to how the modulational amplitude θ_o of the director varies across the transition point (since θ_o dropped out from the torque-balance equation completely). Since, according to experimental observations, θ_o increases from zero and follows a power-law relation as the system transforms from its low-voltage to its high-voltage state, θ_o can be taken as an order parameter as in the Landau theory of phase transition. Taking this idea one step further, in this section, we propose using an energy method to describe the critical behavior of the normal rolls. In the following, we postulate a phenomenological free energy for the nematic system driven slightly out of equilibrium. Then, making use of the linear and the nonlinear solutions found in the previous sections and minimizing the free energy with respect to the appropriate parameters, the critical behavior of the normal rolls is displayed through a series of bifurcation diagrams.

The use of the energy method in dissipative systems is still controversial. Nevertheless, in a recent review by Cross and Hohenberg [32], it has been pointed out that although in general no free energy or Lyapunov potential can be defined for nonequilibrium systems, there remain notable exceptions in which the evolution equations can be written in a gradient form

$$\frac{\partial \psi}{\partial t} = -\Gamma \frac{\delta G}{\delta \psi^*} \tag{3.73}$$

with Γ being a positive kinetic coefficient and G a generalized free energy functional of the complex order parameter ψ and ψ^*. Moreover, the functional G can be shown to be equivalent to a Lyapunov function. In fact, the above evolution equation has been found to be applicable to many physical phenomena involving non-equilibrium processes [33], such as second-order phase transition of a junction laser [34] and propagation of a two-phase interface [35]. For the non-equilibrium systems, Eqn.

(3.73) describes the time relaxation of the (non-conserved) order parameter towards its stationary state. In the case where the stationary state is of primary interest, the time-independent equation is used instead and a minimization principle is applied to the generalized free energy to determine the stationary solution. Common examples of such are Rayleigh-Benard convection [36] and superconductivity [37, 38, 39]. The use of minimization principle in non-equilibrium phase transitions has also been rigorously justified by Graham [40].

3.4.1 A Phenomenological Free energy

To account for the elasticity, the interaction with the electric field and the coupling between the director and the flow, we postulate that the free energy density is made up of three separate contributions:

$$f = f_E + f_d + f_v \tag{3.74}$$

where f_E represents the dielectric free energy density, f_d the deformation free energy density and f_v the free energy density due to the coupling with the viscous flow. We have already encountered the first two contributions on the right previously, so they can be written down quite straightforwardly although the algebra becomes very involved at this stage. The dielectric free energy density has already been given in Eqn. (3.63). We shall expand it in powers of the director tilt angle θ. But we must be careful to keep a sufficient number of high-order terms because, as in any one-dimensional problem, the lowest-order terms determine where the bifurcation takes place; however, it is the high-order terms that determine the order of the transition. For this purpose, we decide to retain terms up to the fourth-order in θ consistently throughout the rest of the calculation. However, from previous sections, our solutions to the electro-hydrodynamic problem are expanded only up to the second-order in θ_o. This means, not all of the third- and the fourth-order terms (in θ_o) will be present in the final expression of the free energy. Returning to the dielectric free energy density,

we expand (3.63) in powers of θ as

$$f_E = -\frac{\Delta\varepsilon}{2}\Big(E_x^2 - E_x^2\theta^2 + 2E_xE'_z\theta + 2E_xE_a\theta - \frac{4}{3}E_xE_a\theta^3 + E'^2_z\theta^2 + 2E'_zE_a\theta^2 + E_a^2\theta^2 - \frac{1}{3}E_a^2\theta^4\Big). \tag{3.75}$$

Note that the first term on the right is independent of θ and does not describe an interaction with the director. Therefore, it can be dropped without any loss of generality. In view of the solutions we obtained in the last section, we see that this free energy density is spatially as well as time dependent. Therefore, the mean free energy is obtained by taking average over space and time. Once the perturbative expansions (3.7) are used and the solutions (3.15) to (3.17) are inserted into the above expression, the integrations can be carried out in a straightforward manner. It can be shown that all third-order terms vanish identically as a result of the integrations and that the resultant dielectric mean free energy F_E can be written in even powers of the order-parameter θ_o with the coefficients dependent upon r and ω. Since these operations tend to produce rather lengthy and tedious expressions which do not illustrate any interesting physics, we shall omit the intermediate steps and simply present the final result:

$$F_E = C_2^E\,\theta_o^2 + C_4^E\,\theta_o^4 + \ldots \tag{3.76}$$

where

$$C_2^E = \frac{\Delta\varepsilon(2b-g)E_o^2}{16g}, \tag{3.77}$$

$$\begin{aligned} C_4^E = {} & -\frac{\Delta\varepsilon\,E_o^2 r^2}{256\,g^2}(b^2 + a^2\omega^2) + \frac{3\,\Delta\varepsilon\,E_o^2}{256\,g^2}(3\,b^2 - 4\,b\,g + g^2 + 3\,a^2\omega^2) \\ & + \frac{\Delta\varepsilon\,E_o^2 r^2}{256\,g^2}(4\,A_1\tau\omega^2 - 4\,A_2 - g^2) + \frac{\Delta\varepsilon\,E_o^2 r^2}{128\,g^3}(2\,A_2\,b \\ & - b^2\,g + 2\,b\,g^2 + 2\,a\,A_1\omega^2 - a^2\,g\,\omega^2 + 2\,a\,A_2\tau\omega^2 - 2\,A_1\,b\,\tau\omega^2\Big) \\ & + \frac{\Delta\varepsilon\,E_o^2}{64\,g^3(\sigma_\perp^2 + \varepsilon_\perp^2\omega^2)}\Big(A_2\,b\,g\,\sigma_\perp - A_2\,g^2\,\sigma_\perp + A_2\,b\,r^2\,\sigma_\perp^2 - A_2\,g\,r^2\,\sigma_\perp^2 \\ & + a\,A_2\,\varepsilon_\perp\,g\,\omega^2 - A_1\,b\,\varepsilon_\perp\,g\,\omega^2 + A_1\,\varepsilon_\perp\,g^2\,\omega^2 + A_2\,b\,\varepsilon_\perp^2\,r^2\,\omega^2 \\ & - A_2\,\varepsilon_\perp^2\,g\,r^2\,\omega^2 + a\,A_1\,g\,\sigma_\perp\,\omega^2 + a\,A_1\,r^2\,\sigma_\perp^2\,\omega^2 + a\,A_2\,r^2\,\sigma_\perp^2\,\tau\omega^2 \end{aligned}$$

$$- A_1 b r^2 \sigma_\perp^2 \tau \omega^2 + A_1 g r^2 \sigma_\perp^2 \tau \omega^2 + a A_1 \varepsilon_\perp^2 r^2 \omega^4 + a A_2 \varepsilon_\perp^2 r^2 \tau \omega^4$$
$$- A_1 b \varepsilon_\perp^2 r^2 \tau \omega^4 + A_1 \varepsilon_\perp^2 g r^2 \tau \omega^4 \Big). \tag{3.78}$$

The deformation free energy density, given in (3.66), can be treated in a similar way. Expanding it in powers of the tilt angle θ, we obtain

$$f_d = \left(\frac{k_{33} - k_{11}}{2}\right)\left[2\theta \frac{\partial\theta}{\partial x}\frac{\partial\theta}{\partial z} - \theta^2\left(\frac{\partial\theta}{\partial x}\right)^2 + \theta^2\left(\frac{\partial\theta}{\partial z}\right)^2\right]$$
$$+ \frac{k_{11}}{2}\left(\frac{\partial\theta}{\partial z}\right)^2 + \frac{k_{33}}{2}\left(\frac{\partial\theta}{\partial x}\right)^2. \tag{3.79}$$

Using the perturbative expansion for the tilt angle as in (3.7) and inserting the solutions (3.15) and (3.28), we average this free energy over space and turn it into a quartic polynomial of θ_o. Again, the third-order term vanishes identically after the integrations. Thus, we find

$$F_d = C_2^d \, \theta_o^2 + C_4^d \, \theta_o^4 + \ldots \tag{3.80}$$

where

$$C_2^d = \frac{\pi^2}{8d^2}\left(k_{11} + \frac{k_{33}}{r^2}\right), \tag{3.81}$$

$$C_4^d = \frac{q^2}{128}\left[3(k_{11} - k_{33})\left(\frac{1}{r^2} - 3\right) + 4(k_{11} r^2 + k_{33})\right]. \tag{3.82}$$

The free energy density due to the viscous flow is something we have not considered explicitly before. The only information available to us is that the viscous torque that the flow exerts on the director is given by the antisymmetric part of the viscous stress tensor. Although we propose this free energy density as a phenomenological model, it is still desirable to write down f_v in such a way that the viscous torque is derivable from it. Hence, to obtain an expression for the free energy f_v, it seems logical to look for an energy function that is dependent on $\vec{v}$ and $\vec{n}$ only, even with respect to $\vec{n}$ and produces the correct viscous torque. So, our first step is to examine this viscous torque more closely.

As we have pointed out earlier, the only non-zero component of the torque that the flow exerts on the director is the y-component given by $\Gamma_v = -(\sigma'_{xz} - \sigma'_{zx})$. We have already worked out this y-component in Section 3.3 and the expression in the linear approximation is given in (3.70). However, because of the presence of nonlinearities in our model, it is important that we obtain a more exact expression for it. Beginning with the molecular field $\vec{h}$ given in (2.99) where the field is expressed in terms of the conjugate thermodynamic fluxes, we can write it in the conduction regime as

$$\begin{aligned} h_x &= -\frac{1}{2}(\alpha_3 - \alpha_2) n_z \left(\frac{\partial v_x}{\partial z} - \frac{\partial v_z}{\partial x} \right) \\ &\quad + (\alpha_2 + \alpha_3) \left[n_x \frac{\partial v_x}{\partial x} + \frac{n_z}{2} \left(\frac{\partial v_x}{\partial z} + \frac{\partial v_z}{\partial x} \right) \right], \\ h_y &= 0, \qquad (3.83) \\ h_z &= \frac{1}{2}(\alpha_3 - \alpha_2) n_x \left(\frac{\partial v_x}{\partial z} - \frac{\partial v_z}{\partial x} \right) \\ &\quad + (\alpha_2 - \alpha_3) \left[n_z \frac{\partial v_z}{\partial z} + \frac{n_x}{2} \left(\frac{\partial v_x}{\partial z} + \frac{\partial v_z}{\partial x} \right) \right] \qquad (3.84) \end{aligned}$$

where all convective terms have been omitted, in accordance with the electro-hydrodynamic calculation presented in the last section. Since the y-component of the viscous torque is the only non-vanishing component, the viscous torque is simply given by $\Gamma_v = -(\vec{n} \times \vec{h})_y = -(n_z h_x - n_x h_z)$. Inserting the above expressions for the components of $\vec{h}$, we can simplify it to

$$\begin{aligned} \Gamma_v &= \frac{1}{2}(\alpha_3 - \alpha_2) \left(\frac{\partial v_x}{\partial z} - \frac{\partial v_z}{\partial x} \right) - \frac{1}{2}(\alpha_2 + \alpha_3) \left[\left(\frac{\partial v_x}{\partial x} - \frac{\partial v_z}{\partial z} \right) \sin(2\theta) \right. \\ &\quad \left. - \left(\frac{\partial v_x}{\partial z} + \frac{\partial v_z}{\partial x} \right) \cos(2\theta) \right]. \qquad (3.85) \end{aligned}$$

Since the viscous torque is given by the cross product $-(\vec{n} \times \vec{h})$, naively, we can express the corresponding free energy density in terms of the dot product $(\vec{n} \cdot \vec{h})/2$, analogous to the dielectric torque an electric dipole experiences in an electric field. It is not difficult to see that, this trial free energy density can be further written as

$$f = \frac{1}{2}(\vec{n} \cdot \vec{h})$$

$$= \frac{\alpha_2+\alpha_3}{2}\left[\cos^2\theta\frac{\partial v_x}{\partial x}+\sin^2\theta\frac{\partial v_z}{\partial z}+\sin\theta\cos\theta\left(\frac{\partial v_x}{\partial z}+\frac{\partial v_z}{\partial x}\right)\right] \quad (3.86)$$

and the corresponding viscous torque is

$$\begin{aligned}\tau &= \frac{\delta f}{\delta\theta}\\ &= -\frac{\alpha_2+\alpha_3}{2}\left[\left(\frac{\partial v_x}{\partial x}-\frac{\partial v_z}{\partial z}\right)\sin(2\theta)-\left(\frac{\partial v_x}{\partial z}+\frac{\partial v_z}{\partial x}\right)\cos(2\theta)\right]. \quad (3.87)\end{aligned}$$

This torque corresponds to only the last two terms on the right of Eqn. (3.85). Thus, f alone does not suffice. However, the total viscous torque can be enitrely accounted for if we add to f an extra term

$$j = -\left(\frac{\alpha_3-\alpha_2}{2}\right)\vec{v}\cdot\left[(\vec{\nabla}\cdot\vec{n})\vec{n}+\vec{n}\times(\vec{\nabla}\times\vec{n})\right]. \quad (3.88)$$

Although it looks very complex, it can be shown to be reduced to

$$j = -\frac{\alpha_3-\alpha_2}{2}\left(v_x\frac{\partial\theta}{\partial z}-v_z\frac{\partial\theta}{\partial x}\right). \quad (3.89)$$

Then, taking the functional derivative of j with respect to θ, we find that the corresponding torque is given by

$$\tau = \frac{\alpha_3-\alpha_2}{2}\left(\frac{\partial v_x}{\partial z}-\frac{\partial v_z}{\partial x}\right). \quad (3.90)$$

This is exactly the first term on the right of Eqn. (3.85). Therefore, the energy function that produces the correct viscous torque is given by

$$f_v = \frac{1}{2}(\vec{n}\cdot\vec{h})-\frac{1}{2}(\alpha_3-\alpha_2)\vec{v}\cdot\left[(\vec{\nabla}\cdot\vec{n})\vec{n}+\vec{n}\times(\vec{\nabla}\times\vec{n})\right]. \quad (3.91)$$

Rearranging this expression, we can put it in a more compact form:

$$f_v = -\frac{1}{2}(\vec{n}\cdot\vec{\mathcal{H}}) \quad (3.92)$$

where

$$\vec{\mathcal{H}} = (\alpha_3-\alpha_2)\left[(\vec{\nabla}\cdot\vec{n})\vec{v}+(\vec{\nabla}\times\vec{n})\times\vec{v}\right]-\vec{h}. \quad (3.93)$$

We shall call the field $\vec{\mathcal{H}}$ the *generalized molecular field* thereafter, in contrast to the molecular field $\vec{h}$ due to de Gennes [20]. Thus, this free energy density favors a parallel alignment with the generalized molecular field.

Having written down the explicit expression for f_v, we make use of the expressions (3.86) and (3.89) and expand it in powers of the infinitesimal quantities:

$$\begin{aligned} f_v &= \left(\frac{\alpha_2+\alpha_3}{2}\right)\left[\frac{\partial v_x}{\partial x}(1-\theta^2)+\frac{\partial v_z}{\partial z}\theta^2+\left(\frac{\partial v_x}{\partial z}+\frac{\partial v_z}{\partial x}\right)\left(1-\frac{2}{3}\theta^2\right)\theta\right] \\ &\quad -\left(\frac{\alpha_3-\alpha_2}{2}\right)\left(v_x\frac{\partial\theta}{\partial z}-v_z\frac{\partial\theta}{\partial x}\right). \end{aligned} \tag{3.94}$$

If we insert the expansions for θ and $\vec{v}$ as listed in (3.7) and the solutions we obtained in Section 2.7 into the above equation, we can again write it as a quartic polynomial of the order-parameter θ_o. Then, after averaging, we get

$$F_v = C_2^v\,\theta_o^2 + C_4^v\,\theta_o^4 + \ldots \tag{3.95}$$

where

$$\begin{aligned} C_2^v &= -\frac{E_o^2 a(\alpha_3 r^2-\alpha_2)}{8(\omega^2\tau^2+1)\xi}, \\ C_4^v &= -\frac{E_o^2 a}{128(\omega^2\tau^2+1)\xi}\Big[(\alpha_2+\alpha_3)(3+12Br-5r^2-4Br^3) \\ &\quad -4B(\alpha_3-\alpha_2)r(r^2+1)\Big]. \end{aligned} \tag{3.96}$$

The total mean free energy for the nematic system can now be constructed by summing the quartic polynomials (3.76), (3.80) and (3.95):

$$F = C_2\,\theta_o^2 + C_4\,\theta_o^4 + \ldots \tag{3.97}$$

where

$$\begin{aligned} C_2 &= \frac{\pi^2}{8d^2}\left(k_{11}+\frac{k_{33}}{r^2}\right)+\frac{V_{rms}^2}{d^2}\left[\frac{a(\alpha_2-\alpha_3 r^2)}{4(\omega^2\tau^2+1)\xi}+\frac{\triangle\varepsilon(2b-g)}{8g}\right], \\ C_4 &= \frac{\pi^2}{128d^2}\left[k_{11}\left(4r^2+\frac{3}{r^2}-9\right)+k_{33}\left(13-\frac{3}{r^2}\right)\right] \\ &\quad -\frac{V_{rms}^2}{8d^2}\left\{\frac{\triangle\varepsilon r^2}{16g^2}\left[b^2+a^2\omega^2+4(A_2-A_1\tau\omega^2)+g^2-\frac{2S_1}{g}\right]\right. \end{aligned} \tag{3.98}$$

$$
\begin{aligned}
&- \frac{3\triangle\varepsilon}{16g^2}\left[3b^2 - 4bg + g^2 + 3a^2\omega^2 + \frac{4S_2}{3g(\sigma_\perp^2 + \varepsilon_\perp^2\omega^2)}\right] \\
&+ \frac{a}{8(\tau^2\omega^2+1)\xi}\left[(\alpha_2+\alpha_3)(3 + 12Br - 5r^2 - 4Br^3)\right. \\
&\left.-4B(\alpha_3 - \alpha_2)r(r^2+1)\right]\Big\}, \qquad (3.99)
\end{aligned}
$$

$$
S_1 = b(2A_2 - bg + 2g^2) + a(2A_1 - ag)\omega^2 + 2\tau\omega^2(aA_2 - bA_1), \qquad (3.100)
$$

$$
\begin{aligned}
S_2 = {} & g[a\omega^2(A_2\varepsilon_\perp + A_1\sigma_\perp) + (b-g)(A_2\sigma_\perp - A_1\omega^2\varepsilon_\perp)] \\
& + r^2(\sigma_\perp^2 + \varepsilon_\perp^2\omega^2)[a\omega^2(A_2\tau + A_1) + (b-g)(A_2 - A_1\tau\omega^2)]. \qquad (3.101)
\end{aligned}
$$

The substitution $V_{rms} = E_o d/\sqrt{2}$ has been made to simplify the above expressions. Since the phenomenon involves a continuous (second-order) phase transition, we expect F to bifurcate from a single well form to a double well one as the applied voltage exceeds its threshold value V_c. Consequently, the essential physics is captured by the first two terms in the expansion. For simplicity, we shall therefore truncate the expansion at the fourth-order term as

$$
F = C_2\,\theta_o^2 + C_4\,\theta_o^4. \qquad (3.102)
$$

By applying the minimization principle, this mean free energy allows us to determine the stationary state of the system at any given voltage and angular frequency. Considering the complexity of this mean free energy, we believe that a global search for the minimum may not be feasible either analytically or numerically. We have thus decided to limit the search region to a subset consistent with experimental observations and a stability criterion and to resort to numerical techniques for the remainder of the analysis.

We already know that, in the neighborhood of the transition point, θ_o is close to zero and the width of the rolls remains comparable to the thickness of the cell. Experimental observations [16] have further indicated that r decreases slightly as the voltage continues to increase. It is therefore reasonable to limit our search region first to $[0,1] \times [0,1]$ in the θ_o-r parameter plane. In addition to these experimental indications, for stability reasons, the fourth-order coefficient must always be positive

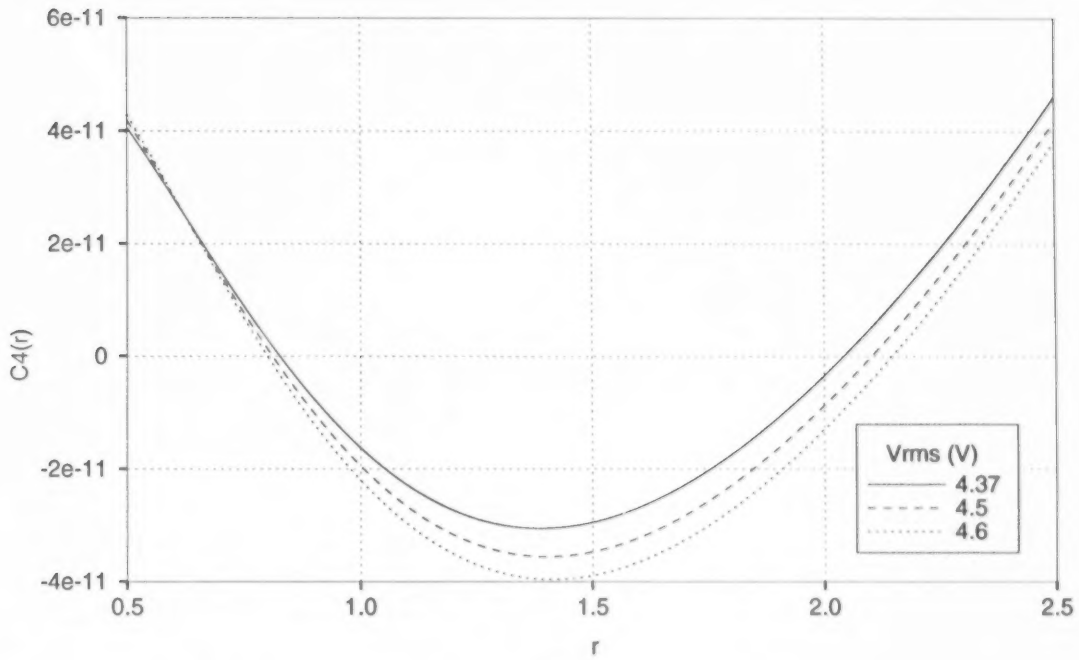

Figure 3.5: The fourth-order coefficient plotted as a function of the normalized domain spacing r at $\omega' = 0.5$ for different values of V_{rms}.

in the region of our search. Using the standard material parameters for the room temperature nematic liquid crystal MBBA (see Table 3.1), in Fig. 3.5, we display typical plots of C_4 at the reduced angular frequency of $\omega' = \omega\varepsilon_{\parallel}/\sigma_{\parallel} = 0.5$ for three different values of the applied *rms* voltage. We readily note that the coefficient becomes negative in the central region of the graph. This anomaly could be caused by the inexactness due to the truncation of the series solutions as pointed out earlier. It could also mean the presence of a metastable state, which is allowed to exist when the fourth-order coefficient becomes negative while the sixth-order coefficient is positive i.e. when the free energy develops local minima. To prove that a metastable state actually exists in our system, we would have to calculate the sixth-order coefficient

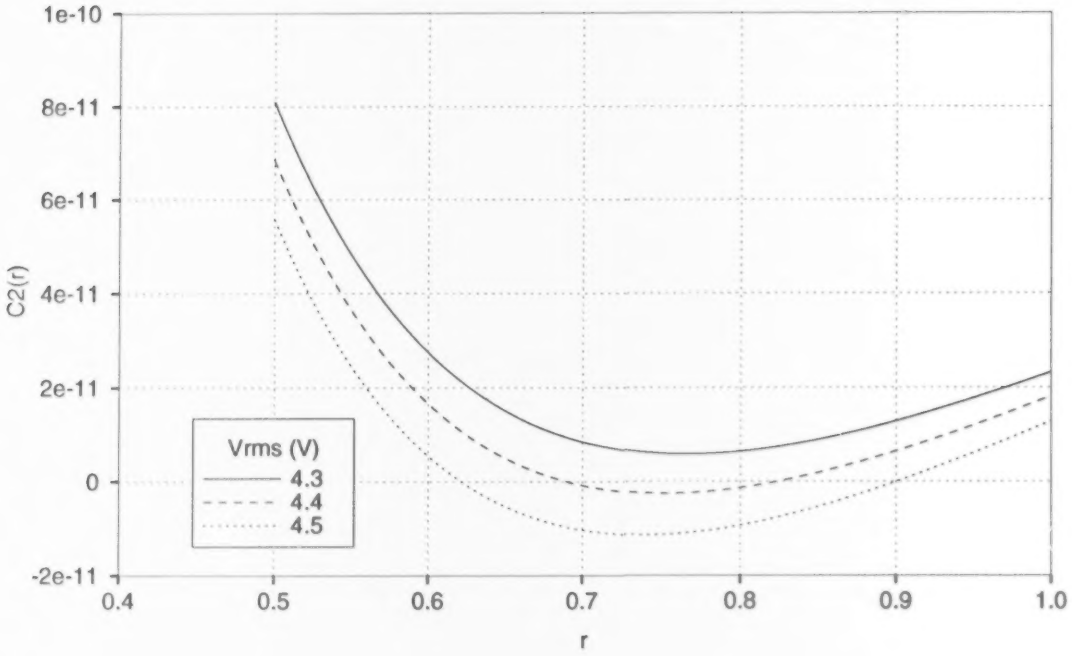

Figure 3.6: The second-order coefficient plotted as a function of the normalized domain spacing r at $\omega' = 0.5$ for different values of V_{rms}.

explicitly and this is beyond the scope of our analysis. It will, therefore, be feasible to limit our search interval of r to the range $[0, \delta)$ where δ is the critical point at which C_4 first crosses the r-axis in Fig. 3.5.

We again fix the reduced field angular frequency ω' at 0.5 for the purpose of illustration and plot the second-order coefficient C_2 as a function of r for three different values of the applied voltage in Fig. 3.6. Evidently, so long as the voltage is below a critical value, the coefficient is positive everywhere. Since C_4 is also positive within the region of our search, this indicates that a single well with its minimum located somewhere on the r-axis is present in the potential. The corresponding stationary state ($\theta_o = 0$) can therefore be interpreted as the rest-state of the nematic cell.

However, as shown in the corresponding figure, once the voltage exceeds its critical value even slightly, the coefficient becomes negative over a small range of r meaning that the single well in the potential has split into two wells and these wells have drifted away from the r-axis. Although there are now two equivalent minima, one with $\theta_o > 0$ and the other with $\theta_o < 0$, physical constraints on θ_o demand that the minimum located in the positive quadrant of the parameter plane corresponds to the true stationary state of the system. Since this state has a non-zero θ_o, it corresponds very naturally to the normal rolls.

It is now clear that the bifurcation must take place at the point where the C_2 curve in Fig. 3.6 just touches the r-axis. Setting C_2 to zero, we can re-arrange the equation and express the rms voltage as a function of r and ω as follows:

$$V_{rms}^2 = \frac{\pi^2}{r^2}(k_1 r^2 + k_3)(\tau^2\omega^2 + 1)\left\{\frac{2(\alpha_3 r^2 - \alpha_2)(\sigma_\parallel \varepsilon_\perp - \varepsilon_\parallel \sigma_\perp)(r^2+1)}{(\sigma_\parallel + \sigma_\perp r^2)\xi} + \triangle\varepsilon\left[\frac{\sigma_\perp(r^2+2) - \sigma_\parallel}{\sigma_\parallel + \sigma_\perp r^2} + \frac{\tau^2\omega^2[\varepsilon_\perp(r^2+2) - \varepsilon_\parallel]}{\varepsilon_\parallel + \varepsilon_\perp r^2}\right]\right\}^{-1}. \quad (3.103)$$

Except for some numerical factors (factors of 2's), this equation is identical in form to the compatibility condition (3.72) derived in the linear theory. The reason that these two equations are not identical is still unclear to us at this point. We hope to resolve this issue in the future. To obtain the transition curve for the purpose of comparing theory with experiment, we minimize the above rms voltage numerically with respect to r over a range of angular frequency. Taking the material parameters for MBBA directly from Table 3.1 and setting the conductivity $\sigma_\parallel$ to $1.19 \times 10^{-8}\Omega^{-1}m^{-1}$, we compare our theoretical transition line with the experimental measurements [13] in Fig. 3.7. We see that the result of our analysis does not agree with the experimental data quite as well as the linear theory does. However, the discrepancy is not too large and the transition line does fit the data qualitatively well. If we allow the ratio $\sigma_\parallel/\sigma_\perp$ to deviate from its generally accepted value 1.5 and re-calibrate $\sigma_\parallel$ to $1.85 \times 10^{-8}\Omega^{-1}m^{-1}$, then the resultant transition curve as shown in Fig. 3.8 compares very favorably with the experimental measurements [13]. Therefore, a small shift in the

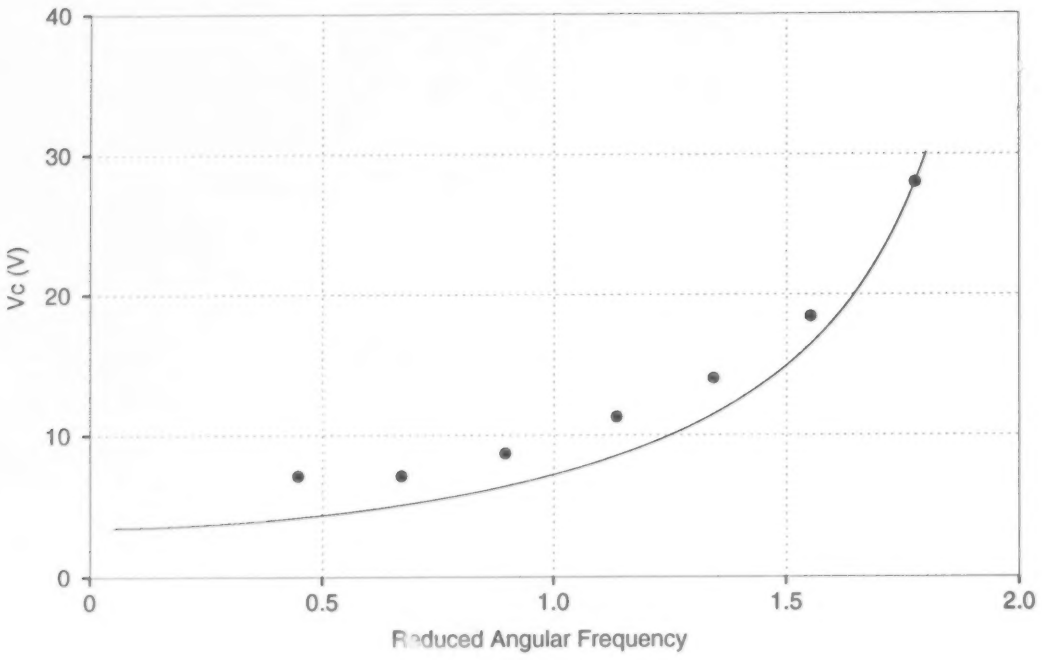

Figure 3.7: The transition line for the rest-state to normal-roll transition. The solid line is calculated by minimizing Eqn. (3.103) with respect to r; the dots represent the experimental measurements.

ratio $\sigma_{\parallel}/\sigma_{\perp}$ has resulted in a very good agreement with the experimental observations. This however is to be expected since lowering the ratio $\sigma_{\parallel}/\sigma_{\perp}$ corresponds to reducing the hydrodynamic torques and the threshold voltage must increase to compensate.

3.4.2 Bifurcation Diagrams

We finally turn our attention to the bifurcation diagrams for the continuous rest-state to normal rolls transition. These diagrams can be constructed by minimizing F with respect to the state parameters r and θ_o. With all the physical parameters for MBBA taken directly from Table 3.1, we have employed a multidimensional minimization

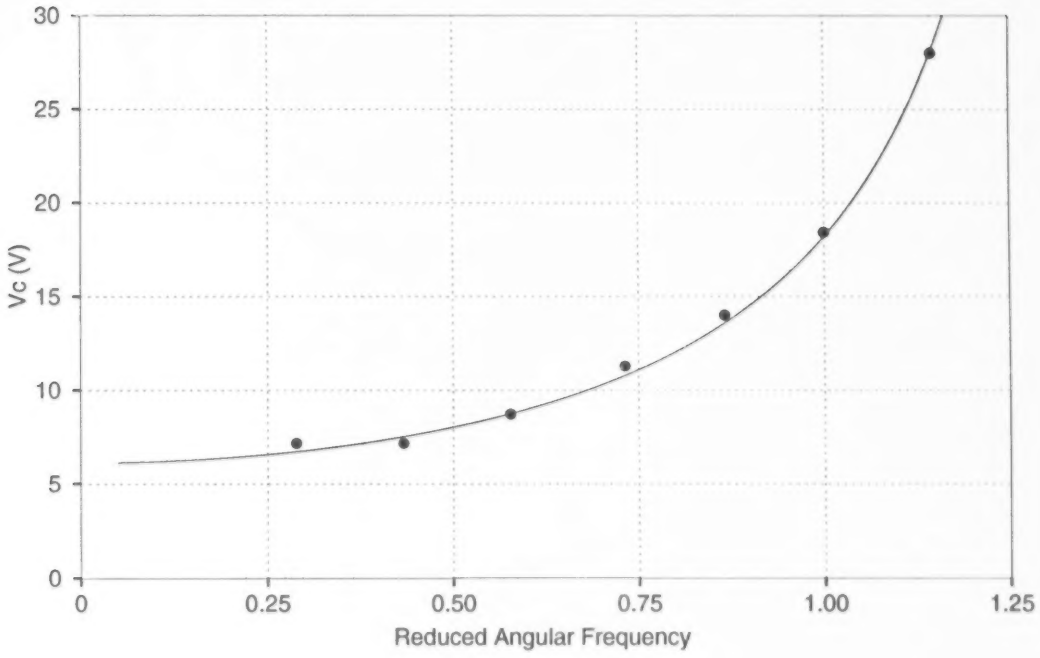

Figure 3.8: The transition line for the rest-state to normal-roll transition. The solid line is calculated at $\sigma_{\parallel}/\sigma_{\perp} = 1.15$; the dots represent the experimental measurements.

algorithm [41] to minimize F at $\omega' = 0.5$ for a range of V slightly above the threshold voltage. For the conductivity $\sigma_{\parallel}$, we have chosen the value $1.19 \times 10^{-8}\Omega^{-1}m^{-1}$ so that the reduced angular frequency corresponds to the actual frequency $f = 22.7\ Hz$ where a continuous transition has indeed been observed [13, 14, 15]. Fig. 3.9 displays the trajectory made by the minimum of F on the positive quadrant of the parameter plane as the voltage increases from the threshold value. Quite clearly, the normal-roll structure emerges with a finite periodicity (normalized domain width of $r \approx 0.755$) regardless how minute the modulation of the director is; furthermore, θ_o can be seen to increase nonlinearly with the applied voltage. In Fig. 3.10, we plot the amplitude θ_o as a function of the reduced voltage ϵ. We can see that θ_o does increase nonlinearly

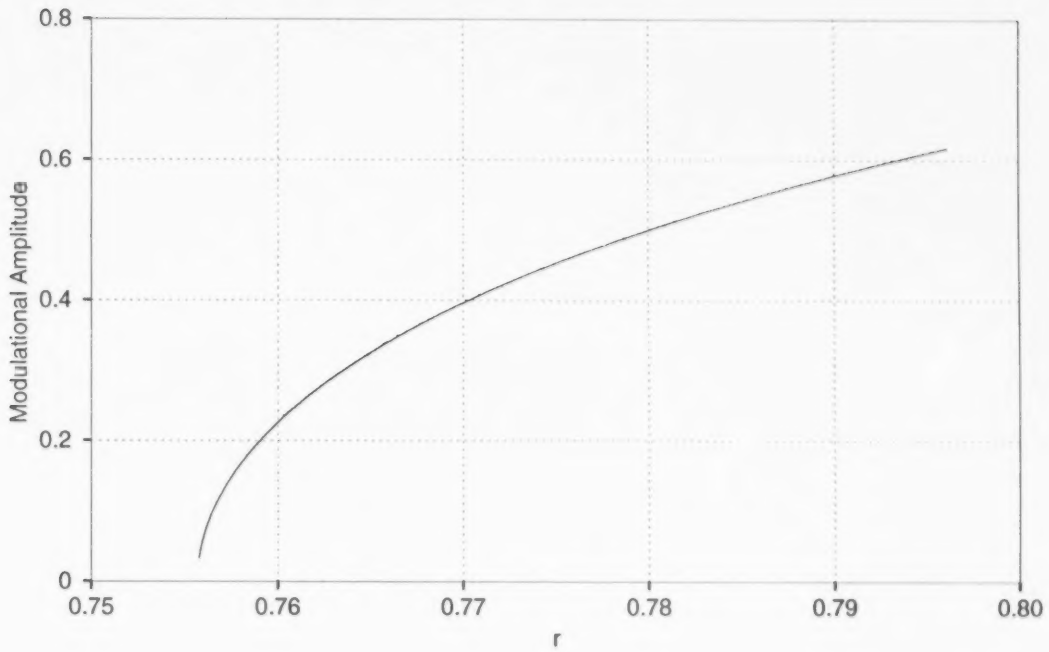

Figure 3.9: The trajectory made by the minimum of F in the positive quadrant of the parameter plane.

with ϵ near criticality. As for the question whether it has the observed power-law behavior, we turn to the log-log plot as shown in Fig. 3.11 where θ_o is seen to increase with ϵ according to

$$\theta_o = \mathcal{A}\epsilon^{\beta} \tag{3.104}$$

where the critical amplitude $\mathcal{A}$ and the critical exponent β have been found to be 3.43 and 0.50, respectively. Our critical exponent is therefore in excellent agreement (within a 0.6% error) with the experimental observation [17].

Next, we present the bifurcation diagram for the normalized domain spacing r in Figure 3.12. As shown in the figure, near criticality ($\epsilon \leq 0.001$), the domain width increases linearly with the reduced voltage. Although an experiment performed by

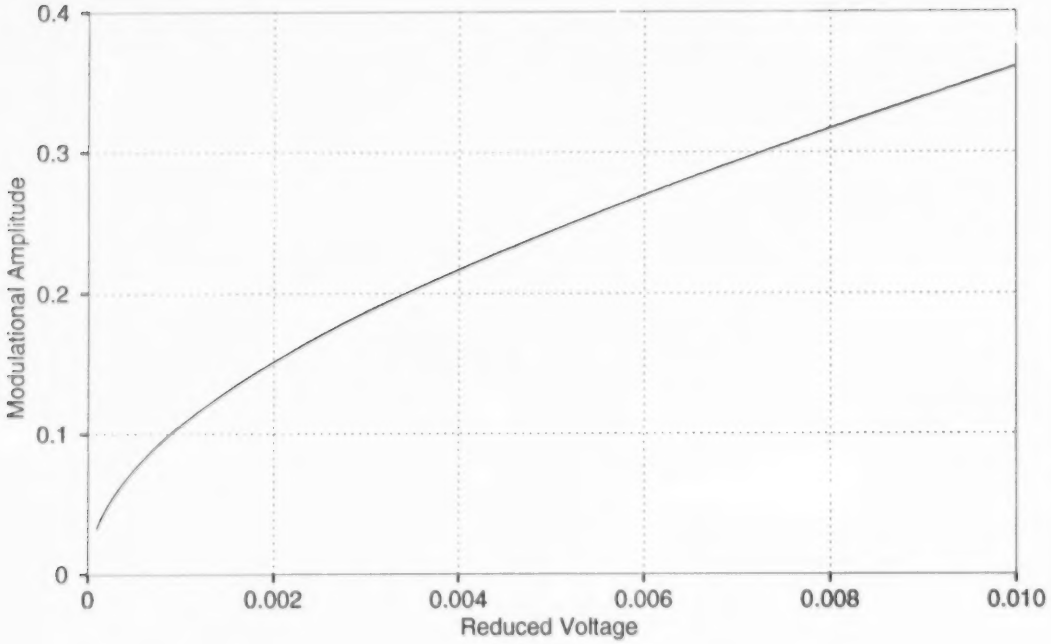

Figure 3.10: Bifurcation diagram for θ_o near criticality.

Joets and Ribota [16] shows that the domain width decreases with the reduced voltage, since their data were collected in a region where ϵ was much greater than 10^{-3}, their findings may not be in direct contradiction with ours. Perhaps, a cross over behavior exists somewhere between these two regimes. We could in principle extend our calculation to the region where ϵ would be of the order 10^{-1} so that comparisons with experiments would be possible. However, in this region, the amplitude θ_o becomes sufficiently large so that the higher order terms become significant. Since the fourth-order coefficient in our mean free energy expansion is not exact, we do not expect the bifurcation diagrams to truly reflect the behavior of the nematic system when θ_o is sufficiently large. Knowing from experiment that the $\epsilon^{1/2}$-dependence continues to hold true up to at least $\epsilon = 0.1$ [17], we can determine the range in which our

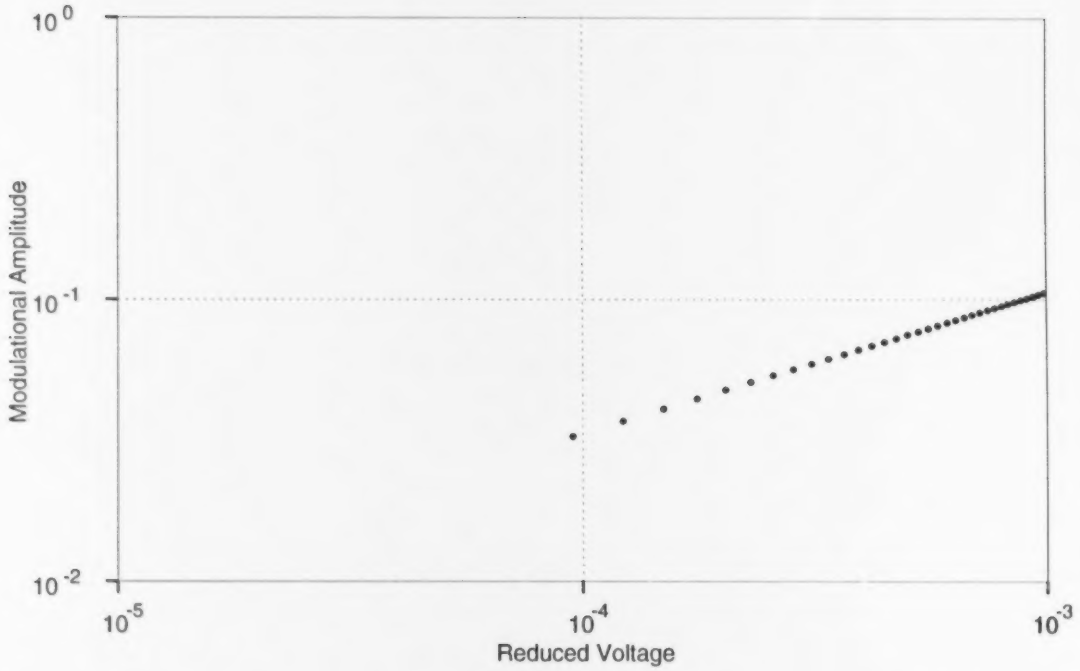

Figure 3.11: A log-log plot of the bifurcation diagram for θ_o.

analysis applies by extending the bifurcation diagrams until a significant departure from the experimental observation appears. The bifurcation diagrams for r and θ_o constructed over an extended range of ϵ are shown in Figure 3.13 and 3.14 respectively. We can clearly see that the amplitude θ_o departs from its $\epsilon^{1/2}$-dependence and increases drastically as ϵ becomes sufficiently greater than 10^{-3} while the normalized domain spacing r deviates from its linear dependence as ϵ exceeds the same value. Therefore, we must conclude that our model is valid only for $\epsilon \leq 0.001$.

So far, we have examined bifurcation diagrams for a fixed angular frequency. Here, we allow the angular frequency to vary and examine if this has an impact on our model. Figures 3.15 and 3.16 display, for a selection of reduced frequencies, the bifurcation curves for the normalized domain width r and the log-log plot of the

bifurcation curves for the amplitude θ_o, respectively. These diagrams strongly suggest that the dependence of these curves on ϵ is independent of angular frequency. The angular frequency dependence of the second-order coefficient C_2 has already been investigated previously: in effect, increasing the angular frequency simply leads to higher and higher threshold voltages until a cut-off angular frequency is reached. The fourth-order coefficient C_4 as a function of r and V_{rms} has once been shown in Fig. 3.5. Varying the angular frequency does not lead to any significant changes in these curves and thus no interesting observations can be made. However, if we plot the value of C_4 at the transition point as a function of the reduced angular frequency as shown in Fig. 3.17, we see that the critical value of C_4 is a decreasing function of ω' and becomes negative for ω' greater than a critical value $\omega'_c \approx 1.03$. As is well known in the theory of phase transition, the sign of C_4 determines the order of the transition: the transition is of the first-order if C_4 is negative but of the second-order if C_4 is positive. Hence, from Fig. 3.17, we predict that the transition line for the normal rolls is of second-order for ω' up to the critical value ω'_c and of first-order for $\omega' > \omega'_c$. In other words, there exists a tricritical point (a point where the order of transition changes from the second to the first order or vice versa) on the transition line at $\omega' = \omega'_c$. For the purpose of illustration, we have used the standard material parameters for MBBA to compute the curve for the critical C_4 in Fig. 3.17. We have then found that the curve behaves qualitatively the same even if a non-standard value (1.15) for the conductivity ratio $\sigma_\parallel/\sigma_\perp$ is used. If we choose $\sigma_\parallel = 1.19 \times 10^{-8}\Omega^{-1}m^{-1}$, the above critical value ω_c corresponds to the actual frequency $f_c = 46.8\ Hz$. Since our fourth-order coefficient is only approximate, a precise determination of the location of this tricritical point is not possible at this time and hence the above critical value should only be taken as a rough estimate.

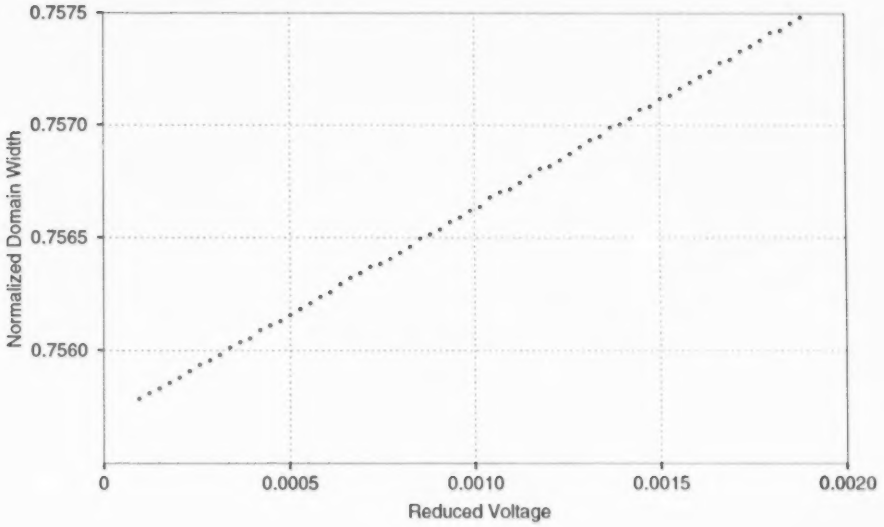

Figure 3.12: Bifurcation diagram for the normalized domain width r.

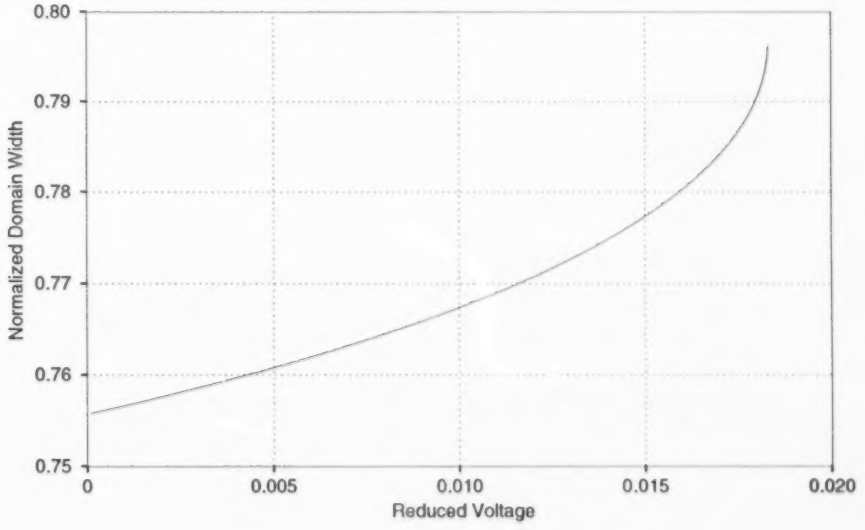

Figure 3.13: Bifurcation diagram for r plotted over an extended range of ϵ.

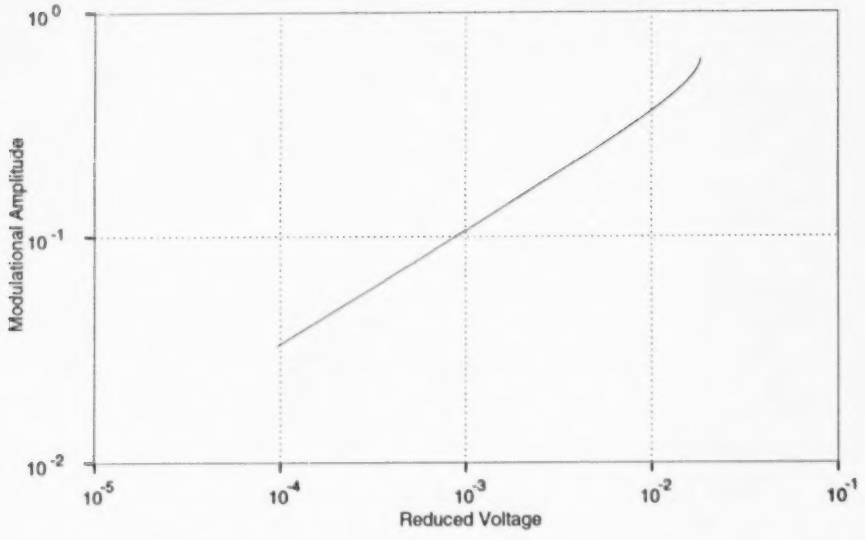

Figure 3.14: A log-log plot of the bifurcation diagram for θ_o over an extend range of the reduced voltage ϵ.

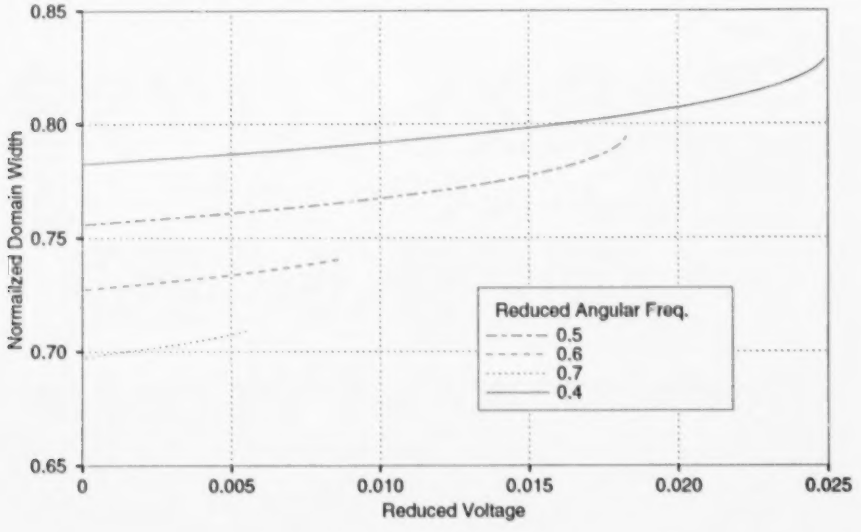

Figure 3.15: Bifurcation curves for r for various values of the reduced angular frequency.

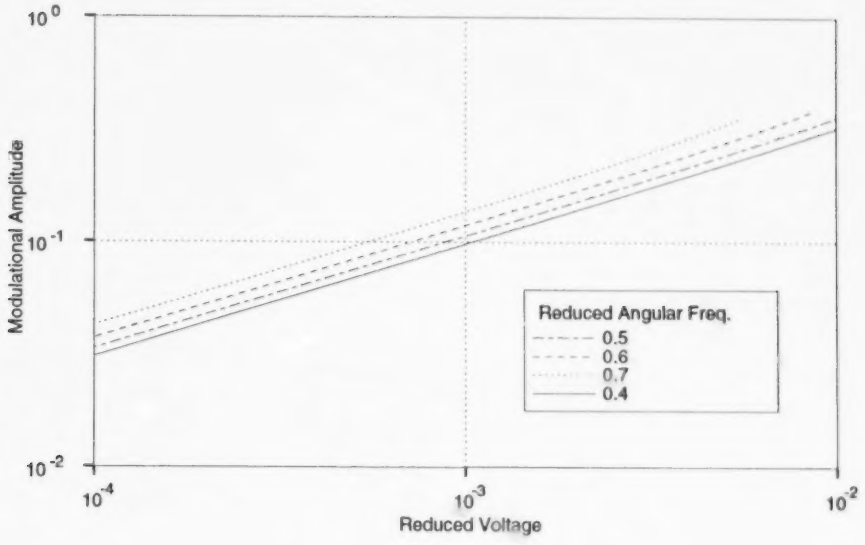

Figure 3.16: A log-log plot of the bifurcation curves for θ_o for different values of the reduced angular frequency.

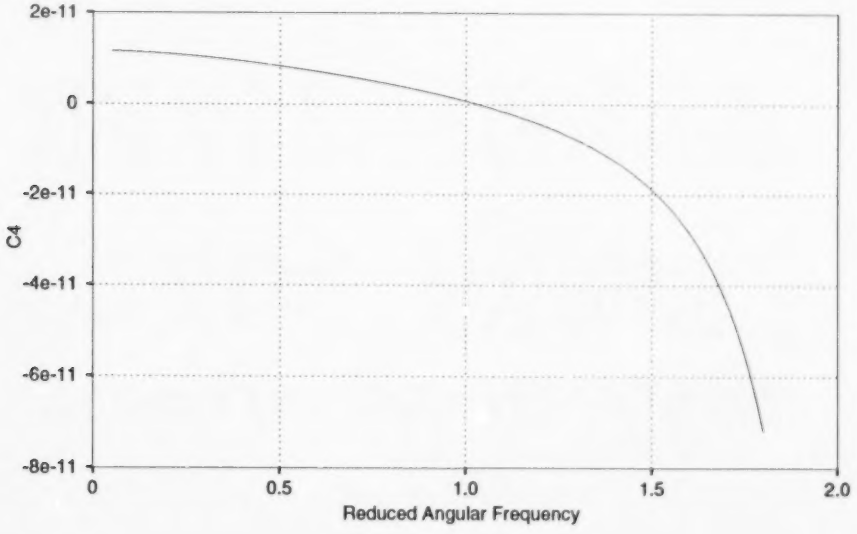

Figure 3.17: The value of C_4 at the transition point plotted as a function of the reduced angular frequency.

3.5 Summary

The use of a generalized free energy description in nonequilibrium processes is still open to debate. Nevertheless, we have proposed to use a phenomenological free energy to describe the voltage dependence of a nematic layer driven slightly out of equilibrium. In order to describe the evolution of the normal rolls slightly above the transition threshold, we have gone beyond the linear approximation and obtained the first nonlinear corrections through the use of series expansions similar to the ϵ-expansions. Our results compare qualitatively well with experimental observations. A good quantitative agreement is also obtained: the critical exponent for the amplitude θ_o deduced from the bifurcation diagram agrees with the experiment to within 0.6%. Although the results of our analysis have a rather limited range of validity ($0 < \epsilon < 0.001$) probably due to the early truncation of the series expansions of the field variables, the present model has an advantage over the multi-scale/amplitude description in that the $\epsilon^{1/2}$-behavior near the threshold is a direct consequence of the model and is not an a priori assumption.

Finally, our model has yielded another important prediction in regard to the formation of normal rolls. Unlike earlier results, the present model suggests that, at sufficiently high angular frequencies of the electric field, the regular straight rolls could be formed via a first-order transition. This prediction immediately points to the presence of a tricritical point on the low-lying transition line.

While discontinuous transitions from the rest-state to the oblique rolls have been commonly observed at low angular frequencies [15, 16, 44], a discontinuous transition from the rest-state to the normal straight rolls at a higher frequency has only been reported once so far. In a recent paper by Rehberg et. al [7], a subcritical (discontinuous) bifurcation of the uniformly aligned state to the normal straight rolls is reported and a bifurcation diagram demonstrating hysteretic behavior is also shown. The experiment however was performed at the fixed driving frequency of $45Hz$ (which comes close to our predicted tricritical point at $f = 46.8Hz$); therefore, the presence

of a tricritical point on the primary transition line cannot be established based on their experimental observations. From the theoretical point of view, the standard model (the linear and the weakly nonlinear analyses on the macroscopic deterministic equations of motion) predicts only a forward stationary (supercritical/continuous) bifurcation and no other method has yet implied subcritical bifurcations at the first transition thresholds. This puts our energy formalism in a very good perspective. Although obtaining further quantitative agreements with the experiment would certainly exceed the scope of our present analysis, the present approach allows one to see that the possibility of a subcritical bifurcation is due to the existence of local minima (metastable states) in the phenomenological free energy and thermal fluctuations is associated with fluctuations between these metastable states.

Chapter 4

Weakly Nonlinear Analysis

It was assumed for some time that a uniformly aligned nematic thin film in the presence of an *a.c.* electric field always transforms first into the normal straight rolls, as the field strength increases gradually. However, experiments later demonstrated that such a nematic thin film can also transform into the oblique (zigzag) rolls first provided the field angular frequencies are sufficiently low [15]. This observation immediately implied the existence of an unexpected triple point in the primary transition line, separating the rest state, the normal rolls and the oblique rolls. This subsequently led to a number of investigations attempting to provide theoretical models for the formation of oblique rolls at low angular frequencies [6, 42]. Since an additional periodicity is added to the convective structure in a new orthogonal direction, a three-dimensional analysis is indeed necessary. Furthermore, based on the notion that oblique rolls can be formed only if the director is given the necessary freedom, the director field is allowed to have two rotational degrees of freedom in all available models thus far. These include i) a comprehensive three-dimensional model based on a direct linearization of the basic equations of motion [42] and ii) a weakly nonlinear analysis which involves the use of multi-scale expansions [6]. The former demonstrated successfully that formation of the oblique rolls from the rest state is feasible below a critical angular frequency; however, quantitative agreement with experimen-

tal observations is still lacking. In the latter case, the extra degree of freedom given to the director combined with the use of fully rigid boundary conditions led to a system of very elaborate equations and expressions so complex that they can be analyzed only with the aid of a computer.

In this chapter, we re-examine the formation of oblique rolls from the uniformly aligned state. Using the technique of multi-scale expansion, we hope to demonstrate that the extra degree of freedom given to the director by the previous authors is not required for the oblique rolls to form and that an amplitude equation of Landau-Ginzburg type remains a valid equation for the small scale variations near the critical point. Semi-rigid (stress-free) boundary conditions will again be used throughout the chapter in the hope that our solutions will be expressible in closed analytical form and our expressions will become somewhat more manageable. Comparison with experimental observations will be made whenever possible.

4.1 The Multi-Scale Expansions

The underlying geometry of our calculation is identical to the setup described in the previous chapters. To recapitulate, we provide a simplified view of the nematic cell in a distorted state in Fig. 4.1 where the appropriate coordinate axes have been attached. Again, the applied electric field is denoted by $\vec{E}_a = E_o \cos(\omega t)\vec{k}$. We assume that the horizontal dimensions of the cell are so large that the effects of the lateral boundaries can be safely ignored.

In order to demonstrate that the extra rotational degree of freedom of the director is not needed for the oblique rolls to form, we ignore the azimuthal deviation of $\vec{n}$ and write it as a planar vector $\vec{n} = (\cos\theta, 0, \sin\theta)$. Then, the variation in the roll axes is a result of a phase modulation of these two components along the y-direction. This view is at least backed up by experimental observations: Joets et al. [16] and Ribotta et al. [15] have both concluded, based on their experiments, that deviations

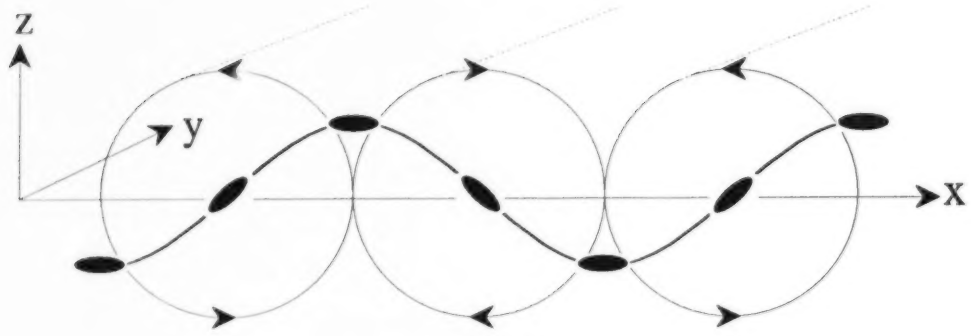

Figure 4.1: Basic setup of a nematic liquid crystal cell.

of $\vec{n}$ from the vertical (xOz) plane is not observable. This is also plausible in the vicinity of the triple point M. For simplicity, we express the total (sum of the applied and the induced fields) electric field in terms of the gradient of an electric potential ϕ as $\vec{E}_{tot} = \vec{E}_a - \vec{\nabla}\phi$ so that Ampere's law is satisfied automatically.

The fundamental equations of motion are again the same as those listed in Section 2.7.2. To repeat them once more, besides the constitutive equations, they are Maxwell's equations, the hydrodynamic equations, the incompressibility condition and the balance of torques relation. The solutions to be determined are the tilt angle θ, the velocity components $v_{(x,y,z)}$, the electric potential ϕ and the pressure P.

Since, as we have already mentioned in the previous chapter, it has been demonstrated experimentally by Rasenat et al. [17] that the modulational amplitude of the director field bifurcates as a square root of the reduced voltage $\epsilon = (V^2 - V_c^2)/V_c^2$ (where V and V_c are the *rms* applied and transition voltages respectively) slightly above a normal-roll instability, we can assume that this critical behavior is common to all of our solutions and we can further incorporate their nonlinear response into

the model by expanding each of them (denoted by g) in fractional powers of ϵ as

$$g = g_o\,\epsilon^{1/2} + g_1\,\epsilon + g_2\,\epsilon^{3/2} + \ldots \tag{4.1}$$

where g_i's are functions of space and possibly time to be determined later on and, by adopting solutions of this form, we have assumed a zero reference value for the scalar pressure P at the transition point.

Next, we follow the method of multi-scale analysis [36, 43]. Not too far from the transition threshold, nonlinearities are weak; both spatial and temporal modulations (due to these nonlinearities) of the basic periodic pattern are therefore slow. In order to separate the small scale variations in the alignment and the flow patterns near an instability, we introduce a set of slow space-time coordinates (X, Y, T) by scaling the regular coordinates according to [6]

$$X = \epsilon^{1/2}\,x, \quad Y = \epsilon^{1/2}\,y \quad \text{and} \quad T = \epsilon t \tag{4.2}$$

and demand that the coefficients g_i's be dependent upon both sets of coordinates i.e. $g_i(x, y, z, t; X, Y, T)$. This causes the spatial and the time derivatives appearing in the fundamental equations of motion to transform accordingly:

$$\begin{aligned}
\frac{\partial}{\partial x} &\longrightarrow \frac{\partial}{\partial x} + \epsilon^{1/2}\frac{\partial}{\partial X} \\
\frac{\partial}{\partial y} &\longrightarrow \frac{\partial}{\partial y} + \epsilon^{1/2}\frac{\partial}{\partial Y} \\
\frac{\partial}{\partial z} &\longrightarrow \frac{\partial}{\partial z} \\
\frac{\partial}{\partial t} &\longrightarrow \frac{\partial}{\partial t} + \epsilon\frac{\partial}{\partial T}
\end{aligned} \tag{4.3}$$

Furthermore, we expand the applied *rms* voltage V according to

$$V = V_c\left(1 + \frac{1}{2}\epsilon - \frac{1}{8}\epsilon^2 + \ldots\right). \tag{4.4}$$

Once the expansions in (4.1) are inserted into the equations of motion and the transformations of the spatial and the time derivatives are carried out, the equations of

motion can be immediately divided into sets of simultaneous equations, each of which is associated with a different order of ϵ. In a manner analogous to applying multi-scale analysis to the Rayleigh-Bénard convection[36], one sees that the lowest order set of equations will establish the lowest order solutions (the fundamental harmonics), θ_o, $v_o^{(x,y,z)}$, ϕ_o and p_o; the first higher order set will generate the second-order harmonics and the second higher order set a solvability condition that will quickly lead to an amplitude equation for the anisotropic system. The coefficient θ_o is not to be confused with the modulational amplitude of the director described in the previous chapter. Here, θ_o, $v_o^{(x,y,z)}$, ϕ_o and p_o are the lowest order coefficients in the ϵ-expansions of the form (4.1).

4.2 The Linear Balance

In this section, we will examine the equations due to the linear balance or, in other words, the lowest order ($O\left(\epsilon^{1/2}\right)$) set of equations. These equations are found to be:

(conservation of charge)

$$(\sigma_\parallel + \epsilon_\parallel \frac{\partial}{\partial t})\frac{\partial^2 \phi_o}{\partial x^2} + (\sigma_\perp + \epsilon_\perp \frac{\partial}{\partial t})\left(\frac{\partial^2 \phi_o}{\partial y^2} + \frac{\partial^2 \phi_o}{\partial z^2}\right) + \frac{\sqrt{2}V_c}{d}\left[\Delta\epsilon\omega\sin(\omega t) - \cos(\omega t)(\Delta\sigma + \Delta\epsilon\frac{\partial}{\partial t})\right]\frac{\partial \theta_o}{\partial x} = 0; \tag{4.5}$$

(incompressibility)

$$\frac{\partial v_o^x}{\partial x} + \frac{\partial v_o^y}{\partial y} + \frac{\partial v_o^z}{\partial z} = 0; \tag{4.6}$$

(torque-balance)

$$-\Delta\epsilon\frac{\sqrt{2}V_c}{d}\cos(\omega t)\left[\frac{\sqrt{2}V_c}{d}\theta_o\cos(\omega t) - \frac{\partial \phi_o}{\partial x}\right] - \left(k_{11}\frac{\partial^2 \theta_o}{\partial z^2} + k_{22}\frac{\partial^2 \theta_o}{\partial y^2} + k_{33}\frac{\partial^2 \theta_o}{\partial x^2}\right) + \alpha_3\frac{\partial v_o^x}{\partial z} + \alpha_2\frac{\partial v_o^z}{\partial x} + (\alpha_3 - \alpha_2)\frac{\partial \theta_o}{\partial t} = 0; \tag{4.7}$$

(x-component of hydrodynamic equation)

$$\rho\frac{\partial v_o^x}{\partial t} = \frac{1}{2}(\alpha_4 + \alpha_6 + \alpha_3)\frac{\partial^2 v_o^x}{\partial z^2} + \alpha_3\frac{\partial^2 \theta_o}{\partial t \partial z} - \frac{\partial p_o}{\partial x} + \frac{1}{2}(\alpha_4 + \alpha_6 - \alpha_3)\frac{\partial^2 v_o^z}{\partial x \partial z}$$

$$+\frac{1}{2}\left[(\alpha_4+\alpha_6+\alpha_3)\frac{\partial^2 v_o^x}{\partial y^2}+(\alpha_4+\alpha_6-\alpha_3)\frac{\partial^2 v_o^y}{\partial x\partial y}\right]$$
$$+(\alpha_1+\alpha_4+\alpha_5+\alpha_6)\frac{\partial^2 v_o^x}{\partial x^2}; \tag{4.8}$$

(y-component)

$$\rho\frac{\partial v_o^y}{\partial t} = \frac{1}{2}\frac{\partial}{\partial x}\left[(\alpha_4+\alpha_5+\alpha_2)\frac{\partial v_o^x}{\partial y}+(\alpha_4+\alpha_5-\alpha_2)\frac{\partial v_o^y}{\partial x}\right]$$
$$+\frac{1}{2}\alpha_4\frac{\partial}{\partial z}\left(\frac{\partial v_o^y}{\partial z}+\frac{\partial v_o^z}{\partial y}\right)+\alpha_4\frac{\partial^2 v_o^y}{\partial y^2}-\frac{\partial p_o}{\partial y}; \tag{4.9}$$

(z-component)

$$\rho\frac{\partial v_o^z}{\partial t} = \frac{1}{2}\alpha_4\frac{\partial}{\partial y}\left(\frac{\partial v_o^y}{\partial z}+\frac{\partial v_o^z}{\partial y}\right)+\alpha_4\frac{\partial^2 v_o^z}{\partial z^2}-\frac{\partial p_o}{\partial z}+\alpha_2\frac{\partial^2\theta_o}{\partial t\partial x}$$
$$-\left[\epsilon_\parallel\frac{\partial^2\phi_o}{\partial x^2}+\epsilon_\perp\left(\frac{\partial^2\phi_o}{\partial y^2}+\frac{\partial^2\phi_o}{\partial z^2}\right)-\triangle\epsilon\frac{\sqrt{2}V_c}{d}\cos(\omega t)\frac{\partial\theta_o}{\partial x}\right]\frac{\sqrt{2}V_c}{d}\cos(\omega t)$$
$$+\frac{1}{2}(\alpha_4+\alpha_5+\alpha_2)\frac{\partial^2 v_o^x}{\partial x\partial z}+\frac{1}{2}(\alpha_4+\alpha_5-\alpha_2)\frac{\partial^2 v_o^z}{\partial x^2} \tag{4.10}$$

where $\triangle\varepsilon$ and $\triangle\sigma$ are respectively the dielectric anisotropy $(\varepsilon_\parallel-\varepsilon_\perp)$ and the conduction anisotropy $(\sigma_\parallel-\sigma_\perp)$. The constitutive equation $J_i=\sigma_{ij}E_j$ and Gauss's law have been used to replace the current $\vec{J}$ and the charge density q in the conservation of charge equation.

In order to write down their solutions in closed analytical form, we impose the semi-rigid boundary conditions on them. This means that we allow the tangential velocities at the vertical boundary surfaces to be small but nonzero i.e. $v_{(x,y)}\neq 0$ at $z=\pm d/2$.

Following the usual approach in the amplitude description of pattern-forming systems, we separate the small scale variations of the pattern near threshold by introducting a complex amplitude $A(X,Y,T)$ and then write each solution as a basic periodic wave with a slowly varying amplitude. If the spatial frequencies in the x-, the y- and the z-directions are denoted by p_x, p_y and q, respectively, the solutions can be written as

$$\theta_o = [A(X,Y,T)e^{i\vec{p}\cdot\vec{r}}+c.c.]\cos(qz); \tag{4.11}$$

$$v_o^x = [A(X,Y,T)e^{i\vec{p}\cdot\vec{r}} + c.c.]D_1 \sin(qz); \tag{4.12}$$

$$v_o^y = [A(X,Y,T)e^{i\vec{p}\cdot\vec{r}} + c.c.]D_2 \sin(qz); \tag{4.13}$$

$$v_o^z = [A(X,Y,T)e^{i\vec{p}\cdot\vec{r}} - c.c.]D_3 \cos(qz); \tag{4.14}$$

$$p_o = [A(X,Y,T)e^{i\vec{p}\cdot\vec{r}} - c.c.]G \sin(qz); \tag{4.15}$$

$$\phi_o = [A(X,Y,T)e^{i\vec{p}\cdot\vec{r}} - c.c.][B_1 \cos(\omega t) + B_2 \sin(\omega t)] \cos(qz) \tag{4.16}$$

where the dot product $\vec{p}\cdot\vec{r}$ denotes $p_x x + p_y y$; $c.c$ is the complex conjugate of $A(X,Y,T)e^{i\vec{p}\cdot\vec{r}}$ and $B_{1,2}$, $D_{1,2,3}$ and G are constant coefficients. Note that, under the previously stated experimental conditions (below the cut off frequency), the director, the flow and the pressure are all time independent. The only time dependent part comes in through the charge oscillation driven by the *a.c.* electric field. This is manifested by a time dependent electric potential.

Substituting these solutions into the above lowest order equations (4.5)-(4.10) results in a set of algebraic equations for the constant coefficients appearing in Eqs. (4.11)-(4.16). Due to the tediousness of the algebra involved, which does not seem to be particularly instructive, we omit the intermediate steps and only report here the expressions for these constant coefficients found by solving these algebraic equations:

$$B_1 = \frac{-iap_x(l_2\Delta\sigma + \omega^2 l_1 \Delta\varepsilon)}{\omega^2 l_1^2 + l_2^2} \tag{4.17}$$

$$B_2 = \frac{-ia\omega p_x(l_2\Delta\varepsilon - l_1\Delta\sigma)}{\omega^2 l_1^2 + l_2^2} \tag{4.18}$$

$$D_1 = \frac{aqp_x\Omega}{l_3} \tag{4.19}$$

$$D_2 = \frac{aqp_y l_5 \Omega}{2l_3 l_4} \tag{4.20}$$

$$D_3 = \frac{i}{q}(D_1 p_x + D_2 p_y) \tag{4.21}$$

$$G = \frac{i[(2n_4 - n_6)p_x p_y D_1 + l_4 D_2]}{2p_y} \tag{4.22}$$

where

$$a = \frac{\sqrt{2}V_c}{d} \tag{4.23}$$

$$n_1 = \alpha_1 + \alpha_4 + \alpha_5 + \alpha_6 \tag{4.24}$$

$$n_2 = \frac{1}{2}(\alpha_4 + \alpha_6 + \alpha_3) \tag{4.25}$$

$$n_3 = \frac{1}{2}(\alpha_4 + \alpha_6 - \alpha_3) \tag{4.26}$$

$$n_4 = \frac{1}{2}(\alpha_4 + \alpha_5 + \alpha_2) \tag{4.27}$$

$$n_5 = \frac{1}{2}(\alpha_4 + \alpha_5 - \alpha_2) \tag{4.28}$$

$$n_6 = \alpha_4 \tag{4.29}$$

$$l_1 = \varepsilon_{\|}p_x^2 + \varepsilon_{\perp}(q^2 + p_y^2) \tag{4.30}$$

$$l_2 = \sigma_{\|}p_x^2 + \sigma_{\perp}(q^2 + p_y^2) \tag{4.31}$$

$$l_3 = [(n_1 - n_3 - n_4 + n_6)p_x^2 + n_2(q^2 + p_y^2)](q^2 + p_y^2) + n_5 p_x^4 \tag{4.32}$$

$$l_4 = 2n_5 p_x^2 + n_6(q^2 + p_y^2) \tag{4.33}$$

$$l_5 = (2n_1 - 2n_3 - 2n_4 + n_6)p_x^2 + 2n_2(q^2 + p_y^2) \tag{4.34}$$

$$\Omega = a\triangle\varepsilon p_x - il_1 B_1. \tag{4.35}$$

Besides these algebraic expressions, the above equations also impose a compatibility condition on the coefficients. After some re-arrangement, this condition takes on the following form:

$$V_c^2 = -\frac{\pi^2}{\varepsilon_{\perp}}(k_{11} + k_{22}r_y^2 + k_{33}r_x^2)\left\{\left[(\alpha_3 - \alpha_2 r_x^2)r_x^2 - \alpha_2 r_x^2 r_y^2 \xi_1\right]\left(\frac{a - \tau\beta - 1}{\xi_o}\right)\right.$$
$$\left.+(a-1)\left(\frac{\beta r_x^2}{br_x^2 + r_y^2 + 1} - 1\right)\right\}^{-1} \tag{4.36}$$

with

$$r_i = \frac{p_i}{q};\ a = \frac{\varepsilon_{\|}}{\varepsilon_{\perp}};\ b = \frac{\sigma_{\|}}{\sigma_{\perp}};\ \tau = \frac{ar_x^2 + r_y^2 + 1}{br_x^2 + r_y^2 + 1};\ \omega' = \omega\frac{\varepsilon_{\perp}}{\sigma_{\perp}}; \tag{4.37}$$

$$\beta = \left[(b-1) + \omega'^2\tau(a-1)\right]/(1 + \omega'^2\tau^2); \tag{4.38}$$

$$\xi_o = \left[(\alpha_1 - \alpha_2 + \alpha_4 + \alpha_6)r_x^2 + (\alpha_4 + \alpha_6 + \alpha_3)(1 + r_y^2)/2\right](1 + r_y^2)$$

$$+ (\alpha_4 + \alpha_5 - \alpha_2) r_x^4/2; \tag{4.39}$$

$$\xi_1 = \left[(2\alpha_1 - 2\alpha_2 + 2\alpha_6 + \alpha_4) r_x^2 + (\alpha_4 + \alpha_3 + \alpha_6)(1 + r_y^2)\right] / \left[(\alpha_4 + \alpha_5 - \alpha_2) r_x^2 + \alpha_4 (1 + r_y^2)\right]. \tag{4.40}$$

This condition functions in exactly the same way as the compatibility condition (3.72) derived in the linear theory. Moreover, comparing these two conditions, we see that the above condition has an extra dimension (r_y), thereby allowing oblique rolls to form.

With r_x and r_y taken as the state parameters, at each modified angular frequency ω', the transition voltage is a three-dimensional surface and the threshold voltage that makes physical sense must correspond to its minimum. We display in Fig. 4.2 contour plots of V_c^2 at three different reduced angular frequencies. As shown in the figure, the surface bifurcates from a single-well to a double-well type as ω' falls below a critical value ω_c'. Since having a non-zero value of r_y at the threshold means the presence of a periodic distortion in the y-direction, this bifurcation can be interpreted as the normal-to-oblique rolls transition. Moreover, the precise location of this transition point on the reduced angular frequency axis can be determined by plotting the value of r_y at the threshold as a function of ω' as in Fig. 4.3 where it can be seen that the threshold value of r_y rises very sharply from zero near the transition angular frequency ω_c'. Since, for $\omega' > \omega_c'$, the rest state transforms into the normal rolls at the threshold but, for $\omega' < \omega_c'$, the oblique rolls are formed instead, the above bifurcation point must correspond to a triple point in the V-ω' stability diagram.

This triple point has been observed in a number of experiments [15, 44] involving MBBA and Merck Phase-V nematic liquid crystals. Unfortunately, only measurements made on Merck Phase-V compound have been reported so far. Due to the lack of experimental information on the physical parameters of this compound, a direct comparison of our analysis with experiments is not possible at this time. However, an indirect indication on the validity of our calculation can be obtained by using different sets of commonly known physical parameters. For this purpose, we have chosen to

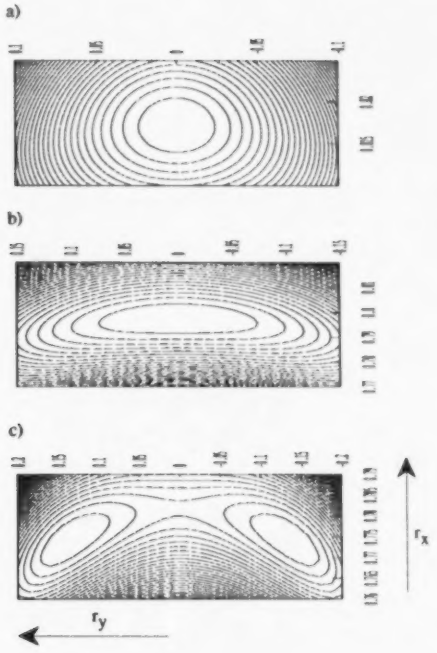

Figure 4.2: Contour plots of the surface (4.36) at **a)** $\omega' > \omega_c'$; **b)** $\omega' \approx \omega_c'$ and **c)** $\omega' < \omega_c'$.

use the parameters for MBBA [6] and PAA [45] to carry out our comparison. We constrast, in Fig. 4.4, the material properties of MBBA with those of Merck Phase-V by superimposing their first transition thresholds on the same graph. The threshold voltage of MBBA is seen to rise more sharply as the cut-off frequency is approached. Clearly, the physical parameters of MBBA can be quite different from those of Merck Phase-V. To account for these material differences, we adjust the elastic constant k_{33} to obtain an optimal fit to the experimental data, still using the highest experimental voltage point as a calibration for the floating parameter $\sigma_\perp$. Then, the elastic constant k_{22} which is mainly responsible for the elastic torque against any twist deformation is finely tuned so that the calculated triple-point falls within the observed range of angular frequency without losing the overall agreement. The experimental

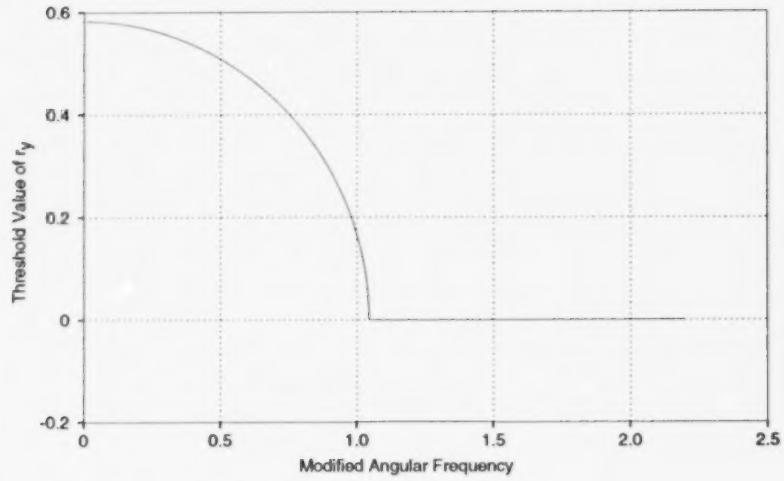

Figure 4.3: The threshold value of the state parameter r_y as a function of the modified angular frequency ω'.

data on Merck Phase-V together with the first- and the second-order transition lines, calculated from the MBBA material parameters by means of minimization of (4.36), are shown in Fig. 4.5 where excellent agreement with the experiments is evident. A similar fit is also obtained for PAA and is shown in Fig. 4.6. The physical parameters for MBBA and PAA used in the theoretical calculation are listed in Table 4.2. Comparing these two sets of parameters, we see that the results obtained using the PAA parameters are more favorable for two following reasons. First, PAA has a natural dielectric anisotropy of -0.19 which corresponds very closely to that (-0.2) of Merck Phase-V used in the experiments [15, 44]; whereas, for MBBA, its dielectric constants had to be modified in the calculation. Secondly, the changes made to the elastic constants of PAA are within 58% of their original values while, for MBBA, the changes made to the same constants can be as large as 141% of their original values.

It is now necessary to combine all the low-order equations introduced in this section into a single homogeneous equation involving only one of the field variables

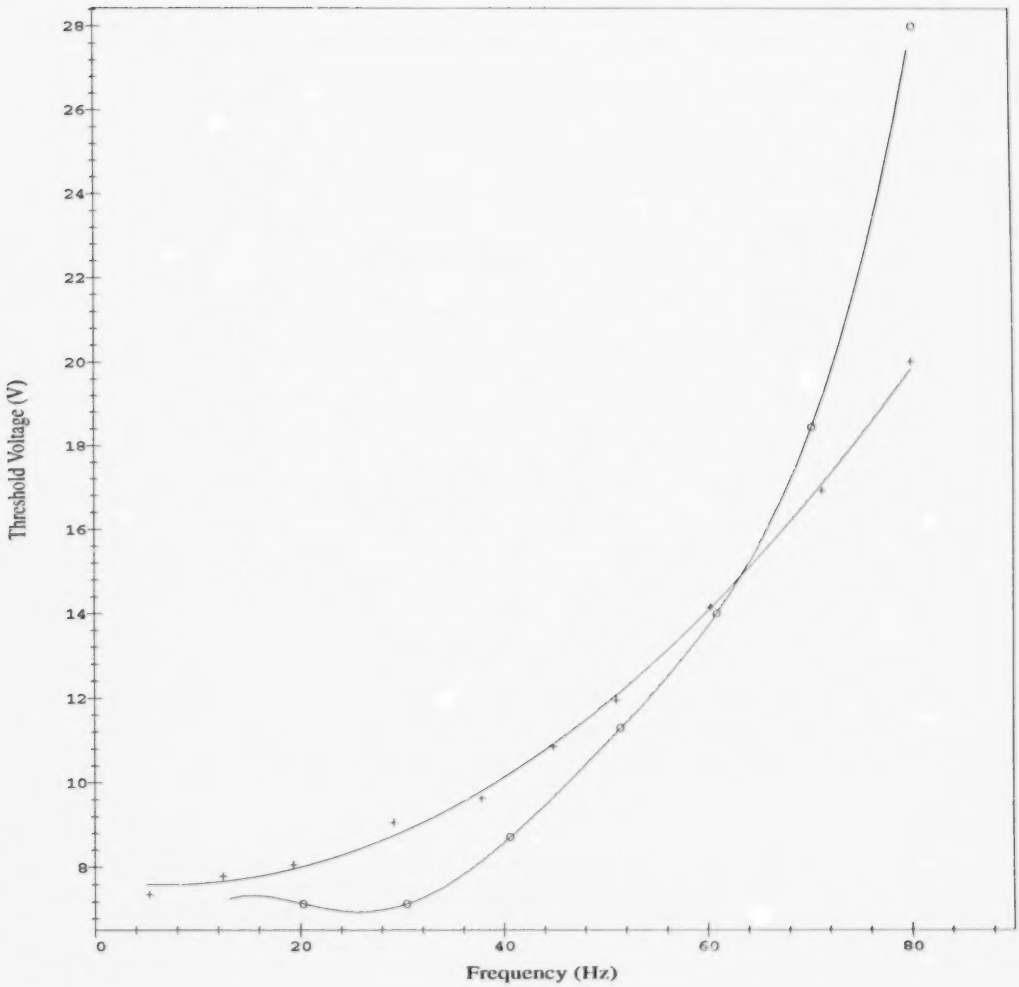

Figure 4.4: Observed first transition thresholds of MBBA [13] (circle) and Merck Phase-V [15] ("+").

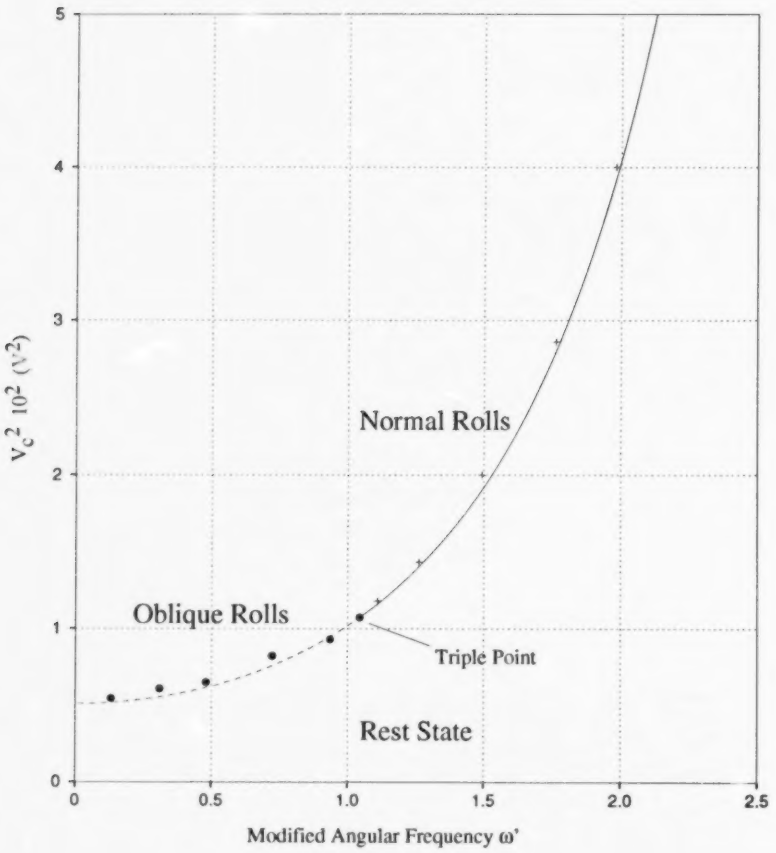

Figure 4.5: Structure diagram for the low-order instabilities using MBBA material parameters. The solid and the dashed lines represent respectively the calculated threshold voltages for the normal- and the oblique-roll formations. The "+" and the dots, on the other hand, correspond to the experimentally measured threshold voltages for the normal- and the oblique-roll formations in Merck Phase-V, respectively.

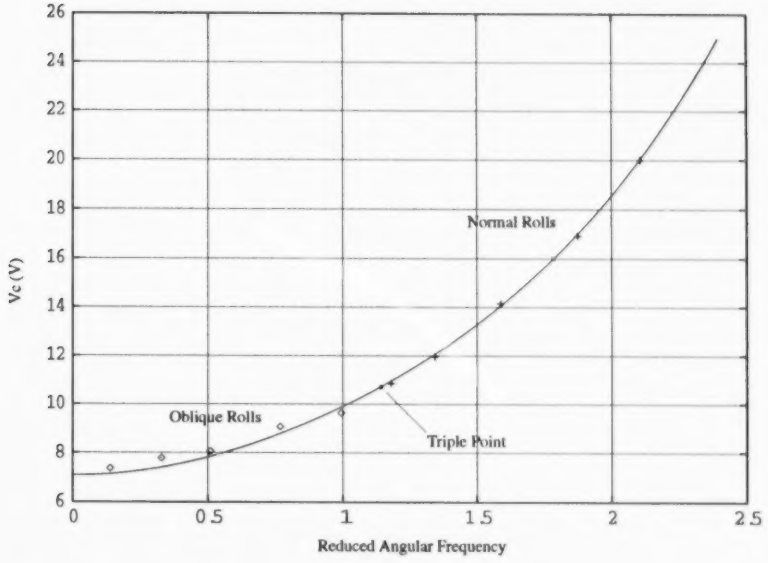

Figure 4.6: Structure diagram for the low-order instabilities using PAA material parameters. The solid line is the theoretical transition line. The "+" and the diamonds correspond to the experimentally measured threshold voltages for the normal- and the oblique-roll formations in Merck Phase-V, respectively.

Parameter	*PAA (122°C)*	*MBBA*
k_{11}	6.9×10^{-12} N	6.10×10^{-12} N
k_{22}	6.0×10^{-12} N	0.5×10^{-12} N
k_{33}	15.0×10^{-12} N	17.5×10^{-12} N
$\alpha 1$	4.0×10^{-3} Kg/m/s	6.5×10^{-3} Kg/m/s
$\alpha 2$	-6.9×10^{-3} Kg/m/s	-77.5×10^{-3} Kg/m/s
$\alpha 3$	-0.2×10^{-3} Kg/m/s	-1.2×10^{-3} Kg/m/s
$\alpha 4$	6.8×10^{-3} Kg/m/s	83×10^{-3} Kg/m/s
$\alpha 5$	5.0×10^{-3} Kg/m/s	46×10^{-3} Kg/m/s
$\alpha 6$	-2.0×10^{-3} Kg/m/s	-35×10^{-3} Kg/m/s
$\epsilon_{\parallel}$	$5.61 \times \varepsilon_o$	$4.937 \times \varepsilon_o$
$\epsilon_{\perp}$	$5.8 \times \varepsilon_o$	$5.137 \times \varepsilon_o$
$\sigma_{\perp}$	$1.23 \times 10^{-8}\Omega^{-1}m^{-1}$	$1.15 \times 10^{-8}\Omega^{-1}m^{-1}$
$\sigma_{\parallel}/\sigma_{\perp}$	≈ 1.5	≈ 1.5

Table 4.1: Physical parameters for MBBA [6] and PAA [45] nematic liquid crystals. These values are used in the calculations of the stability diagrams in Figs. 4.5 and 4.6. The elastic constants k_{22} and k_{33} have been adjusted to yield optimal fits.

i.e.

$$\mathcal{L}_o \zeta_o = 0 \tag{4.41}$$

where $\mathcal{L}_o$ is a linear differential operator and ζ_o is one of the low-order field components. This step is extremely important in the method of multi-scale expansions because it allows us to establish a criterion of uniformity (non-singular behavior) for the ϵ-expansion (4.1) [36, 43]. As our analysis continues, the linear differential operator $\mathcal{L}_o$ will emerge once again in a higher order equation of the form

$$\mathcal{L}_o \zeta_i = L\zeta_o + \ldots \tag{4.42}$$

where ζ_i is a higher order coefficient in the ϵ-expansion, L is another linear opera-

tor and "..." represents the driving terms not proportional to the eigenfunction ζ_o. Since a driving term proportional to the eigenfunction of the operator $\mathcal{L}_o$ will lead to singular behavior in ζ_i, if we insist that the ϵ-expansion be uniform, then the term $L\zeta_o$ (the secular term) must vanish identically. This condition

$$L\zeta_o = 0 \tag{4.43}$$

will eventually lead to an equation for the slowly varying amplitude $A(X, Y, T)$.

To begin, we differentiate the x- (4.8) and the y- (4.9) components of the hydrodynamic equation with respect to y and x, respectively. Then, after subtracting these two equations to remove the pressure term and applying the incompressibility condition (4.6), we obtain the following equation:

$$\mathcal{L}_1 \frac{\partial v_o^x}{\partial y} - \mathcal{L}_2 \frac{\partial v_o^y}{\partial x} = 0 \tag{4.44}$$

where the operators $\mathcal{L}_1$ and $\mathcal{L}_2$ are defined respectively as

$$\mathcal{L}_1 = (\alpha_1 - \alpha_2 + \frac{\alpha_4}{2} + \alpha_6)\frac{\partial^2}{\partial x^2} + \frac{1}{2}(\alpha_4 + \alpha_6 + \alpha_3)\left(\frac{\partial^2}{\partial y^2} + \frac{\partial^2}{\partial z^2}\right) \tag{4.45}$$

$$\mathcal{L}_2 = \frac{1}{2}(\alpha_4 + \alpha_5 - \alpha_2)\frac{\partial^2}{\partial x^2} + \frac{\alpha_4}{2}\left(\frac{\partial^2}{\partial y^2} + \frac{\partial^2}{\partial z^2}\right). \tag{4.46}$$

If, instead, we differentiate the x- and the z- (4.10) components of the hydrodynamic equation with respect to z and x, respectively, and combine the equations in exactly the same way as above, then we get

$$\frac{\partial}{\partial x}\left[\varepsilon_\parallel \frac{\partial^2 \phi_o}{\partial x^2} + \varepsilon_\perp \left(\frac{\partial^2 \phi_o}{\partial y^2} + \frac{\partial^2 \phi_o}{\partial z^2}\right) - \triangle\varepsilon a\cos(\omega t)\frac{\partial \theta_o}{\partial x}\right] a\cos(\omega t) + \mathcal{L}_1 \frac{\partial v_o^x}{\partial z} - \mathcal{L}_2 \frac{\partial v_o^z}{\partial x} = 0 \tag{4.47}$$

where $a = \sqrt{2}V_c/d$. Differentiating Eqn. (4.44) with respect to y and Eqn. (4.47) with respect to z and adding them, we can simplify the resultant equation to

$$\mathcal{L}v_o^x + \frac{\partial^2}{\partial z \partial x}\left[\varepsilon_\parallel \frac{\partial^2 \phi_o}{\partial x^2} + \varepsilon_\perp \left(\frac{\partial^2 \phi_o}{\partial y^2} + \frac{\partial^2 \phi_o}{\partial z^2}\right) - \triangle\varepsilon a\cos(\omega t)\frac{\partial \theta_o}{\partial x}\right] a\cos(\omega t) = 0 \tag{4.48}$$

where

$$\mathcal{L} = (\alpha_1 - \alpha_2 + \alpha_4 + \alpha_6)\frac{\partial^2}{\partial x^2}\left(\frac{\partial^2}{\partial y^2} + \frac{\partial^2}{\partial z^2}\right) + \frac{1}{2}(\alpha_4 + \alpha_6 + \alpha_3)\left(\frac{\partial^2}{\partial y^2} + \frac{\partial^2}{\partial z^2}\right)\left(\frac{\partial^2}{\partial y^2} + \frac{\partial^2}{\partial z^2}\right) + \frac{1}{2}(\alpha_4 + \alpha_5 - \alpha_2)\frac{\partial^4}{\partial x^4}. \tag{4.49}$$

We will now leave this equation and return to it momentarily. Next, we operate on the torque-balance equation (4.7) with the operator $\mathcal{L}_2$ from the left and combine it with Eqn. (4.47) to eliminate the term involving v_o^z. This results in

$$-\triangle\varepsilon a\cos(\omega t)\mathcal{L}_2\left[\theta_o a\cos(\omega t) - \frac{\partial\phi_o}{\partial x}\right] - \mathcal{L}_2\tilde{\triangle}\theta_o + (\alpha_3\mathcal{L}_2 + \alpha_2\mathcal{L}_1)\frac{\partial v_o^x}{\partial z} + \alpha_2\frac{\partial}{\partial x}\left[\varepsilon_\parallel\frac{\partial^2\phi_o}{\partial x^2} + \varepsilon_\perp\left(\frac{\partial^2\phi_o}{\partial y^2} + \frac{\partial^2\phi_o}{\partial z^2}\right) - \triangle\varepsilon a\cos(\omega t)\frac{\partial\theta_o}{\partial x}\right] \times a\cos(\omega t) = 0 \tag{4.50}$$

where

$$\tilde{\triangle} = k_{11}\frac{\partial^2}{\partial z^2} + k_{22}\frac{\partial^2}{\partial y^2} + k_{33}\frac{\partial^2}{\partial x^2}. \tag{4.51}$$

If we now operate on this equation from the left with the operator $\mathcal{L}$, we can make use of Eqn. (4.48) to eliminate the remaining velocity term. The resultant equation, after being differentiated with respect to x and averaged over time (one cycle), can be written as

$$\left\langle a\cos(\omega t)\left(\triangle\varepsilon\mathcal{L}\mathcal{L}_2 + \lambda_1\lambda_2\right)\frac{\partial^2\phi_o}{\partial x^2}\right\rangle - \left[\mathcal{L}\mathcal{L}_2\tilde{\triangle} + \frac{\triangle\varepsilon a^2}{2}\left(\mathcal{L}\mathcal{L}_2 + \lambda_1\frac{\partial^2}{\partial x^2}\right)\right]\frac{\partial\theta_o}{\partial x} = 0 \tag{4.52}$$

where the angle brackets denote average over time t and the operators λ_1 and λ_2 are defined respectively as

$$\lambda_1 = \alpha_2\mathcal{L} - (\alpha_3\mathcal{L}_2 + \alpha_2\mathcal{L}_1)\frac{\partial^2}{\partial z^2} \tag{4.53}$$

$$\lambda_2 = \varepsilon_\parallel\frac{\partial^2}{\partial x^2} + \varepsilon_\perp\left(\frac{\partial^2}{\partial y^2} + \frac{\partial^2}{\partial z^2}\right). \tag{4.54}$$

Finally, we use the conservation of charge equation (4.5) to eliminate one of the field components from the above equation. This can be accomplished by multiplying

Eqn. (4.5) by $\cos(\omega t)$ from the left and averaging it over t:

$$\frac{\triangle\sigma a}{2}\frac{\partial\theta_o}{\partial x} = \langle\cos(\omega t)\lambda_3\phi_o\rangle \tag{4.55}$$

where the operator λ_3 is written as

$$\lambda_3 = (\sigma_\parallel + \varepsilon_\parallel\frac{\partial}{\partial t})\frac{\partial^2}{\partial x^2} + (\sigma_\perp + \varepsilon_\perp\frac{\partial}{\partial t})\left(\frac{\partial^2}{\partial y^2} + \frac{\partial^2}{\partial z^2}\right). \tag{4.56}$$

Then, substituting the above expression for $\partial\theta_o/\partial x$ into Eqn. (4.52), we arrive at the following homogeneous equation for the spatial part of ϕ_o:

$$\mathcal{L}_o\phi_o = 0 \tag{4.57}$$

where $\mathcal{L}_o$ is given by

$$\cos(\omega t)\left\{\left[\mathcal{L}\mathcal{L}_2\tilde{\triangle} + \frac{\triangle\varepsilon a^2}{2}\left(\mathcal{L}\mathcal{L}_2 + \lambda_1\frac{\partial^2}{\partial x^2}\right)\right]\lambda_3 - \frac{\triangle\sigma a^2}{2}\left(\triangle\varepsilon\mathcal{L}\mathcal{L}_2 + \lambda_1\lambda_2\right)\frac{\partial^2}{\partial x^2}\right\} \tag{4.58}$$

and average over time is automatically implied. Since (4.16) is a solution to the low-order fundamental equations and we have chosen $\vec{p}$ to satisfy Eqn. (4.36), (4.16) is automatically an eigenfunction of $\mathcal{L}_o$.

4.3 First Nonlinear Balance

We present, in this section, the set of equations due to the first nonlinear balance (i.e. the ϵ-order equations) and their solutions. Employing some of the linear operators from the previous section, we can express the conservation of charge equation at order ϵ as follows:

$$\begin{aligned}
&\lambda_3\phi_1 + a\left[\triangle\varepsilon\omega\sin(\omega t) - \cos(\omega t)\left(\triangle\sigma - \triangle\varepsilon\frac{\partial}{\partial t}\right)\right]\frac{\partial\theta_1}{\partial x} \\
&+ 2\left[\left(\sigma_\parallel + \varepsilon_\parallel\frac{\partial}{\partial t}\right)\frac{\partial^2}{\partial x\partial X} + \left(\sigma_\perp + \varepsilon_\perp\frac{\partial}{\partial t}\right)\frac{\partial^2}{\partial y\partial Y}\right]\phi_o \\
&+ \left(\triangle\sigma + \triangle\varepsilon\frac{\partial}{\partial t}\right)\left[\frac{\partial}{\partial x}\left(\theta_o\frac{\partial\phi_o}{\partial z}\right) + \frac{\partial}{\partial z}\left(\theta_o\frac{\partial\phi_o}{\partial x}\right)\right] \\
&+ a\left[\triangle\varepsilon\omega\sin(\omega t) - \cos(\omega t)\left(\triangle\sigma - \triangle\varepsilon\frac{\partial}{\partial t}\right)\right]\left(\frac{\partial\theta_o}{\partial X} + 2\vartheta_o\frac{\partial\theta_o}{\partial z}\right) = 0.
\end{aligned} \tag{4.59}$$

This equation can be used immediately to solve for the electric potential ϕ_1 if we assume that

$$\theta_1 = 0 \tag{4.60}$$

With this assumption, we substitute the neutral solutions ϕ_o and θ_o found in the previous section into Eqn. (4.59) and put

$$\begin{aligned}
\phi_1 &= \left\{\left(A^2 e^{2i\vec{p}\cdot\vec{r}} + A^{*2} e^{-2i\vec{p}\cdot\vec{r}}\right)\left[a_1 \sin(\omega t) + a_2 \cos(\omega t)\right]\right. \\
&\quad \left. + |A|^2 \left[a_3 \sin(\omega t) + a_4 \cos(\omega t)\right]\right\} \sin(2qz) \\
&\quad + \left\{\left(\frac{\partial A}{\partial X} e^{i\vec{p}\cdot\vec{r}} + \frac{\partial A^*}{\partial X} e^{-i\vec{p}\cdot\vec{r}}\right)\left[a_5 \sin(\omega t) + a_6 \cos(\omega t)\right]\right. \\
&\quad \left. + \left(\frac{\partial A}{\partial Y} e^{i\vec{p}\cdot\vec{r}} + \frac{\partial A^*}{\partial Y} e^{-i\vec{p}\cdot\vec{r}}\right)\left[a_7 \sin(\omega t) + a_8 \cos(\omega t)\right]\right\} \cos(qz).
\end{aligned} \tag{4.61}$$

This leads us to the following expressions for the coefficients a_1 to a_8:

$$a_1 = \frac{-q\left[(2\mu_2 - \beta_2)\omega\chi_1 + (\beta_1 - 2\mu_1)\chi_2\right]}{4(\chi_2^2 + \omega^2\chi_1^2)} \tag{4.62}$$

$$a_2 = \frac{-q\left[(2\mu_2 - \beta_2)\chi_2 - (\beta_1 - 2\mu_1)\chi_1\omega\right]}{4(\chi_2^2 + \omega^2\chi_1^2)} \tag{4.63}$$

$$a_3 = -\frac{(\beta_1 - \mu_1)\sigma_\perp + (\mu_2 - \beta_2)\varepsilon_\perp\omega}{2q(\sigma_\perp^2 + \varepsilon_\perp^2\omega^2)} \tag{4.64}$$

$$a_4 = \frac{(\beta_2 - \mu_2)\sigma_\perp + (\beta_1 - \mu_1)\varepsilon_\perp\omega}{2q(\sigma_\perp^2 + \varepsilon_\perp^2\omega^2)} \tag{4.65}$$

$$a_5 = \frac{\chi_2(\beta_1 - 2\mu_3) + \omega\chi_1(2\mu_4 - \beta_2)}{\chi_2^2 + \omega^2\chi_1^2} \tag{4.66}$$

$$a_6 = \frac{\chi_2(2\mu_4 - \beta_2) - \omega\chi_1(\beta_1 - 2\mu_3)}{\chi_2^2 + \omega^2\chi_1^2} \tag{4.67}$$

$$a_7 = 2\left(\frac{\omega\chi_1\mu_6 - \chi_2\mu_5}{\chi_2^2 + \omega^2\chi_1^2}\right) \tag{4.68}$$

$$a_8 = 2\left(\frac{\omega\chi_1\mu_5 + \chi_2\mu_6}{\chi_2^2 + \omega^2\chi_1^2}\right) \tag{4.69}$$

with

$$\mu_1 = ip_x(\Delta\varepsilon B_1\omega - \Delta\sigma B_2) \tag{4.70}$$

$$\mu_2 = ip_x(\Delta\sigma B_1 + \Delta\varepsilon B_2\omega) \tag{4.71}$$

$$\mu_3 = ip_x(\varepsilon_\parallel B_1\omega - \sigma_\parallel B_2) \tag{4.72}$$

$$\mu_4 = ip_x(\varepsilon_\parallel B_2\omega + \sigma_\parallel B_1) \tag{4.73}$$

$$\mu_5 = ip_y(\varepsilon_\perp B_1\omega - \sigma_\perp B_2) \tag{4.74}$$

$$\mu_6 = ip_y(\varepsilon_\perp B_2\omega + \sigma_\perp B_1) \tag{4.75}$$

$$\beta_1 = a\triangle\varepsilon\omega \tag{4.76}$$

$$\beta_2 = a\triangle\sigma \tag{4.77}$$

$$\chi_1 = \varepsilon_\parallel p_x^2 + \varepsilon_\perp(p_y^2 + q^2) \tag{4.78}$$

$$\chi_2 = \sigma_\parallel p_x^2 + \sigma_\perp(p_y^2 + q^2). \tag{4.79}$$

We now turn to the hydrodynamic equations at the order ϵ for the velocities $v_1^{(x,y,z)}$. It is typical of the multi-scale expansion that these equations are coupled to the low order coefficients $v_o^{(x,y,z)}$, θ_o, ϕ_o and p_o. In our case, the z-component of the hydrodynamic equation is also coupled to the higher order coefficients ϕ_1 and θ_1. Therefore, time averages (over one cycle) have to be performed on these equations. After substituting the neutral solutions found in the previous section and the next order coefficients derived earlier in this section, we express these equations (after averaged over time) as follows:

(x-component)

$$\begin{aligned} 0 = {} & g_1\frac{\partial^2 v_1^x}{\partial x^2} + g_2\left(\frac{\partial^2 v_1^x}{\partial y^2} + \frac{\partial^2 v_1^x}{\partial z^2}\right) - \frac{\partial p_1}{\partial x} \\ & + \left(A^2 e^{2i\vec{p}\cdot\vec{r}} - A^{*2}e^{-2i\vec{p}\cdot\vec{r}}\right)\left[\frac{\tau_1}{2} + \left(\frac{\tau_1}{2} + \tau_2\right)\cos(2qz)\right] \\ & + \left[\tau_3\left(\frac{\partial A}{\partial X}e^{i\vec{p}\cdot\vec{r}} - \frac{\partial A^*}{\partial X}e^{-i\vec{p}\cdot\vec{r}}\right) + \tau_4\left(\frac{\partial A}{\partial Y}e^{i\vec{p}\cdot\vec{r}} - \frac{\partial A^*}{\partial Y}e^{-i\vec{p}\cdot\vec{r}}\right)\right] \\ & \times \sin(qz) \end{aligned} \tag{4.80}$$

(y-component)

$$\begin{aligned} 0 = {} & g_3\frac{\partial^2 v_1^y}{\partial x^2} + \frac{\alpha_4}{2}\left(\frac{\partial^2 v_1^y}{\partial y^2} + \frac{\partial^2 v_1^y}{\partial z^2}\right) + g_4\frac{\partial^2 v_1^x}{\partial x\partial y} - \frac{\partial p_1}{\partial y} \\ & + \left(A^2 e^{2i\vec{p}\cdot\vec{r}} - A^{*2}e^{-2i\vec{p}\cdot\vec{r}}\right)\left[\frac{\delta_1}{2} + \left(\frac{\delta_1}{2} + \delta_2\right)\cos(2qz)\right] \end{aligned}$$

$$+\left[\delta_3\left(\frac{\partial A}{\partial Y}e^{i\vec{p}\cdot\vec{r}}-\frac{\partial A^*}{\partial Y}e^{-i\vec{p}\cdot\vec{r}}\right)+\delta_4\left(\frac{\partial A}{\partial X}e^{i\vec{p}\cdot\vec{r}}-\frac{\partial A^*}{\partial X}e^{-i\vec{p}\cdot\vec{r}}\right)\right]$$
$$\times\sin(qz) \tag{4.81}$$

(z-component)

$$\begin{aligned}0 &= g_3\frac{\partial^2 v_1^z}{\partial x^2}+\frac{\alpha_4}{2}\left(\frac{\partial^2 v_1^z}{\partial y^2}+\frac{\partial^2 v_1^z}{\partial z^2}\right)+g_5\frac{\partial^2 v_1^x}{\partial x\partial z}+\frac{\alpha_4}{2}\frac{\partial^2 v_1^y}{\partial y\partial z}-\frac{\partial p_1}{\partial z}\\ &+\left[\eta_1\left(A^2e^{2i\vec{p}\cdot\vec{r}}+A^{*2}e^{-2i\vec{p}\cdot\vec{r}}\right)+\eta_2|A|^2\right]\sin(2qz)\\ &+\left[\eta_3\left(\frac{\partial A}{\partial X}e^{i\vec{p}\cdot\vec{r}}-\frac{\partial A^*}{\partial X}e^{-i\vec{p}\cdot\vec{r}}\right)+\eta_4\left(\frac{\partial A}{\partial Y}e^{i\vec{p}\cdot\vec{r}}-\frac{\partial A^*}{\partial Y}e^{-i\vec{p}\cdot\vec{r}}\right)\right]\\ &\times\cos(qz)\end{aligned} \tag{4.82}$$

where

$$g_1 = \alpha_1+\alpha_4/2+\alpha_5+\alpha_6/2+\alpha_3/2 \tag{4.83}$$

$$g_2 = (\alpha_4+\alpha_6+\alpha_3)/2 \tag{4.84}$$

$$g_3 = (\alpha_4+\alpha_5-\alpha_2)/2 \tag{4.85}$$

$$g_4 = (\alpha_5+\alpha_2)/2 \tag{4.86}$$

$$g_5 = (\alpha_4+\alpha_5+\alpha_2)/2 \tag{4.87}$$

$$\begin{aligned}\tau_1 &= 2ip_x[i(\alpha_1+\alpha_6)D_3p_x+qD_1(\alpha_1+\alpha_5)]+ip_y[i(\alpha_6+\alpha_3)D_3p_y+qD_2(\alpha_6-\alpha_3)]\\ &-\frac{i}{2}p_x(B_1^2+B_2^2)[\varepsilon_\parallel p_x^2+\varepsilon_\perp(p_y^2+q^2)]+2ip_x(k_{33}p_x^2+k_{22}p_y^2)\\ &-p_xB_1\triangle\varepsilon a\end{aligned} \tag{4.88}$$

$$\tau_2 = ik_{11}p_xq^2+q[iD_1p_x(\alpha_1+\alpha_5)-qD_3\alpha_6] \tag{4.89}$$

$$\begin{aligned}\tau_3 &= [2(\alpha_1+\alpha_4+\alpha_5+\alpha_6)-(\alpha_4+\alpha_6-\alpha_3)/2]ip_xD_1-G\\ &+(\alpha_4+\alpha_6-\alpha_3)(ip_yD_2-qD_3)/2\end{aligned} \tag{4.90}$$

$$\tau_4 = i(\alpha_4+\alpha_6+\alpha_3)p_yD_1 \tag{4.91}$$

$$\begin{aligned}\delta_1 &= -p_x[(\alpha_5+\alpha_2)D_3p_y+iqD_2(\alpha_2-\alpha_5)]+2ip_y(k_{33}p_x^2+k_{22}p_y^2)\\ &-\frac{i}{2}p_y(B_1^2+B_2^2)[\varepsilon_\parallel p_x^2+\varepsilon_\perp(p_y^2+q^2)]-p_xB_1\triangle\varepsilon a\end{aligned} \tag{4.92}$$

$$\delta_2 = ik_{11}p_yq^2-\frac{i}{2}q[D_2p_x(\alpha_2-\alpha_5)-D_1p_y(\alpha_2+\alpha_5)] \tag{4.93}$$

$$\delta_3 = \alpha_4 i p_y D_2 + \frac{i}{2}(\alpha_5+\alpha_2)p_x D_1 - G \tag{4.94}$$

$$\delta_4 = i(\alpha_4+\alpha_5-\alpha_2)p_x D_2 + \frac{i}{2}(\alpha_5+\alpha_2)p_y D_1 \tag{4.95}$$

$$\begin{aligned}\eta_1 = {} & \left[\frac{q}{4}\left(B_1^2+B_2^2\right)+2aa_2\right]\left[\varepsilon_\parallel p_x^2+\varepsilon_\perp(p_y^2+q^2)\right]-q(k_{11}q^2+k_{22}p_y^2+k_{33}p_x^2)\\ & -\frac{p_y}{2}\left[(\alpha_6+\alpha_3)p_y D_1+(\alpha_6-\alpha_3)p_x D_2\right]-q(\alpha_6 q D_1+2i\alpha_5 p_x D_3)\\ & -p_x^2(\alpha_6+\alpha_1)D_1+\frac{a}{2}\Delta\varepsilon q(\frac{5}{2}iB_1p_x-a)\end{aligned} \tag{4.96}$$

$$\begin{aligned}\eta_2 = {} & 2a\varepsilon_\perp q^2 a_4-2q(\alpha_6 q D_1+i\alpha_5 p_x D_3)-2k_{11}q^3\\ & -\frac{q}{2}\left(B_1^2+B_2^2\right)\left[\varepsilon_\parallel p_x^2+\varepsilon_\perp(p_y^2+q^2)\right]+a\Delta\varepsilon q\left(\frac{i}{2}p_x B_1-a\right)\end{aligned} \tag{4.97}$$

$$\begin{aligned}\eta_3 = {} & \frac{a}{2}\left[\varepsilon_\parallel p_x^2+\varepsilon_\perp(p_y^2+q^2)\right]a_6+i(\alpha_4+\alpha_5-\alpha_2)p_x D_3+(\alpha_4+\alpha_5+\alpha_2)qD_1\\ & -i\varepsilon_\parallel p_x B_1 a+\frac{1}{2}a^2\Delta\varepsilon\end{aligned} \tag{4.98}$$

$$\eta_4 = \frac{a}{2}\left[\varepsilon_\parallel p_x^2+\varepsilon_\perp(p_y^2+q^2)\right]a_8+\frac{\alpha_4}{2}qD_2+i\alpha_4 p_y D_3-i\varepsilon_\perp p_y B_1 a. \tag{4.99}$$

These equations combined with the incompressibility condition at the order ϵ

$$\begin{aligned}\frac{\partial v_1^x}{\partial x}+\frac{\partial v_1^y}{\partial y}+\frac{\partial v_1^z}{\partial z}+\left(\frac{\partial A}{\partial X}e^{i\vec{p}\cdot\vec{r}}-\frac{\partial A^*}{\partial X}e^{-i\vec{p}\cdot\vec{r}}\right)D_1\sin(qz)\\ +\left(\frac{\partial A}{\partial Y}e^{i\vec{p}\cdot\vec{r}}-\frac{\partial A^*}{\partial Y}e^{-i\vec{p}\cdot\vec{r}}\right)D_2\sin(qz) = 0\end{aligned} \tag{4.100}$$

completely specify the pressure and the velocity coefficients. If we put

$$\begin{aligned}p_1 = {} & \left(A^2e^{2i\vec{p}\cdot\vec{r}}+A^{*2}e^{-2i\vec{p}\cdot\vec{r}}\right)\left[c_1-\frac{il}{4}+c_2\cos(2qz)\right]-\frac{\eta_2}{2q}|A|^2\cos(2qz)\\ & +\left[c_3\left(\frac{\partial A}{\partial X}e^{i\vec{p}\cdot\vec{r}}+\frac{\partial A^*}{\partial X}e^{-i\vec{p}\cdot\vec{r}}\right)+c_4\left(\frac{\partial A}{\partial Y}e^{i\vec{p}\cdot\vec{r}}-\frac{\partial A^*}{\partial Y}e^{-i\vec{p}\cdot\vec{r}}\right)\right]\\ & \times\sin(qz)\end{aligned} \tag{4.101}$$

$$\begin{aligned}v_1^x = {} & \left(A^2e^{2i\vec{p}\cdot\vec{r}}-A^{*2}e^{-2i\vec{p}\cdot\vec{r}}\right)\left[u_{x1}+u_{x2}\cos(2qz)\right]\\ & +u_{x3}\left(\frac{\partial A}{\partial X}e^{i\vec{p}\cdot\vec{r}}-\frac{\partial A^*}{\partial X}e^{-i\vec{p}\cdot\vec{r}}\right)\sin(qz)\\ & +u_{x4}\left(\frac{\partial A}{\partial Y}e^{i\vec{p}\cdot\vec{r}}-\frac{\partial A^*}{\partial Y}e^{-i\vec{p}\cdot\vec{r}}\right)\sin(qz)\end{aligned} \tag{4.102}$$

$$\begin{aligned}v_1^y = {} & \left(A^2e^{2i\vec{p}\cdot\vec{r}}-A^{*2}e^{-2i\vec{p}\cdot\vec{r}}\right)\left[u_{y1}+u_{y2}\cos(2qz)\right]\\ & +u_{y3}\left(\frac{\partial A}{\partial Y}e^{i\vec{p}\cdot\vec{r}}-\frac{\partial A^*}{\partial Y}e^{-i\vec{p}\cdot\vec{r}}\right)\sin(qz)\end{aligned}$$

$$+ u_{y4}\left(\frac{\partial A}{\partial X}e^{i\vec{p}\cdot\vec{r}} - \frac{\partial A^*}{\partial X}e^{-i\vec{p}\cdot\vec{r}}\right)\sin(qz) \tag{4.103}$$

$$\begin{aligned} v_1^z &= -\frac{i}{q}\left(A^2e^{2i\vec{p}\cdot\vec{r}} + A^{*2}e^{-2i\vec{p}\cdot\vec{r}}\right)(p_x u_{x2} + p_y u_{y2})\sin(2qz) \\ &+ \frac{1}{q}\left(\frac{\partial A}{\partial X}e^{i\vec{p}\cdot\vec{r}} + \frac{\partial A^*}{\partial X}e^{-i\vec{p}\cdot\vec{r}}\right)(ip_x u_{x3} + ip_y u_{y4} + D1)\cos(qz) \\ &+ \frac{1}{q}\left(\frac{\partial A}{\partial Y}e^{i\vec{p}\cdot\vec{r}} + \frac{\partial A^*}{\partial Y}e^{-i\vec{p}\cdot\vec{r}}\right)(ip_x u_{x4} + ip_y u_{y3} + D2)\cos(qz) \end{aligned} \tag{4.104}$$

where

$$\begin{aligned} l &= 2i(k_{33}p_x^2 + k_{22}p_y^2) - \frac{i}{2}(B_1^2 + B_2^2)[\varepsilon_\parallel p_x^2 + \varepsilon_\perp(p_y^2 + q^2)] \\ &+ \frac{a}{2}B_1\triangle\varepsilon p_x \end{aligned} \tag{4.105}$$

and c_i, u_{xi} and u_{yi} are constant coefficients, then, providing

$$u_{y1} = -\frac{p_x u_{x1}}{p_y}, \tag{4.106}$$

the above coefficients are found to be

$$c_1 = \frac{\delta_1' p_y e_1 - \tau_1' e_2}{4i(p_y^2 e_1 - p_x e_2)} \tag{4.107}$$

$$c_2 = \frac{-ip_y(\delta_1 + 2\delta_2)/2 - q\eta_1 + e_4(\tau_1 + 2\tau_2)p_x}{4ip_x^2 e_4 + 2(p_y^2 + q^2)} \tag{4.108}$$

$$c_3 = \frac{-ip_y\delta_4 + q\eta_3 - [\alpha_4(2q^2 + p_y^2)/2 + g_3 p_x^2]D_1 - ie_5\tau_3}{e_5 p_x + q^2 + p_y^2} \tag{4.109}$$

$$c_4 = \frac{-ip_y\delta_3 + q\eta_4 - [\alpha_4(2q^2 + p_y^2)/2 + g_3 p_x^2]D_2 - ie_5\tau_4}{e_5 p_x + q^2 + p_y^2} \tag{4.110}$$

$$u_{x1} = \frac{\tau_1' - 4ip_x c_1}{8(g1p_x^2 + g2p_y^2)} \tag{4.111}$$

$$u_{x2} = \frac{\tau_1 + 2\tau_2 - 4ip_x c_2}{8[g1p_x^2 + g2(p_y^2 + q^2)]} \tag{4.112}$$

$$u_{x3} = \frac{\tau_3 - ip_x c_3}{g2(q^2 + p_y^2) + g_1 p_x^2} \tag{4.113}$$

$$u_{x4} = \frac{\tau_4 - ip_x c_4}{g2(q^2 + p_y^2) + g_1 p_x^2} \tag{4.114}$$

$$u_{y2} = \frac{\delta_1 + 2\delta_2 - 4ip_y c_2 - 8g4p_x p_y u_{x2}}{4[\alpha_4(q^2 + p_y^2) + 2g_3 p_x^2]} \tag{4.115}$$

$$u_{y3} = \frac{\delta_3 - g_4 p_x p_y u_{x4} - i p_y c_4}{g3 p_x^2 + \alpha_4 (q^2 + p_y^2)/2} \tag{4.116}$$

$$u_{y4} = \frac{\delta_4 - g_4 p_x p_y u_{x3} - i p_y c_3}{g3 p_x^2 + \alpha_4 (q^2 + p_y^2)/2} \tag{4.117}$$

where

$$\begin{aligned} \tau_1' &= 2ip_x[i(\alpha_1 + \alpha_6) D_3 p_x + q D_1(\alpha_1 + \alpha_5)] \\ &\quad + ip_y[i(\alpha_6 + \alpha_3) D_3 p_y + q D_2(\alpha_6 - \alpha_3)] \end{aligned} \tag{4.118}$$

$$\delta_1' = -p_x[D_3 p_y(\alpha_5 + \alpha_2) + i D_2 q(\alpha_2 - \alpha_5)] \tag{4.119}$$

$$e_1 = 8(g_1 p_x^2 + g_2 p_y^2) \tag{4.120}$$

$$e_2 = 4[2g_4 p_x p_y^2 - (\alpha_4 p_y^2 + 2g_3 p_x^2) p_x] \tag{4.121}$$

$$e_3 = \frac{2i}{q}(2g_3 p_x^2 + \alpha_4 p_y^2) \tag{4.122}$$

$$e_4 = \frac{4ig_4 p_y^2 - q e_3 - 4iq^2(\alpha_4 - g_5)}{8[g2(q^2 + p_y^2) + g_1 p_x^2]} \tag{4.123}$$

$$e_5 = \frac{[\alpha_4(2q^2 + p_y^2)/2 + g_3 p_x^2 - g_5 q^2 - g_4 p_y^2] p_x}{g2(q^2 + p_y^2) + g_1 p_x^2} \tag{4.124}$$

Therefore, through extensive algebra, we have obtained solutions to the equations of order ϵ and we have shown that the first nonlinear balance leads to the generation of second harmonics. In the next section, we will write down the equations due to the next nonlinear balance (at the order of $\epsilon^{3/2}$). Then, by combining these equations in exactly the same way as outlined in Section 4.2, we will obtain a condition necessary for the uniformity of the ϵ-expansions.

4.4 The Amplitude Equation

We are now entering the final stage of our analysis. Our purpose in this section is not to obtain solutions to the next higher order equations. Instead, our aim is to derive an evolution equation for the slowly varying amplitude $A(X, Y, T)$, as a consequence of a uniformity condition. Let us begin with the equation of conservation of charge at the order $\epsilon^{3/2}$. As stated above, we are to follow exactly the same procedure as

in Section 4.2 to combine the $\epsilon^{3/2}$-order equations into a single equation for one of the fields. We have already seen that the revelant equations include not simply the charge conservation equation but its time average weighted with respect to $\cos(\omega t)$. At the order $\epsilon^{3/2}$, this leads to

$$-\cos(\omega t)\lambda_3\phi_2 + \frac{\Delta\sigma a}{2}\frac{\partial\theta_2}{\partial x} + MW_1^- \cos(qz) + \ldots = 0 \tag{4.125}$$

where the operator M and the associated coefficients are defined as

$$M = \xi_{m1}\frac{\partial}{\partial T} + \xi_{m2}\frac{\partial^2}{\partial X^2} + \xi_{m3}\frac{\partial^2}{\partial Y^2} + \xi_{m4}\frac{\partial^2}{\partial X\partial Y} + \xi_{m5}|A|^2 + \xi_{m6} \tag{4.126}$$

$$\xi_{m1} = \frac{1}{2}\left[\Delta\varepsilon a i p_x - (\varepsilon_\parallel p_x^2 + \varepsilon_\perp p_y^2)B_2\right] \tag{4.127}$$

$$\xi_{m2} = -\frac{1}{2}\left[(\sigma_\parallel B_1 + \varepsilon_\parallel \omega B_2) + 2ip_x(\sigma_\parallel a_6 + \varepsilon_\parallel \omega a_5)\right] \tag{4.128}$$

$$\xi_{m3} = -\frac{1}{2}\left[(\sigma_\perp B_1 + \varepsilon_\perp \omega B_2) + 2ip_y(\sigma_\perp a_8 + \varepsilon_\perp \omega a_7)\right] \tag{4.129}$$

$$\xi_{m4} = -i\left[(\sigma_\parallel a_8 + \varepsilon_\parallel \omega a_7)p_x + p_y(\sigma_\perp a_6 + \varepsilon_\perp \omega a_5)\right] \tag{4.130}$$

$$\begin{aligned}\xi_{m5} = -\Big[&2ip_x q(\Delta\sigma a_2 + \Delta\varepsilon\omega a_1) + \frac{3}{4}\Delta\sigma i a \\ &+\frac{1}{8}(\Delta\sigma B_1 + \Delta\varepsilon\omega B_2)(9p_x^2 - q^2) + \frac{i}{2}p_x q(\Delta\sigma a_4 + \Delta\varepsilon\omega a_3)\Big]\end{aligned} \tag{4.131}$$

$$\xi_{m6} = \frac{1}{2}\left(\frac{ip_x a\Delta\sigma}{2} + \varepsilon_\perp \omega q^2 B_2\right) \tag{4.132}$$

We have again employed the linear operator λ_3 from Section 4.2 to simplify the above equation. For convenience, we have introduced the following notation:

$$W_1^\pm = Ae^{i\vec{p}\cdot\vec{r}} \pm A^* e^{-i\vec{p}\cdot\vec{r}}. \tag{4.133}$$

The ellipsis "..." in Eqn. (4.125) represents terms not proportional to $W_1^\pm$. This notation will also be used throughout this section. Although we have not made explicit use of the angle brackets as we did previously, we should remind ourselves that average over t is implied automatically.

We now turn to the hydrodynamic equations at the order of $\epsilon^{3/2}$. Following the same steps as in the case above, these hydrodynamic equations can be expressed in

a similar form. They are listed as follows:

(x-component)

$$\left(\alpha_1+\frac{\alpha_4}{2}+\alpha_5+\frac{\alpha_6}{2}+\frac{\alpha_3}{2}\right)\frac{\partial^2 v_2^x}{\partial x^2}+\frac{1}{2}(\alpha_4+\alpha_6+\alpha_3)\left(\frac{\partial^2 v_2^x}{\partial y^2}+\frac{\partial^2 v_2^x}{\partial z^2}\right)-\frac{\partial p_2}{\partial x}$$
$$+H_x W_1^+\sin(qz)+\ldots=0 \tag{4.134}$$

(y-component)

$$\frac{1}{2}(\alpha_4+\alpha_5-\alpha_2)\frac{\partial^2 v_2^y}{\partial x^2}+\frac{\alpha_4}{2}\left(\frac{\partial^2 v_2^y}{\partial y^2}+\frac{\partial^2 v_2^y}{\partial z^2}\right)+\frac{1}{2}(\alpha_5+\alpha_2)\frac{\partial^2 v_2^x}{\partial x\partial y}$$
$$-\frac{\partial p_2}{\partial y}+H_y W_1^+\sin(qz)+\ldots=0 \tag{4.135}$$

(z-component)

$$\frac{1}{2}(\alpha_4+\alpha_5-\alpha_2)\frac{\partial^2 v_2^z}{\partial x^2}+\frac{\alpha_4}{2}\left(\frac{\partial^2 v_2^z}{\partial y^2}+\frac{\partial^2 v_2^z}{\partial z^2}\right)+\frac{1}{2}(\alpha_5+\alpha_2)\frac{\partial^2 v_2^x}{\partial x\partial z}$$
$$-\frac{\partial p_2}{\partial z}-\left[\lambda_2\phi_2-\triangle\varepsilon a\cos(\omega t)\frac{\partial\theta_2}{\partial x}\right]a\cos(\omega t)$$
$$+H_z W_1^-\cos(qz)+\ldots=0 \tag{4.136}$$

where the operators H_x, H_y, H_z and their associated coefficients are written as

$$H_x = \xi_{x1}\frac{\partial}{\partial T}+\xi_{x2}\frac{\partial^2}{\partial X^2}+\xi_{x3}\frac{\partial^2}{\partial Y^2}+\xi_{x4}\frac{\partial^2}{\partial X\partial Y}+\xi_{x5}|A|^2 \tag{4.137}$$

$$H_y = \xi_{y1}\frac{\partial}{\partial T}+\xi_{y2}\frac{\partial^2}{\partial X^2}+\xi_{y3}\frac{\partial^2}{\partial Y^2}+\xi_{y4}\frac{\partial^2}{\partial X\partial Y}+\xi_{y5}|A|^2 \tag{4.138}$$

$$H_z = \xi_{z1}\frac{\partial}{\partial T}+\xi_{z2}\frac{\partial^2}{\partial X^2}+\xi_{z3}\frac{\partial^2}{\partial Y^2}+\xi_{z4}\frac{\partial^2}{\partial X\partial Y}+\xi_{z5}|A|^2+\xi_{z6} \tag{4.139}$$

$$\xi_{x1} = -\rho D_1 \tag{4.140}$$

$$\xi_{x2} = \left(\alpha_1+\frac{\alpha_4}{2}+\alpha_5+\frac{\alpha_6}{2}+\frac{\alpha_3}{2}\right)(D_1+2ip_x u_{x3})-c_3 \tag{4.141}$$

$$\xi_{x3} = \frac{1}{2}(\alpha_4+\alpha_6+\alpha_3)(D_1+2ip_y u_{x4}) \tag{4.142}$$

$$\xi_{x4} = 2ip_x\left(\alpha_1+\frac{\alpha_4}{2}+\alpha_5+\frac{\alpha_6}{2}+\frac{\alpha_3}{2}\right)u_{x4}+(\alpha_4+\alpha_6+\alpha_3)ip_y u_{x3}$$
$$-c_4 \tag{4.143}$$

$$\xi_{x5} = \frac{1}{4}(2\alpha_1+\alpha_5+\alpha_6)p_x^2 D_1+\frac{i}{q}(p_x u_{x2}+p_y u_{y2})(\gamma_1 p_x^2+\alpha_6 q^2+\frac{1}{2}\gamma_1' p_y^2)$$

$$
\begin{aligned}
&- \frac{1}{2}(k_{11}-k_{33})p_x^2 q + i(\frac{1}{2}-p_x)[\varepsilon_\parallel p_x^2 + \varepsilon_\perp(p_y^2+q^2)](B_1 a_2 + B_2 a_1) \\
&- i\gamma_2 p_x q u_{x2} + \frac{1}{8}\gamma_1' p_y^2 D_1 + \frac{1}{8}\gamma_2' p_x p_y D_2 - \frac{9}{4}(\alpha_1 - \alpha_6 + \alpha_5)q^2 D_1 \\
&- \frac{10}{4}\alpha_1 i p_x q D_3 - \frac{1}{2}\gamma_2' i p_y q u_{y2} - \gamma_2 i p_x q(u_{x2} + 2u_{x1}) - \frac{a_2}{2}\Delta\varepsilon a p_x^2 \\
&+ \frac{3}{4}\Delta\varepsilon a i p_x q B_1 + \Delta\varepsilon p_x^2 q(B_1^2 + B_2^2) \\
&- i p_x \varepsilon_\perp q^2(a_3 B_2 + a_4 B_1)
\end{aligned} \tag{4.144}
$$

$$
\xi_{y1} = -\rho D_2 \tag{4.145}
$$

$$
\xi_{y2} = \frac{1}{2}(\alpha_4 + \alpha_5 - \alpha_2)(D_2 + 2ip_x u_{y4}) + \frac{1}{2}(\alpha_5 + \alpha_2) i p_y u_{x3} \tag{4.146}
$$

$$
\xi_{y3} = \frac{1}{2}\alpha_4 D_2 + \alpha_4 i p_y u_{y3} + \frac{1}{2}(\alpha_5 + \alpha_2) i p_x u_{x4} - c_4 \tag{4.147}
$$

$$
\begin{aligned}
\xi_{y4} = {} & (\alpha_4 + \alpha_5 - \alpha_2) i p_x u_{y3} + \frac{1}{2}(\alpha_5 + \alpha_2)(D_1 + i p_x u_{x3} + i p_y u_{x4}) \\
& - c_3 + \alpha_4 i p_y u_{y4}
\end{aligned} \tag{4.148}
$$

$$
\begin{aligned}
\xi_{y5} = {} & -\frac{1}{2}(k_{11}-k_{33}) p_x p_y q - \frac{i}{2}[\varepsilon_\parallel p_x^2 + \varepsilon_\perp(p_y^2+q^2)] p_y (a_2 B_1 + a_1 B_2) \\
& + \frac{1}{8}(\alpha_5 - \alpha_2) D_2 (p_x^2 - 9q^2) + \frac{1}{2}\Delta\varepsilon a p_y \left(\frac{3}{2} i q B_1 - p_x a_2\right) \\
& - \frac{1}{2}(\alpha_5 + \alpha_2)\left[\frac{9}{4} i D_3 q + i q(2u_{x1} + u_{x2}) - \frac{i}{q} p_x (p_x u_{x2} + p_y u_{y2}) - \frac{1}{4} D_1 p_x\right] p_y \\
& + q p_y \left[\Delta\varepsilon p_x (B_1^2 + B_2^2) - \varepsilon_\perp (a_4 B_1 + a_3 B_2) 1 q\right] \\
& - (\alpha_5 - \alpha_2) i p_x q (u_{y1} + u_{y2})
\end{aligned} \tag{4.149}
$$

$$
\xi_{z1} = -\rho D_3 \tag{4.150}
$$

$$
\begin{aligned}
\xi_{z2} = {} & \frac{1}{2}(\alpha_5 + \alpha_2) q u_{x3} + \frac{1}{2}(\alpha_4 + \alpha_5 - \alpha_2)\left[D_3 + \frac{2ip_x}{q}(i p_x u_{x3} + i p_y u_{y4} + D_1)\right] \\
& - \frac{\varepsilon_\parallel a}{2}(B_1 + 2i p_x a_6)
\end{aligned} \tag{4.151}
$$

$$
\xi_{z3} = \frac{\alpha_4 i p_y}{q}(i p_x u_{x4} + i p_y u_{y3} + D_2) + \frac{\alpha_4}{2} D_3 - \frac{\varepsilon_\perp a}{2}(B_1 + 2i p_y a_8) \tag{4.152}
$$

$$
\begin{aligned}
\xi_{z4} = {} & \frac{\alpha_4 i p_y}{q}(i p_x u_{x3} + i p_y u_{y4} + D_1) + \frac{1}{2}(\alpha_5 + \alpha_2) q u_{x4} \\
& + (\alpha_4 + \alpha_5 - \alpha_2)\frac{i p_x}{q}(i p_x u_{x4} + i p_y u_{y3} + D_2) \\
& - i a(\varepsilon_\parallel p_x a_8 + \varepsilon_\perp p_y a_6)
\end{aligned} \tag{4.153}
$$

$$
\xi_{z5} = \frac{1}{2}(k_{11}-k_{33}) i p_x q^2 - (u_{x1} + \frac{1}{2}u_{x2})[2\gamma_1 p_x^2 + \gamma_1' p_y^2]
$$

$$
\begin{aligned}
&- \frac{a}{2}\Delta\varepsilon iqp_x(2a_4+a_2) - \frac{a}{8}\Delta\varepsilon B_1(q^2+9p_x^2) + q^3(B_1a_4+B_2a_3) \\
&- \frac{q}{2}[\varepsilon_\parallel p_x^2 + \varepsilon_\perp(p_y^2+q^2)][B_1(a_2+a_4)+B_2(a_1+a_3)] \\
&- \frac{1}{4}[(\alpha_5+\alpha_6)q^2 + 9(\alpha_1+\alpha_2+\alpha_3)p_x^2]D_3 + \frac{10}{4}i\alpha_1 qp_xD_1 \\
&- \gamma_2' p_x p_y(u_{y1}+\frac{u_{y2}}{2}) - \alpha_6 q^2 u_{x2} - \frac{3}{4}\Delta\varepsilon a^2 ip_x \\
&+ \frac{9}{8}p_y(\gamma_2' iqD_2 - \gamma_1' p_y D_3) \\
&+ 2\alpha_5 p_x(p_x u_{x2} + p_y u_{y2})
\end{aligned} \tag{4.154}
$$

$$
\xi_{z6} = \frac{a}{4}\left\{2\Delta\varepsilon aip_x + B_1[\varepsilon_\parallel p_x^2 + \varepsilon_\perp(p_y^2+q^2)]\right\} \tag{4.155}
$$

with

$$
\gamma_1 = \alpha_1 + \alpha_6 \tag{4.156}
$$

$$
\gamma_2 = \alpha_1 + \alpha_5 \tag{4.157}
$$

$$
\gamma_1' = \alpha_6 + \alpha_3 \tag{4.158}
$$

$$
\gamma_2' = \alpha_6 - \alpha_3 \tag{4.159}
$$

Finally, we write down the torque-balance at order $\epsilon^{3/2}$:

$$
\begin{aligned}
&-\Delta\varepsilon a\cos(\omega t)\left[\theta_2 a\cos(\omega t) - \frac{\partial\phi_2}{\partial x}\right] - \tilde{\Delta}\theta_2 + \alpha_3\frac{\partial v_2^x}{\partial z} + \alpha_2\frac{\partial v_2^z}{\partial x} \\
&+ SW_1^+\cos(qz) + \ldots = 0
\end{aligned} \tag{4.160}
$$

where the operator S and its coefficients are

$$
S = \xi_{s1}\frac{\partial^2}{\partial X^2} + \xi_{s2}\frac{\partial^2}{\partial Y^2} + \xi_{s3}\frac{\partial^2}{\partial X\partial Y} + \xi_{s4}|A|^2 + \xi_{s5} \tag{4.161}
$$

$$
\xi_{s1} = \frac{\alpha_2}{q}(ip_x u_{x3} + ip_y u_{y4} + D_1) - k_{33} + \frac{a}{2}\Delta\varepsilon a_6 \tag{4.162}
$$

$$
\xi_{s2} = -k_{22} \tag{4.163}
$$

$$
\xi_{s3} = \frac{\alpha_2}{q}(ip_x u_{x4} + ip_y u_{y3} + D_2) + \frac{a}{2}\Delta\varepsilon a_8 \tag{4.164}
$$

$$
\begin{aligned}
\xi_{s4} = {} & \frac{3}{2}(k_{33}-k_{11})(q^2-p_x^2) + \frac{9}{4}(\alpha_5-\alpha_6)(ip_xD_3 + qD_1) \\
& + \frac{\Delta\varepsilon}{4}\left[3a^2 - 9aip_xB_1 + 4aq(a_2+a_4) - \frac{1}{2}(B_1^2+B_2^2)(9p_x^2-q^2)\right]
\end{aligned}
$$

$$+(\alpha_5-\alpha_6)[2ip_x(u_{x1}+u_{x2})+ip_yu_{y2}]$$
$$-\frac{i}{2}\triangle\varepsilon p_xq\,[B_1(2a_2+a_4)+B_2(2a_1+a_3)] \tag{4.165}$$

$$\xi_{s5} = \frac{\triangle\varepsilon}{4}a(ip_xB_1-2a). \tag{4.166}$$

It is now quite straightforward to follow exactly the same steps described in the latter half of Section 4.2 to combine these 3/2-order equations into a single equation for ϕ_2. Since the procedures have been well illustrated in Section 4.2, we will omit the intermediate steps and proceed to write down the final equation in the form below:

$$\mathcal{L}_o\phi_2+[j_o(j_1H_x+j_2H_y+j_3H_z+j_4S+j_5R)+j_6M]\,W_1^-\cos(qz)+\ldots=0 \tag{4.167}$$

where the operator R is defined as

$$R=u_{x3}\frac{\partial^2}{\partial X^2}+u_{y3}\frac{\partial^2}{\partial Y^2}+(u_{x4}+u_{y4})\frac{\partial^2}{\partial X\partial Y} \tag{4.168}$$

and the coefficients j_i are

$$j_o = -\frac{\triangle\sigma a}{2} \tag{4.169}$$
$$j_1 = ip_xq[\alpha_2\nu_o+(p_y^2+q^2)(\alpha_3\nu_2+\alpha_2\nu_1)] \tag{4.170}$$
$$j_2 = -ip_x^2p_yq(\alpha_3\nu_2+\alpha_2\nu_1) \tag{4.171}$$
$$j_3 = p_x^2[\alpha_2\nu_o+q^2(\alpha_3\nu_2+\alpha_2\nu_1)] \tag{4.172}$$
$$j_4 = i\nu_o\nu_2p_x \tag{4.173}$$
$$j_5 = p_x^2q\nu_2(\alpha_3\nu_2+\alpha_2\nu_1) \tag{4.174}$$
$$j_6 = (k_{11}q^2+k_{22}p_y^2+k_{33}p_x^2)\nu_o\nu_2 - \frac{\triangle\varepsilon a^2}{2}[\nu_o\nu_2-\alpha_2p_x^2\nu_o-p_x^2q^2(\alpha_3\nu_2+\alpha_2\nu_1)] \tag{4.175}$$

with

$$\nu_o = (\alpha_1-\alpha_2+\alpha_4+\alpha_6)(p_y^2+q^2)p_x^2+\frac{1}{2}(\alpha_4+\alpha_6+\alpha_3)(p_y^2+q^2)^2 + \frac{1}{2}(\alpha_4+\alpha_5-\alpha_2)p_x^4 \tag{4.176}$$
$$\nu_1 = -(\alpha_1-\alpha_2+\frac{\alpha_4}{2}+\alpha_6)p_x^2-\frac{1}{2}(\alpha_4+\alpha_6+\alpha_3)(p_y^2+q^2) \tag{4.177}$$
$$\nu_2 = -\frac{1}{2}(\alpha_4+\alpha_5-\alpha_2)p_x^2-\frac{\alpha_4}{2}(p_y^2+q^2). \tag{4.178}$$

We see that the operator $\mathcal{L}_o$ reappears once again on the left hand side of the above equation. As we have seen in Section 4.2, the eigenfunction of this operator involves $W_1^- \cos(qz)$ (c.f. Eqns. (4.16) and (4.57)). Therefore, any terms in the above equation proportional to this eigenfunction will lead to singular behavior in ϕ_2. Therefore, to suppress non-uniformity, we demand that the second term on the left of the above equation (the secular term) vanishes identically. After some re-arrangement, this finally leads us to a Landau-Ginzburg type equation for the slowly varying amplitude $A(X, Y, T)$:

$$\xi_T \frac{\partial A}{\partial T} + \xi_{XX} \frac{\partial^2 A}{\partial X^2} + \xi_{YY} \frac{\partial^2 A}{\partial Y^2} + \xi_{XY} \frac{\partial^2 A}{\partial X \partial Y} + \xi_n A|A|^2 + \xi_l A = 0 \tag{4.179}$$

where the coefficients are written as

$$\xi_T = j_o(j_1\xi_{x1} + j_2\xi_{y1} + j_3\xi_{z1}) + j_6\xi_{m1} \tag{4.180}$$

$$\xi_{XX} = j_o(j_1\xi_{x2} + j_2\xi_{y2} + j_3\xi_{z2} + j_4\xi_{s1} + j_5 u_{x3}) + j_6\xi_{m2} \tag{4.181}$$

$$\xi_{YY} = j_o(j_1\xi_{x3} + j_2\xi_{y3} + j_3\xi_{z3} + j_4\xi_{s2} + j_5 u_{y3}) + j_6\xi_{m3} \tag{4.182}$$

$$\xi_{XY} = j_o[j_1\xi_{x4} + j_2\xi_{y4} + j_3\xi_{z4} + j_4\xi_{s3} + j_5(u_{x4} + u_{y4})] + j_6\xi_{m4} \tag{4.183}$$

$$\xi_n = j_o(j_1\xi_{x5} + j_2\xi_{y5} + j_3\xi_{z5} + j_4\xi_{s4}) + j_6\xi_{m5} \tag{4.184}$$

$$\xi_l = j_o(j_3\xi_{z6} + j_4\xi_{s5}) + j_6\xi_{m6}. \tag{4.185}$$

Although the detailed properties of the nematic system are contained within the real coefficients ξ_T, ξ_{XX}, ... and ξ_l, the above amplitude equation can be transformed into a more universal (isotropic) form:

$$\frac{\partial A}{\partial T} = \frac{\partial^2 A}{\partial X^2} + \frac{\partial^2 A}{\partial Y^2} + A - A|A|^2. \tag{4.186}$$

In principle, the term involving the cross derivative $\partial^2 A/\partial X \partial Y$ can be eliminated by a rotation on the X-Y plane and by setting the angle of rotation properly so that the new X and Y axes represent the principal directions [32]. The real coefficients, then, can be removed by re-scaling the coordinates and the amplitude. However, doing so requires a more detailed investigation of these coefficients so that their signs can be

determined. For the available time frame, we are unable to continue our analysis in this direction.

Exact solutions to the above time dependent Landau-Ginzburg (TDLG) equation have been found. For stationary states, this equation has i) a finite amplitude periodic solution with a wave vector either parallel or oblique to the x-axis [36, 46] and ii) a tanh-like saddle-point solution [47]. In the case of coupled TDLG equations, the superposition of two small amplitude periodic solutions whose wave vectors are equal in magnitude but different in direction gives rise to square and hexagonal patterns [32]. For coupled TDLG equations with complex coefficients, travelling and standing waves are found [48]. Furthermore, based on the method of symmetry reduction, Skierski et. al [49] have transformed the isotropic TDLG equation into an *ode* thus allowing a larger class of exact solutions to be classified as rolls, defects, bumps (non-topological solitons) and kinks (topological solitons). Finally, we remark that the isotropic form of the amplitude equation has been found applicable to many pattern forming systems [36, 43, 47, 48, 50]. In particular, it has been found to be a model equation for the Eckhaus (side-band) instability [36, 48, 51, 52, 53] which is considered responsible for the wavelength changing process. Beyond this, the equation has also been applied successfully to describe the second-order phase transition of a junction laser [34], propagation of a two-phase interface [35] and superconductivity [37, 38, 39].

4.5 Summary

We have in this section demonstrated another possible scenario for the formation of oblique rolls at low field angular frequencies. In the present model, the azimuthal derivation of the director from the xOz plane remains zero. The onset of this instability is attributed to the presence of a periodic twist deformation in the y-direction (similar to the initial periodic bend perturbation in the Helfrich-Carr scenario). Once it is present, the deformation energy tends to "untwist" the director while the shear

flow, also modulated periodically (in the y-direction) provides the counter-action. Once the instability sets in, the phase variation of the tilt angle θ along y gives rise to the observed zigzag pattern.

The method of multi-scale analysis is a standard technique in hydrodynamic calculations. Kramer and his co-worker (Universität Bayreuth) [6, 42, 47, 46] were the first to pioneer the application of this technique to the nematic liquid crystals. It is therefore necessary to compare explicitly our present approach with that of the above authors. The fundamental differences between the two approaches lie in the assumption on the director and the boundary conditions. In the previously analysis, the orientation of the director was represented by two spherical angles. This representation coupled with the fully rigid boundary conditions led the previous authors to a set of very complicated equations and solutions which could not be written down in analytical form. Our present approach enjoys a simplistic assumption on the director. Here, the director is given only one rotational degree of freedom and is assumed to be parallel to the vertical (xOz) plane. This assumptions, together with the (relaxed) stress-free boundary conditions, we are able to write down our results in analytic form. Furthermore, in so far as the application of multi-scale analysis to the nematic liquid crystals is concerned, the details of the analysis is reported for the first time. We have also reconstructed the stability diagram for the primary transitions and carried out explicit comparison with experimental observations. Comparison with experiments was not available previously. Perhaps, the only common results shared between the Bayreuth group and us is that the same universal equation (the time dependent Landau-Ginzberg equation) emerges as the governing equation for the slow scale motions. Although the details of the physical system is embedded in the coefficients appearing in the TDLG equation, when speaking of universality, it is the form of the model equation that is relevant. This brings us to a very important point: The slow scale dynamics near the transition point is unaffected by our simplistic assumptions.

Chapter 5

Conclusions

We have concerned ourselves, in this thesis, exclusively with nematic liquid crystals. We have reviewed some of their physical properties and re-derived the quantities vital to the theoretical investigations. Included in this thesis are the preservation of orientational order in the nematic phases, response of the nematics to electromagnetic fields, the hydrostatic equilibrium condition and the total stress tensor for nonequilibrium situations, just to name a few.

The loss of positional order and a small amount of orientational order gives the nematic liquid crystals the right amount of freedom to respond sensitively to an electric field. The local orientational order of the molecules, on the other hand, gives the liquid crystals the ability to demonstrate extraordinary optical properties, reminiscent of many pattern forming systems involving isotropic fluids (Rayleigh-Bénard convection). It is the electro-hydrodynamic instabilities that the latter half of this thesis is devoted to. We have presented two independent investigations, both based on, at least in part, a macroscopic continuum theory in which the hydrodynamic equations, Maxwell's equations and a torque-balance equation are used. In both cases, the nonlinear response of the system has been derived and utilized.

In our first investigation, we focus our effort on a bifurcation problem associated with the primary transition of a nematic liquid crystal thin film. By using an ad

hoc assumption that the concept of free energy is also applicable to systems driven slightly out of equilibrium, we are able to correctly predict the observed power-law behavior of the normal rolls slightly above the transition voltage. Furthermore, our model has also suggested the formation of the normal straight rolls via a subcritical (discontinuous) bifurcation and this prediction has been found to be consistent with experimental observations.

In our second investigation, we re-examine the formation of the oblique (zigzag) rolls at low electric field angular frequencies using the technique of multi-scale analysis. The critical behavior found in our first investigation becomes the basis for our choice of the leading order in the ϵ-expansions. We have shown that a new mechanism responsible for the oblique rolls formation may involve merely a pure twist deformation along the normal roll axis (in addition to the bend deformation along x) and therefore the director field can be kept aligned parallel to the vertical plane. This is in contrast with the common belief that the director must be given two rotational degrees of freedom [54, 55, 56]. Through the linear balance of the equations, we have constructed a three-dimensional surface and a stability diagram in the *rms* voltage-angular frequency plane. We have found excellent agreements with experimental observations.

We have also included significant details of the multi-scale analysis applied to the electro-hydrodynamic equations of the nematic liquid crystals. Although a similar analysis has been performed by other authors [6], their results are too complicated to present in closed analytical form. We believe that the use of semi-rigid boundary conditions and a planar director field has reduced our expressions to a manageable size and given us solutions in closed form.

Finally, at order $\epsilon^{3/2}$, a time dependent Landau-Ginzburg type equation has been found to be the governing equation for the slowly varying amplitude [57]. Therefore, we conclude that the underlying dynamics at small scale remain relatively unaffected by the use of a simplified director field and a set of somewhat unrealistic boundary

conditions.

Bibliography

[1] P.J. Collings, *Liquid Crystals* (Princeton University Press, New Jersey, 1990).

[2] F.B. Priestley, P.J. Wojtowicz and P. Sheng, *Introduction to Liquid Crystals* (Plenum Press, New York, 1975).

[3] W. Helfrich, J. Chem. Phys., **51** (1969) 4092.

[4] E. Dubois-Violette, P.G. de Gennes and O. Parodi, J. Phys. (Paris), **32** (1971) 305.

[5] P.A. Penz and G.W. Ford, Phys. Rev., **A6** (1972) 414.

[6] E. Bodenschatz, W. Zimmermann and L. Kramer, J. Phys. France, **49** (1988) 1875.

[7] I. Rehberg, S. Rasenat, M. de la Torre Juárez, W. Schöpf, F. Hörner, G. Ahlers and H.R. Brand, Phys. Rev. Lett. **67** (1991) 596.

[8] G. Ahlers, L.I. Berge and D.S. Cannell, Phys. Rev. Lett. **70** (1993) 2399.

[9] L.I. Berge, G. Ahlers and D.S. Cannell, Phys. Rev. E **48** (1993) R3236.

[10] E. Bodenschatz, J.R. de Bruyn, G. Ahlers and D.S. Cannell, Phys. Rev. Lett. **67** (1991) 3078.

[11] Quanyuan Feng, W. Pesch and L. Kramer, Phys. Rev. A, **45** (1992) 7242.

[12] Q. Feng, W. Decker, W. Pesch and L. Kramer, J. Phys. II (France), **2** (1992) 1303.

[13] Orsay Liquid Crystal Group, Phys. Rev. Lett., **25** (1970) 1642.

[14] D. Meyerhofer and A. Sussman, Appl. Phys. Lett., **20** (1972) 337.

[15] R. Ribotta, A. Joets and L. Lei, Phys. Rev. Lett., **56** (1986) 1595.

[16] A. Joets and R. Ribotta, J. Physique, **47** (1986) 595.

[17] S. Rasenat, G. Hartung, B.L. Winkler and I. Rehberg, Experiments in Fluids, **7** (1989) 412.

[18] T.O. Carroll, J. Appl. Phys., **43** (1972) 1342.

[19] S. Kai, M. Araoka, H. Yamazaki and K. Hirakawa, J. Phys. Soc. Jpn., **46** (1979) 383.

[20] P.G. de Gennes, *The Physics of Liquid Crystals* (Clarendon Press, Oxford, 1974).

[21] F.C. Frank, Faraday Soc. Disc., **25** (1958) 19.

[22] L.D. Landau and E.M. Lifshitz, *Theory of Elasticity* (Pergamon Press, Reading, Massachusetts, 1959).

[23] L.D. Landau and E.M. Lifshitz, *Fluid Mechanics* (Pergamon Press, London, 1959).

[24] H.J. Kreuzer, *Nonequilibrium Thermodynamics and its Statistical Foundations* (Clarendon Press, Oxford, 1981).

[25] W. Jaunzemis, *Continuum Mechanics* (MacMillan, New York, 1967).

[26] L. Onsager, Phys. Rev., **37**(1931)405; Phys. Rev., **38** (1931) 2265.

[27] F.M. Leslie, Arch. Ration. Mech. Analysis, **28** (1968) 265.

[28] O. Parodi, Journal of Physics (Paris), **31** (1970) 581.

[29] F.H. Busse, in *Cellular Structures in Instability* (Lecture Notes in Physics **210**), J.E. Wesfreid and S. Zaleski, ed. (Springer, 1984), p. 97.

[30] E.F. Carr, in *Ordered fluids and liquid crystals*, Advanced Chemistry Series, American Chemical Society, (Washington DC, 1967) p. 76.

[31] G.F. Smith and R.S. Rivlin, Quart. Appl. Math., **15** (1957) 308.

[32] M.C. Cross and P.C. Hohenberg, Reviews of Modern Physics, **65** (1993) 851.

[33] H. Haken, in *Stochastic Nonlinear Systems*, L. Arnold and R. Lefever ed., (Springer-Verlag, Berlin, 1981), p. 12.

[34] R. Graham and H. Haken, Z. Phys., **237** (1970) 31.

[35] S.K. Chan, J. Chem. Phys., **67** (1977) 5755.

[36] A.C. Newell and J.A. Whitehead, J. Fluid Mech. , **38** (1969) 279.

[37] J.S. Langer and V. Ambegaokar, Phys. Rev., **164** (1967) 498.

[38] D.E. McCumber, Phys. Rev., **172** (1968) 427.

[39] D.E. McCumber and B.I. Halperin, Phys. Rev., **B1** (1970) 1054.

[40] R. Graham, in *Stochastic Nonlinear Systems*, L. Arnold and R. Lefever ed., (Springer-Verlag, Berlin, 1981), p. 202.

[41] W.H. Press, B.P. Flannery, S.A. Teukolsky and W.T. Vetterling, *Numerical Recipes in C* (Cambridge University Press, Cambridge, 1990), p. 305.

[42] W. Zimmermann and L. Kramer, Phys. Rev. Lett., **55** (1985) 402.

[43] A.C. Newell, in *Nonlinear Wave Motion* (Lectures in Applied Mathematics), A.C. Newell, ed. (Americiam Mathematical Society, 1974), p. 157.

[44] A. Joets and R. Ribotta, in *Cellular Structures in Instabilities*, edited by J.E. Wesfreid and S. Zaleski (Springer-Verlag, New York, 1984), p. 294.

[45] W.H. de Jeu, in *Physical Properties of Liquid Crystalline Materials*, edited by G. Gray (Gordon and Breach, New York, 1980).

[46] W. Pesch and L. Kramer, Z. Phys. B, **63** (1986) 121.

[47] L. Kramer and W. Zimmermann, Physica, **16D** (1985) 221.

[48] H. Sakaguchi, Prog. of Theor. Phys. , **89** (1993) 1123.

[49] M. Skierski, A.M. Grundland and J.A. Tuszyński, Phys. Lett. , **133A** (1988) 213; M. Skierski, A.M. Grundland and J.A. Tuszyński, J. Phys. A. , **22** (1989) 3789; M. Skierski, PhD thesis, University of Alberta (1991).

[50] A. Joets and R. Ribotta, Journal of Statistical Physics, **64** (1991) 981.

[51] W. Eckhaus, *Studies in Nonlinear Stability Theory* (Springer, New York, 1965).

[52] J.T. Stuart and R.C. Di Prima, Proc. R. Soc. Lond. , **A362** (1978) 27.

[53] L. Kramer, H.R. Schober and W. Zimmermann, Physica D, **31** (1988) 212.

[54] L. Kramer and W. Pesch, to be published in *Pattern Formation in Liquid Crystals*, editors A. Buka and L. Kramer, (Springer-Verlag, New York, 1995).

[55] M. Treiber and L. Kramer, Phys. Rev. E. **49** (1994) 3184.

[56] L. Kramer, E. Bodenschatz, W. Pesch, W. Thom and W. Zimmermann, Liquid Crystals, **5** (1989) 699.

[57] A. Becker and L. Kramer, Phys. Rev. Lett. **73** (1994) 955.

Appendix A

Anisotropic Tensors

We shall examine some of the transformation properties of the anisotropic tensors and demonstrate how an anisotropic tensor of any rank can be constructed explicitly. Let us consider a subgroup $\{T\}$ of a group of orthogonal transformations $\bar{x}_i = S_{ij}x_j$ with $S_{ij}S_{ik} = \delta_{jk}$. Suppose the tensor $a_{ij\cdots}$ is invariant under the subgroup $\{T\}$ i.e. $a_{\alpha\beta\cdots} = \bar{a}_{\alpha\beta\cdots} = S_{\alpha l}S_{\beta m}\cdots a_{lm\cdots}$. Then, the tensor a is referred to as an anisotropic tensor. Or, if a cylindrical symmetry is present so that $\{T\}$ corresponds to rotations about the symmetry axis, a is also called a *transverse isotropic tensor.*

Let u_i^1, u_i^2, $\cdots u_i^n$ be the components of n independent vectors and suppose that they transform under the subgroup $\{T\}$ as $\bar{u}_i^r = S_{ij}u_j^r$ where $r = 1, 2, \cdots, n$. Then, the scalar polynomial $p = a_{ij\cdots l}u_i^1u_j^2\cdots u_l^n$ is form-invariant under the action of T because

$$\begin{aligned}
\bar{a}_{ij\cdots l}\bar{u}_i^1\bar{u}_j^2\cdots\bar{u}_l^n &= S_{i\alpha}S_{j\beta}\cdots S_{l\xi}a_{\alpha\beta\cdots\xi}S_{ig}u_g^1S_{jh}u_h^2\cdots S_{lt}u_t^n \\
&= \delta_{\alpha g}\delta_{\beta h}\cdots\delta_{\xi t}a_{\alpha\beta\cdots\xi}u_g^1u_h^2\cdots u_t^n \\
&= a_{\alpha\beta\cdots\xi}u_\alpha^1u_\beta^2\cdots u_\xi^n. \qquad \text{(A.1)}
\end{aligned}$$

This form-invariant property implies that p can be constructed from a finite basis which consists of polynomial elements, each of which is also form-invariant under T [31]. Since p is a function of the n independent vectors i.e. $p = p(\vec{u}^1, \vec{u}^2, \cdots, \vec{u}^n)$ and

is linear in each $\vec{u}^i$, these basis elements must be of the form $(\vec{u}^i \cdot \vec{u}^j)$ or $(\vec{n}^r \cdot \vec{u}^s)$ where $i \neq j$ and $\vec{n}^r$ is a vector along an axis of symmetry of T; any combination that leads to a nonlinearity in any $\vec{u}^i$ must be disregarded. We shall denote this polynomial basis by $\{J_1, J_2, \cdots, J_m\}$. Then, in view of the fact that each vector contributes a component to each term in p, we may express p as a linear combination of all possible independent products of the basis elements:

$$p = A_{\alpha\beta\cdots\xi}\, J_\alpha J_\beta \cdots J_\xi \tag{A.2}$$

where each product $(J_\alpha J_\beta \cdots J_\xi)$ consists of a combination of the components of the n distinct vectors so that the multilinearity of p is preserved. Furthermore, each coefficient $A_{\alpha\beta\cdots\xi}$ must be a real scalar under T; otherwise, the above expansion will not remain form-invariant. Then, the anisotropic tensor a is found by differentiations:

$$a_{ij\cdots l} = \frac{\partial^n p}{\partial u_i^1 \partial u_j^2 \cdots \partial u_l^n} = A_{\alpha\beta\cdots\xi} \frac{\partial^n (J_\alpha J_\beta \cdots J_\xi)}{\partial u_i^1 \partial u_j^2 \cdots \partial u_l^n}. \tag{A.3}$$

Appendix B

Total Stress Tensor

Here, we list the exact expressions for all the non-zero elements of the total stress tensor σ in the conduction regime ($\partial\vec{n}/\partial t = 0$):

$$\begin{aligned}
\sigma_{xx} &= \alpha_1 n_x^2 \left[n_x^2 \frac{\partial v_x}{\partial x} + n_x n_z \left(\frac{\partial v_x}{\partial z} + \frac{\partial v_z}{\partial x} \right) + n_z^2 \frac{\partial v_z}{\partial z} \right] \\
&\quad + (\alpha_2 + \alpha_3) n_x \left[(\vec{v} \cdot \vec{\nabla}) n_x - \frac{n_z}{2} \left(\frac{\partial v_x}{\partial z} - \frac{\partial v_z}{\partial x} \right) \right] \\
&\quad + \alpha_4 \frac{\partial v_x}{\partial x} + (\alpha_5 + \alpha_6) n_x \left[n_x \frac{\partial v_x}{\partial x} + \frac{n_z}{2} \left(\frac{\partial v_z}{\partial x} + \frac{\partial v_x}{\partial z} \right) \right] \\
&\quad - k_1 \left(\frac{\partial n_x}{\partial x} + \frac{\partial n_z}{\partial z} \right) \frac{\partial n_x}{\partial x} + k_3 \left(\frac{\partial n_x}{\partial z} - \frac{\partial n_z}{\partial x} \right) \frac{\partial n_z}{\partial x} - p, \qquad \text{(B.1)} \\
\sigma_{yy} &= -p, \qquad \text{(B.2)} \\
\sigma_{xz} &= \alpha_1 n_x n_z \left[n_x^2 \frac{\partial v_x}{\partial x} + n_x n_z \left(\frac{\partial v_x}{\partial z} + \frac{\partial v_z}{\partial x} \right) + n_z^2 \frac{\partial v_z}{\partial z} \right] \\
&\quad + \alpha_2 n_x \left[(\vec{v} \cdot \vec{\nabla}) n_z - \frac{n_x}{2} \left(\frac{\partial v_z}{\partial x} - \frac{\partial v_x}{\partial z} \right) \right] \\
&\quad + \alpha_3 n_z \left[(\vec{v} \cdot \vec{\nabla}) n_x - \frac{n_z}{2} \left(\frac{\partial v_x}{\partial z} - \frac{\partial v_z}{\partial x} \right) \right] + \frac{\alpha_4}{2} \left(\frac{\partial v_x}{\partial z} + \frac{\partial v_z}{\partial x} \right) \\
&\quad + \alpha_5 n_x \left[\frac{n_x}{2} \left(\frac{\partial v_x}{\partial z} + \frac{\partial v_z}{\partial x} \right) + n_z \frac{\partial v_z}{\partial z} \right] \\
&\quad + \alpha_6 n_z \left[n_x \frac{\partial v_x}{\partial x} + \frac{n_z}{2} \left(\frac{\partial v_z}{\partial x} + \frac{\partial v_x}{\partial z} \right) \right] \\
&\quad - k_1 \left(\frac{\partial n_x}{\partial x} + \frac{\partial n_z}{\partial z} \right) \frac{\partial n_x}{\partial z} + k_3 \left(\frac{\partial n_x}{\partial z} - \frac{\partial n_z}{\partial x} \right) \frac{\partial n_z}{\partial z}, \qquad \text{(B.3)}
\end{aligned}$$

$$
\begin{aligned}
\sigma_{xx} &= \alpha_1 n_x n_z \left[n_x^2 \frac{\partial v_x}{\partial x} + n_x n_z \left(\frac{\partial v_x}{\partial z} + \frac{\partial v_z}{\partial x} \right) + n_z^2 \frac{\partial v_z}{\partial z} \right] \\
&\quad + \alpha_2 n_z \left[(\vec{v} \cdot \vec{\nabla}) n_x - \frac{n_z}{2} \left(\frac{\partial v_x}{\partial z} - \frac{\partial v_z}{\partial x} \right) \right] \\
&\quad + \alpha_3 n_x \left[(\vec{v} \cdot \vec{\nabla}) n_z - \frac{n_x}{2} \left(\frac{\partial v_z}{\partial x} - \frac{\partial v_x}{\partial z} \right) \right] + \frac{\alpha_4}{2} \left(\frac{\partial v_z}{\partial x} + \frac{\partial v_x}{\partial z} \right) \\
&\quad + \alpha_5 n_z \left[\frac{n_z}{2} \left(\frac{\partial v_z}{\partial x} + \frac{\partial v_x}{\partial z} \right) + n_x \frac{\partial v_x}{\partial x} \right] \\
&\quad + \alpha_6 n_x \left[n_z \frac{\partial v_z}{\partial z} + \frac{n_x}{2} \left(\frac{\partial v_x}{\partial z} + \frac{\partial v_z}{\partial x} \right) \right] \\
&\quad - k_1 \left(\frac{\partial n_x}{\partial x} + \frac{\partial n_z}{\partial z} \right) \frac{\partial n_z}{\partial x} - k_3 \left(\frac{\partial n_x}{\partial z} - \frac{\partial n_z}{\partial x} \right) \frac{\partial n_x}{\partial x}, \qquad \text{(B.4)} \\
\sigma_{zz} &= \alpha_1 n_z^2 \left[n_x^2 \frac{\partial v_x}{\partial x} + n_x n_z \left(\frac{\partial v_x}{\partial z} + \frac{\partial v_z}{\partial x} \right) + n_z^2 \frac{\partial v_z}{\partial z} \right] \\
&\quad + (\alpha_2 + \alpha_3) n_z \left[(\vec{v} \cdot \vec{\nabla}) n_z - \frac{n_x}{2} \left(\frac{\partial v_z}{\partial x} - \frac{\partial v_x}{\partial z} \right) \right] \\
&\quad + \alpha_4 \frac{\partial v_z}{\partial z} + (\alpha_5 + \alpha_6) n_z \left[n_z \frac{\partial v_z}{\partial z} + \frac{n_x}{2} \left(\frac{\partial v_x}{\partial z} + \frac{\partial v_z}{\partial x} \right) \right] \\
&\quad - k_1 \left(\frac{\partial n_x}{\partial x} + \frac{\partial n_z}{\partial z} \right) \frac{\partial n_z}{\partial z} - k_3 \left(\frac{\partial n_x}{\partial z} - \frac{\partial n_z}{\partial x} \right) \frac{\partial n_x}{\partial z} - p. \qquad \text{(B.5)}
\end{aligned}
$$